UNIVERSITÀ DEGLI STUDI DI PADOVA

DIPARTIMENTO DI INGEGNERIA INDUSTRIALE

TESI DI LAUREA MAGISTRALE

IN INGEGNERIA AEROSPAZIALE

PROGETTAZIONE PRELIMINARE DI UNA TURBINA DI BASSA PRESSIONE PER UN NUOVO MOTORE DI TIPO INTERCOOLED TURBOFAN

RELATORE:

PROF. ERNESTO BENINI

CORRELATORI:

DR. V. SETHI (CRANFIELD UNIVERSITY)

DR. P. LASKARIDIS (CRANFIELD UNIVERSITY)

LAUREANDO: ANDREA BRISTOT

ANNO ACCADEMICO 2012/2013

UNIVERSITÀ DEGLI STUDI DI PADOVA

DIPARTIMENTO DI INGEGNERIA INDUSTRIALE

TESI DI LAUREA MAGISTRALE

IN INGEGNERIA AEROSPAZIALE

PROGETTAZIONE PRELIMINARE DI UNA TURBINA DI BASSA PRESSIONE PER UN NUOVO MOTORE DI TIPO INTERCOOLED TURBOFAN

RELATORE:

PROF. ERNESTO BENINI

CORRELATORI:

DR. V. SETHI (CRANFIELD UNIVERSITY)

DR. P. LASKARIDIS (CRANFIELD UNIVERSITY)

LAUREANDO: ANDREA BRISTOT

ABSTRACT

Una nuova configurazione di motore turbofan per aeromobili a lungo raggio è attualmente in fase di studio. Il modello include un accoppiamento con riduttore di velocità tra turbina di bassa pressione (LPT) e ventola, intercoolers ed un'inversione della direzione del flusso del gas nel motore (reverse-flow core). Questo arrangiamento porterà a raggiungere rapporti di compressione e di bypass molto più elevati dei motori attualmente in produzione. Due configurazioni sono oggetto di studio: un design a due alberi separati, dove una turbina di bassa pressione guida sia la ventola che il compressore intermedio (IPC), ed un design a tre alberi, dove la potenza richiesta dalla ventola è fornita da una turbina di media pressione (IPT) con riduttore, mentre la turbina di bassa pressione guida il compressore intermedio.

In questo lavoro di tesi si è realizzata la progettazione preliminare delle turbine per le due configurazioni, per valutare i potenziali vantaggi di entrambe. Sono risultate realizzabili una LPT a cinque stadi per il motore a due alberi ed una IPT a tre stadi/LPT a due stadi per il motore a tre alberi. Le due configurazioni non presentano differenze rilevanti in termini di dimensioni e massa; sono quindi entrambe potenzialmente adottabili per il motore considerato.

Per consentire una migliore integrazione delle turbine nel motore, è stato realizzato un design perfezionato e più dettagliato con T-AXI, un programma open-source per la progettazione di turbomacchine assiali, che ha permesso di determinare la palettatura delle turbine ed il dimensionamento preliminare dei dischi. Il processo ha permesso di migliorare le stime dell'efficienza delle turbine ed ha individuato il requisito di raffreddamento attivo dei dischi per la IPT, evidenziando quindi una maggiore complessità per la configurazione a tre alberi del motore.

I files dei risultati ottenuti per la palettatura ed i dischi sono ora disponibili per procedere con simulazioni CFD e FEA.

Keywords: *LEMCOTEC, Reverse-Flow Core, Geared Turbine, Ultra-High OPR, Ultra-High BPR, T-AXI*

ACKNOWLEDGEMENTS

This work is financially supported by the E.U. under the “LEMCOTEC – Low Emissions Core Engine Technologies”, a Collaborative Project cofounded by the European Commission within the Seventh Framework Programme (2007-2013) under the Grant Agreement n° 283216.

I would like to express my sincere thanks first of all to Dr Sethi for his guidance and availability in the development of this thesis work. Aside from his useful advices which led to a successful completion of the project, his kindness and helpfulness left me a positive impression which goes beyond the simple acknowledgment of his impressive academic qualities.

I am particularly grateful to my PhD advisor Eduardo, who was available in every moment to help me in the project, providing a reliable support during the progression and always taking care of my work and results. I sincerely wish him all the best for the future, both academic and in life. I would also like to thank my colleagues Rodrigo and Haowen, who shared with me their knowledge and skills during the development of the project, and Prof M. Turner and his team from University of Cincinnati, who kindly provided me all the useful information to use their open-source turbomachinery design software.

I especially thank Prof E. Benini and Dr R. Biollo from the University of Padova, who together with Dr D. Di Cugno made this year of studies possible and provided all the necessary support. My special gratitude goes to all the new friends and people I had the pleasure to meet during this period in Cranfield, who contributed to a very rewarding year of studies and personal growth.

Finally, I would like to thank my parents and my sister for all the support always provided in my life, particularly during the academic studies. Their unique presence made all my achievements possible.

TABLE OF CONTENTS

LIST OF FIGURES

LIST OF TABLES

LIST OF EQUATIONS

LIST OF ABBREVIATIONS

ACARE	Advisory Council for Aeronautical Research in Europe
AR	Aspect Ratio
BMH	Blade Mean Height
BPR	Bypass Ratio
CLEAN	Component Validator of Environmentally Friendly Aero-Engine
DREAM	Validation of Radical Engine Architecture Systems
DP	Design Point
EEE	Energy Efficient Engine
FEA	Finite Elements Analysis
FL	Flight Level
GE	General Electric
HP	High Pressure
HPT	High Pressure Turbine
IP	Intermediate Pressure
IPT	Intermediate Pressure Turbine
ISA	International Standard Atmosphere
LEMCOTEC	Low Emissions Core-Engine Technologies
LP	Low Pressure
LPT	Low Pressure Turbine
NASA	National Aeronautics and Space Administration
NGV	Nozzle Guide Vane
OD	Off-Design
OGV	Outlet Guide Vane
OPR	Overall Pressure Ratio
PDT	Preliminary Design Tool
P&W	Pratt & Whitney
PR	Pressure Ratio
SFC	Specific Fuel Consumption
SPDS	Simplified Preliminary Design Spreadsheet
T/O	Take-off

TET	Turbine Entry Temperature
TOC	Top of climb
VITAL	Environmentally Friendly Aero Engine

Nomenclature

A	Annulus Area
C	Chord Length
c	Specific Heat
H	Enthalpy
h	Blade Height
M	Mach Number
N	Rotational Speed (rpm)
p	Static Pressure
r	Radius
rpm	Revolutions per Minute
S	Blade Spacing
T	Temperature
U	Blade Speed
V	Flow Velocity
W	Mass Flow
WT	Turbine Weight

α	Air Angle
γ	Specific Heat Ratio (= c_P/c_V)
η	Efficiency
ρ	Gas Density
Ψ	Stage Loading Coefficient
Φ	Stage Flow Coefficient or Diameter

Subscripts

0	NGV outlet
1	Rotor Relative Inlet

2	Rotor Relative Outlet
3	Rotor Absolute Outlet
a	Axial
in	NGV Inlet
is	Isentropic
m	Mean
P	Constant Pressure
V	Constant Volume
θ or w	Tangential

1 INTRODUCTION

Environmental protection is currently one of the main design drivers in the development of new engines for aeronautical propulsion. Clear objectives in terms of emissions limitations have been defined by several world aviation organizations.

European Union, through its Advisory Council for Aeronautical Research (ACARE), set precise goals for engine emissions. The Flightpath 2050 Report [1] foresees a reduction in CO_2 and NO_x emissions respectively of 75% and 90%, compared with the values of year 2000, by the year 2050. This forecast is based on predictions of the evolution of engine technology in the future years. Engine designers and manufacturers are therefore encouraged to put every effort in achieving this goal, also through increasingly stringent regulations on emissions.

In order to reduce CO_2 emissions, the most straightforward action is a reduction in specific fuel consumption, defined as the fuel flow per unit thrust of the engine [2]. This can be achieved through an increase in the overall cycle efficiency, as well as with a reduction in engine weight and an increase in the bypass ratio.

1.1 LEMCOTEC

LEMCOTEC is a European research and engineering project addressed to achieve the goals in terms of reduction of emissions set by the European Union. It was created in 2011 by an association of the most important European aero engine manufacturers and the institutions and universities leading in the aeronautical research.

The project has duration of four years. Following the assessment of very-high and ultra-high bypass ratio engines in the previous projects, namely VITAL and DREAM [3], its objective is the improvement of the core-engine thermal efficiency through the increase in the overall pressure ratio. Previous work in this field was made in the NEWAC project [4], which started analysing intercooled engine concepts to achieve very high OPRs.

The main objective for LEMCOTEC is the improvement of the core-engine thermal efficiency by increasing the OPR to ultra-high values compared with the current production turbofans. For example, the Rolls-Royce Trent 900 powering the Airbus A380 has an OPR comprised between 37 and 39 [5]: the objective of LEMCOTEC is to develop the set of technologies needed to produce engines with OPRs up to 70 [3], hence setting a large step forward from their predecessors. This task results to be challenging because of the large amount of work required to compress hot air, giving as a consequence the need for an intercooling device upstream of the high pressure compressor (HPC). Moreover, a very high pressure in the combustion chamber will lead to an increase in NO_x production, thus requiring the development of new combustion technologies [3]. The goal for this project is to go beyond the ACARE targets set for Vision 2020, hence reduction in CO_2 and NO_x emissions respectively by 50% and 80%, and point towards the objectives set in the Flightpath 2050 report [1].

The aim of the project is to obtain an improvement in thermal efficiency for the majority of the engines required in the foreseeable future, with the intention of covering with the new concepts 90% of the commercial aero engine market [3].

Three generic engines capable of covering most of the commercial applications are currently under study:

- Small turbofan engine with OPR=50 for regional aircraft
- Mid-sized open rotor engine with OPR=60 for medium range aircraft
- Large turbofan engine with OPR=70 for long range aircraft

This report addresses to the latter case, hence the object of this study will be the large turbofan engine concept.

1.2 New Concepts

1.2.1 Intercooling

Intercooling is one of the options under analysis in LEMCOTEC to achieve the target OPR value of 70 in the large turbofan engine concept. The resulting engine requires the choice of intercooling modules and their integration in the engine

structure. Some prototypes of modules and connection ducts were developed, rig tested and patented in the NEWAC project; however, several issues such as the reduction of pressure losses within the whole system, as well as the containment of the weight of the modules are still under analysis [6].

1.2.2 Gear

High bypass ratio is the second main aspect characterizing the new engine concept. The VITAL project upstream of LEMCOTEC set as a parameter for the large turbofan engine a BPR of 15 [3], hence much higher than the current engines in production. For example, the Rolls-Royce Trent 900 has a BPR comprised between 8.5 and 8.7 [7]. The main limit in the achievement of very high bypass ratios is given by the fan tip speed limitation, which implies a low rotational speed of the fan shaft. Consequently, the turbine driving the fan is required to have a low rotational speed. On conventional engines the fan is driven by the low pressure stages of the turbine; typically these stages experience a blade speed lower than the optimum due to the constraints imposed by the fan. Therefore, a further decrease in the fan rotational speed will negatively affect the fan turbine performance, thus overcoming the gain in propulsive efficiency given by the high BPR [8].

The solution can be either increase the turbine diameter or adopt a gearbox to allow for the fan turbine to rotate at a higher speed than the fan. The turbine diameter increase would lead to high core diameters and weight in the case of the large turbofan engine, hence the most appealing solution results to be the use of a gearbox.

A positive example of this solution is given by the recently introduced Pratt&Whitney PW1000G geared engine, which claims a reduction in specific fuel consumption up to 15% (compared with current engines), thanks to the higher bypass ratio and the reduction in number of stages, hence weight, allowed by the increase in LPT efficiency [9].

1.2.3 Reverse-Flow Core

The previous engine design presented in NEWAC resulted to have an excessively low blade height in the final stages of the HP compressor, due to the high delivery pressure required. This can be clearly observed by comparing the inlet blade length of the IP compressor and the outlet blade length of the HP compressor in the following sketch from one of the reports on the engine configuration concepts [10].

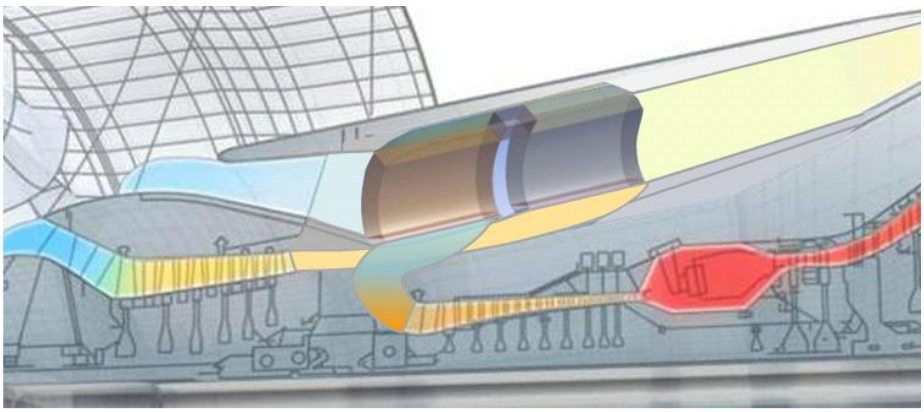

***Figure 1.1 – Compressor and intercooler arrangement in the NEWAC proposed engine* [10]**

A possible solution was reducing the HP compressor diameter. This would have allowed lowering the final stage blade hub to tip ratio, but the presence of the concentric inner IP and LP shaft made this option non-viable. The concept therefore moved to a configuration with separate HP shaft located in the rear part of the engine, such as presented in *Figure 1.2*.

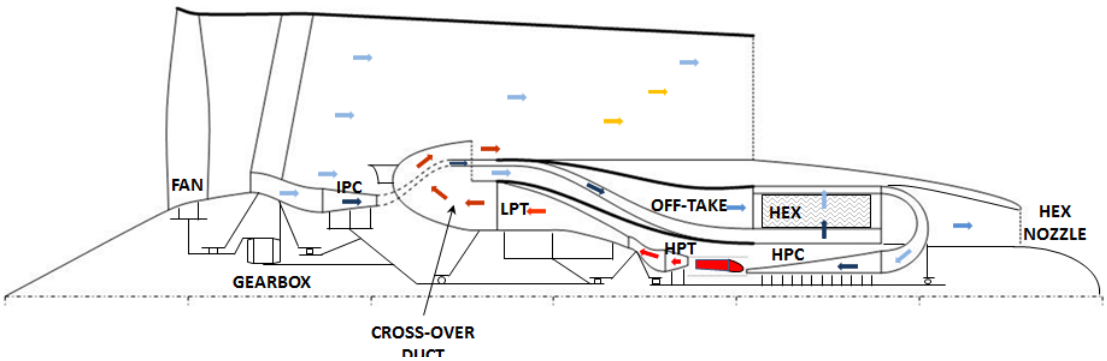

Figure 1.2 – Current LEMCOTEC engine configuration (courtesy of E. Anselmi Palma)

This configuration is characterized by a reverse flow in the HP stages of the engine and in the low pressure turbine. This sets the third new concept differentiating the engine from conventional designs, along with the intercooler and the gearbox.

1.3 Aim of the project

Consequently to the previous considerations, the basic configuration of the high BPR, high OPR LEMCOTEC concept results to be a geared, intercooled, reverse-flow core engine. The simplest configuration would be a two-spool engine, consisting of a fast-rotating LP turbine driving the geared fan and the IP compressor, plus a separate HP shaft. However, further advantage could be taken by the use of the gear to allow for a three-spool configuration. In fact, the aforementioned LP shaft could be separated into two concentric shafts. In this case, a low pressure turbine would drive the intermediate pressure compressor, while the gearbox would connect a faster rotating intermediate pressure turbine with the fan.

The aim of the project is therefore the following:

- Evaluate the differences for a two or three-spool configuration for the LPT, in terms of mass, weight and performance

The project is composed of the following steps:

- Preliminary design of the LPT for the 2-spool configuration
- Preliminary design of the IPT and LPT for the 3-spool configuration
- Turbine mass estimation for both the cases
- Turbine overall length estimation for both the cases

In addition to these steps, it was decided to carry out further investigations to better characterize the turbines. The outcome is:

- Determination of the blading
- Preliminary design of the discs
- Optimization of the disc design for mass minimization

The project relies on the use of different design tools, either internal of Cranfield University or open-source. Further details of the tools and a comparison between their differences will be presented in the following chapters.

2 LITERATURE REVIEW

2.1 Intercooled Engine Concepts after NEWAC

After the baseline configuration was set in the NEWAC project, studies aimed at quantifying the effectiveness of the innovations introduced in the new engine concept. The report presented in Ref. [11] quantifies the potential advantages of heat-exchanged core engines over conventional designs. It results therefore to be useful in understanding the context in which the LEMCOTEC configuration is set up.

The cycle analysed in the report featured an intercooled core, with the fan driven directly by the turbine, hence with no gearbox. The engine had a three-shaft configuration and featured a variable area nozzle. The performance calculations were made for top of climb conditions (FL = 350, ISA + 10 K, Mach = 0.82), with net thrust and propulsive efficiency maintained constant through variations in fan pressure ratio and bypass ratio.

A first performance simulation was made for an OPR = 50 for varying intercooler efficiencies. The intercooler proved to improve the specific fuel consumption, relative to a conventional engine, for low IP compressor pressure ratios (PR from 2 to 6). However, the advantage of intercooling for this OPR was still penalized by the increased engine weight.

Intercooling allowed reaching higher OPRs, thus achieving the indicated value set in LEMCOTEC (see Section 1.1). A second performance simulation was therefore made at OPR = 80. In this case, the thermal efficiency resulted improved, thus implying a reduced SFC relative to the previous case: the SFC at cruise was estimated to be 1.5% less than a conventional core engine, giving a saving in mass of fuel of 3.2% on a reference mission of 5500 km.

According with the paper, the use of an intercooler in the engine cycle is proven therefore to be useful to reduce the engine SFC at very high OPRs. However, the benefits provided by intercooling are strictly related with the associated pressure

losses. The article reports how the total pressure losses both in the cold and hot flow affect the SFC advantage. The results are shown in *Figure 2.1*.

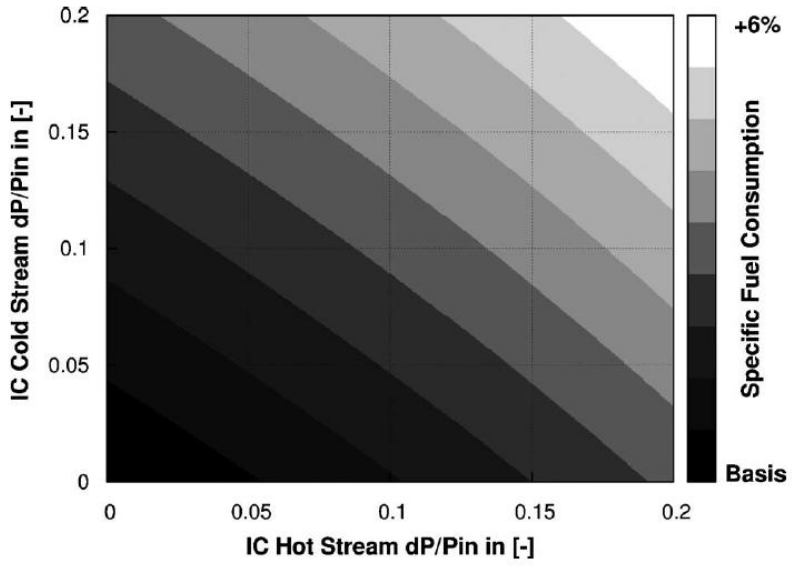

Figure 2.1 - Effect of intercooler pressure losses at OPR = 80 **[11]**

The SFC can rapidly rise up to 6% from the ideal case; this would overcome the advantage given by the intercooling. The intercooler design and integration results therefore a determining step in the overall engine design to achieve an effective SFC improvement. The turbine design and location needs to take into account as well the requirements imposed by the intercooler, such as minimizing the length of the ducting to reduce pressure losses and the matching with the other components.

2.2 Reverse-Flow Core Aero Engine: the Garrett ATF3

The Garrett ATF 3 is a small turbofan engine for executive jets, developed in the late 1960's with the aim of increasing aircraft operative range. This extension could be obtained by reducing the specific fuel consumption, with a target of 30-40% less of its competitor engines [12]. The concepts leading to this objective were an increase in overall pressure ratio and bypass ratio. The result was an innovative three spool turbofan, with a radial HP compressor and three reverse-flow turbines, as presented in *Figure 2.2*.

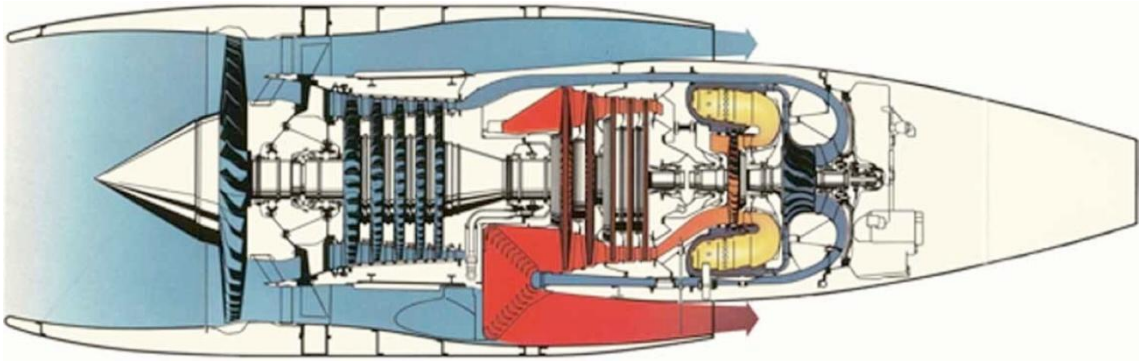

Figure 2.2 - Cross-sectional view of the ATF3 engine **[33]**

This engine shares with the LEMCOTEC concept the reverse-flow core design. The new core engine is characterized as well by a separate HP shaft, reverse-flow turbines and crossover exhaust ducts.

The crossover ducting design improves the stiffness of the ATF3 engine case, thus preventing deformation and variations in the compressor, turbine and sealing clearances [12]. This disposition of the ducts might have a positive contribution also in the LEMCOTEC concept. It is therefore recommended to consider the structural aspect when evaluating the optimum design for the ducting.

Another contribution given by the flow path in the ATF3 engine is noise suppression. The designers claim in fact for a reduction in the noise associated with the HP components of the engine, due to the tortuous ducting between the HP section and the outside air [12]. Further improvements to the acoustic emissions come from the mixed exhaust design.

The main difference between the Garrett ATF3 and the LEMCOTEC turbomachinery components concept lies in the HP compressor. In the first case, the final stage of the compression is given by a radial compressor, while the current engine design relies on a multi-stage axial compressor. The advantages of a radial compressor over an axial one are a higher stage pressure ratio and increased compactness. Studies were conducted in NEWAC to evaluate the suitability of a radial HP compressor for the intercooled engine concept, but the conclusions drawn were an excessive weight,

about four times the weight of the corresponding axial compressor, and a too low efficiency, 85.4% against 89.1% [13]. New compressor concepts for large engines are therefore still based on axial flow, while for small engines radial and axial-radial compressors can be competitive [14].

2.3 Potentialities and Challenges for the LP Turbine Design of a Geared Turbofan

The report presented in Ref. [8] analyses the potential advantages and the challenges related with the development of a geared turbofan engine. Particular attention is dedicated to the impact on the low pressure turbine design.

The objective for this new engine concept is to achieve a high propulsive efficiency through an increase in the bypass ratio. The main limitation to conventional designs is the fan tip speed, which needs to be kept sufficiently low to avoid transonic losses [8]. An increase in the bypass ratio while maintaining acceptable values of the fan tip speed would require reducing the LP spool rotational speed. Considering the turbine, this would imply for a given geometry a lower blade velocity U, hence a higher stage loading coefficient $\frac{\Delta H}{U^2}$ and therefore a decrease in turbine efficiency. To overcome this problem, a conventional engine design would require splitting ΔH among a large number of stages, thus adding weight to the engine. The impact of this approach on the fuel burn would be negative, as shown in the plot of *Figure 2.3*.

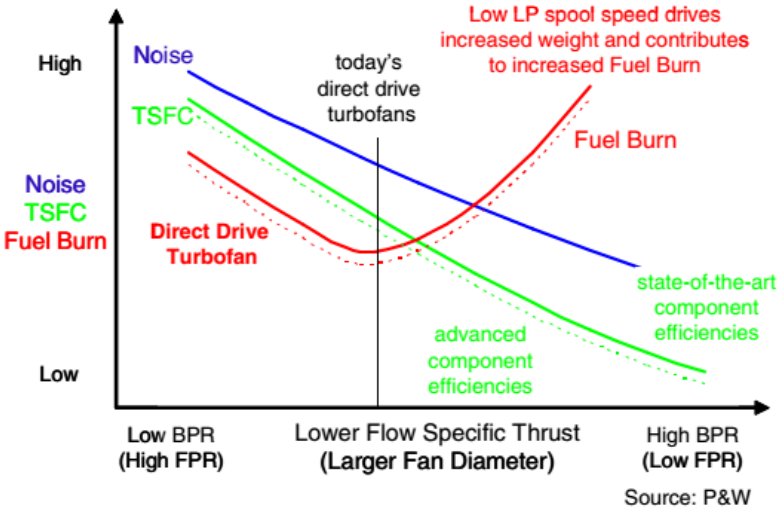

Figure 2.3 - Effect of bypass ratio variations on ungeared turbofan performance **[8]**

The main advantage of the geared turbofan is to allow the LP turbine to rotate at a high speed. This is possible by decoupling the fan speed from the rest of the low pressure spool, therefore introducing an additional degree of freedom useful to achieve an optimal turbine design. In fact, as the rotational speed increases, the blade tangential speed U will be higher, thus reducing $\frac{\Delta H}{U^2}$. A lower stage loading implies higher stage efficiency [15], thus allowing for splitting the energy extraction between a lower number of stages compared with a direct drive turbofan. The added weight due to the gearbox would be therefore offset.

According with Ref. [8], the stage count of the geared LPT could be roughly halved while maintaining a low stage aerodynamic loading. A technology demonstrator, CLEAN, was designed to evaluate the potential advantage over a conventional, slower-rotating LPT. The shaft horse power produced was comparable with the Pratt & Whitney V2500 engine LPT, but for CLEAN the rotational speed was increased by 60%. Consequently, the number of stages was reduced from 5 to 3 and the blade count resulted 40% of the original number. The comparison between the two designs is shown in *Figure 2.4*.

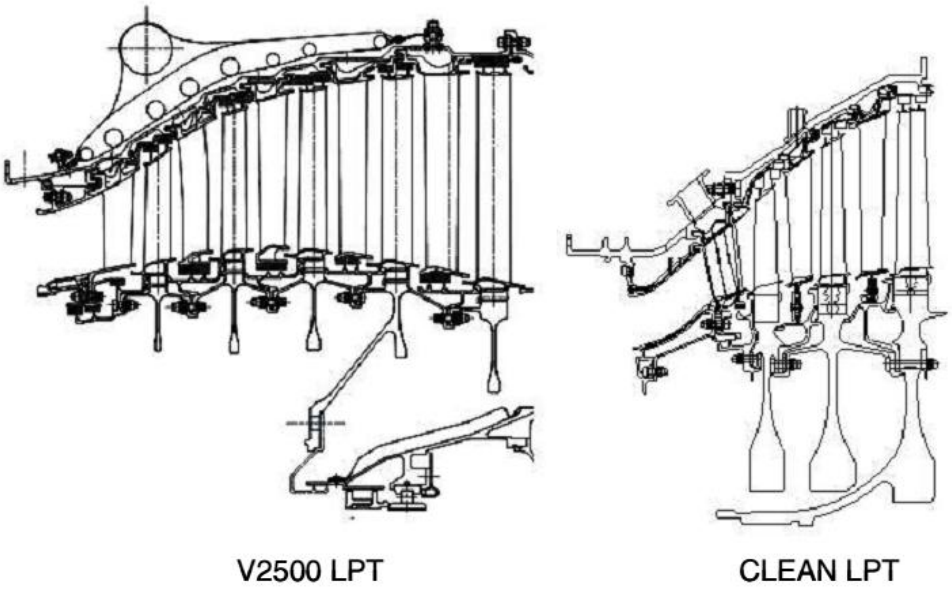

Figure 2.4 - Comparison between conventional and high-speed LPT **[8]**

The discs of the fast-rotating CLEAN LPT are much larger and heavier than those of the V2500, due to the higher dynamic loading involved. The design results however very compact, thus allowing for a lower weight; in this case the mass is 60% the value of the conventional LPT, therefore balancing the penalty introduced by the gearbox [8].

Thanks to the reduced number of stages, the stage pressure ratio will be higher than the conventional engine. This allows increasing the velocity ratios across the rotors, with average values of 2.3 against the typical 1.8 of conventional engines. As a consequence, the area of laminar flow on the blade will be augmented and the friction losses reduced. On the other hand, particular care will be needed in designing the seals in order to minimize the leakages [8].

Mechanical design is one of the most relevant challenges connected with the fast-rotating LP turbine. Centrifugal forces are much higher than a conventional turbine, thus giving a high AN^2 value; particular solutions need therefore to be adopted. First of all, the outer shroud should be as light as possible in order to reduce the load on the underlying blade. The airfoil itself needs to be resistant enough to

withstand the load of the shroud, the aerodynamic loads and its own weight. All the mentioned loads, plus the hub shroud and the blade root, impact on the disc size, which can be considerably larger than that of a conventional turbine, as shown in *Figure 2.4*. Moreover, the casing needs to be sized to contain a possible blade-off, hence its thickness will result larger as well due to the higher inertia forces involved. For all these reasons, a limited blade mass results essential. The design moves towards a tapered blade, thinner at the tip in order to minimize the mass at its extremity. The outer shroud presents cut-backs to reduce its mass without affecting the sealing properties [8]. An example of the resulting shroud compared with a conventional design is shown in *Figure 2.5*.

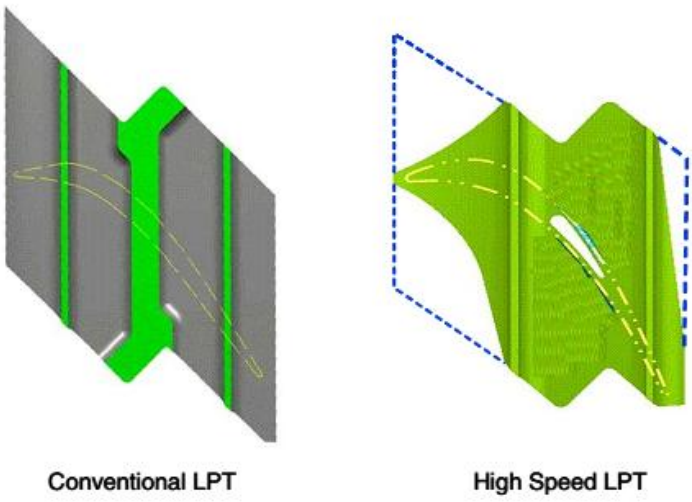

***Figure 2.5 - Comparison between conventional and high-speed LPT shroud design* [8]**

The axial length of the blade root is increased compared with a conventional turbine, in order to allow for a smooth transfer of the high loads into the disc rim [8].

The disc design presents an arrangement similar to that of the high pressure turbines: the spacers and the flanges need in fact to be close to the disc in order to have a limited hoop stress. This increases the mass of the disc web, thus implying a large bore on the lowest possible diameter [8]. A section of the conventional and high-speed LPT disc design is shown in *Figure 2.6*.

Further challenges on the LP turbine design are related with the high relative flow Mach numbers consequent to the high rotational speeds and the elevated stage pressure ratios. In order to avoid excessive pressure losses, the Mach numbers need to be kept limited. Indications for the design suggest increasing the inlet area of the LPT through an upstream diffuser, while keeping a low blockage at the turbine exit to reduce the Mach number [8].

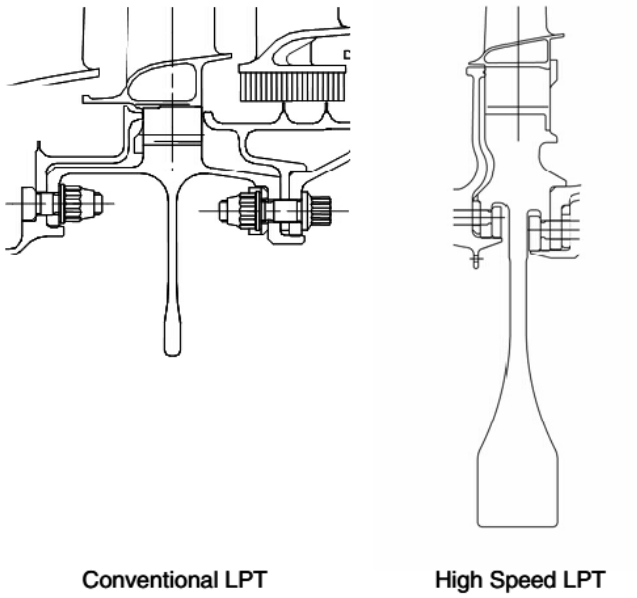

Figure 2.6 - Comparison between conventional and high-speed LPT disc design **[8]**

2.4 Geared Reversed-Flow Core Turbofan Patent

The patent presented in [16] from United Technology Corporation covers many of the characteristics of the LEMCOTEC concept, defining its baseline configuration. The features claimed by the designers include:

- geared turbofan concept
- separate HP spool located aft of the LP spool
- intercooling heat exchanger upstream of the HP compressor
- forward-flow axial HP and IP/LP turbines
- two or three-shaft configuration

A schematic of the proposed engine is shown in *Figure 2.7*.

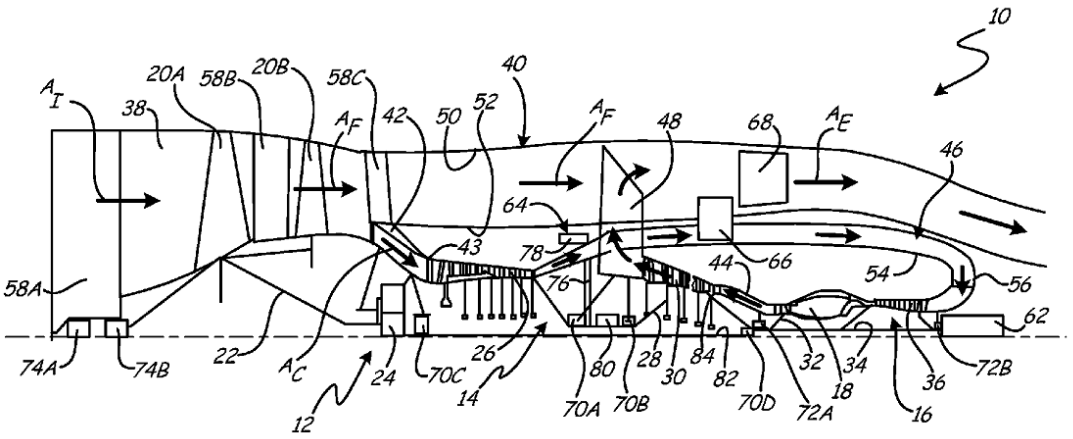

Figure 2.7 - Reverse-flow core, geared, intercooled engine patent illustration (2-spool case) **[16]**

Among the main advantages reported in this patent, the engine presents a reduced LP shaft length, compared with a conventional core. This is due to the lack of need to extend the LP shaft through a coaxial, external HP shaft. As a consequence of the decrease in length, the shaft diameter can be reduced, thus saving weight and obtaining a more compact core. In fact, the main limitation to a reduction in shaft diameter is given by the critical speed, defined as the angular velocity which excites the first natural frequency of the shaft, leading to a resonance condition [17]. The critical speed needs to be higher than the maximum shaft rotational speed, in order to avoid excessive vibratory loads. For a simple shaft, supported at its extremities and with a central mass slightly dislocated from the axis of rotation, the expression for the first natural frequency is given by

$$\omega_n = \sqrt{\frac{48EI}{ml^3}} \qquad (2.1)$$

where E is the elasticity module of the material, I the second moment of area of the section, m the dislocated mass and l the shaft length [17]. From Equation (2.1), the shaft natural frequency results to be proportional to the shaft diameter and inversely

proportional to its length. Therefore, for a given critical speed, a reduced shaft length will correspond to a lower shaft diameter, thus giving advantages in terms of mass and size.

Thanks to the separate LP and HP shaft arrangement, the HP spool diameter results as well reduced compared with the case of a conventional flow engine. The bearings for the HP shaft can be therefore smaller and simpler, thus introducing weight and cost savings [16].

Further advantages presented in the patent are related with the geared fan, which produces most of the thrust, hence improving fuel efficiency and reducing engine noise. Another contribution to noise reduction comes from the mixed-flow nacelle design, which provides for the mixing of the exhaust hot gases with the bypass air before the ejection through the nozzle, thus avoiding uncontrolled mixing outside of the engine [16].

The installation of an intercooler upstream of the HP compressor is taken into account in the patent, stressing the potential benefits given by the configuration of the ducting. The connection between the LP and HP compressor would in fact allow for a relatively simple installation of the heat exchanger, without using excessively long additional ducts [16].

Finally, as it was pointed out for the Garrett ATF3 engine case in Section 2.2, the designers identify a contribution of the cross-flow ducting to the overall stiffness of the engine, claiming a reduction in shaft bending and a possible use as support for mounting accessories on the engine.

The LP turbine described in this patent is proposed in two different configurations. The simplest presents a single turbine, driving the fan and the IP compressor (referred as LP in the patent). A second configuration is then proposed, where the LPT work is split between a faster rotating IPT driving the fan and an LPT driving the IP compressor only. The potential advantages of one configuration over the other are just briefly introduced, since they will depend on the layout and staging,

depending themselves on the engine requirements. The purpose of this thesis work will be in fact to assess for a specific case the differences between the two configurations, from the turbine preliminary design point of view.

3 TOOLS FOR LPT DESIGN

3.1 Design Process Methodology

The first step in the design of the two configurations of the LEMCOTEC LP turbine was the creation of an Excel spreadsheet based on the design process outlined in Ref. [15]. The main purpose of this spreadsheet, referenced as Simplified Preliminary Design Spreadsheet (SPDS), was to obtain a base design for the Preliminary Design Tool (PDT), developed in Cranfield University to facilitate axial-flow turbine preliminary design. An extended description of its features is reported in Section 3.3.

The starting data for both the configurations were provided from the results of a previous performance study completed by the two PhD advisors [18]. Once completed the SPD, the same design was developed with the PDT to compare the results obtained, confirming that both the design modes were reliable for producing a correct design. The process therefore continued with the PDT, which with its features allowed performing a parametric study, in order to evaluate how the changes in the turbine design parameters such as inlet Mach number or temperature distributions affected the overall performance and sizing. The main goal was to achieve a turbine capable of respecting all the constraints imposed by the flow dynamics and mechanical requirements, while having a design as compact as possible in terms of mass, maximum diameter and length. The matching with the upstream HP turbine was considered as well, in order to reduce as much as possible the curvatures of the s-duct connecting the two components, previously shown in *Figure 1.2*. The stage isentropic efficiency was set as a target to be above 90%.

After a design capable of achieving all the target values and respecting all the constraints was obtained for both the two and three-shaft cases, the results were used as a starting point for T-AXI, a sophisticated tool developed by University of Cincinnati for axial-flow turbomachinery design, which allowed to obtain a more detailed design of the turbine and a preliminary blading. After this step, the blade data were used in T-AXI to create a preliminary sizing of the turbine discs, thus estimating their weight. This process gave as result also the disc bore radius, thus allowing for an estimation of the

maximum shaft diameter. The detailed description of T-AXI features is reported in Section 3.4.

The following three sections describe in detail the mentioned tools used for the design process.

3.2 Simplified Preliminary Design Spreadsheet

The first calculations in order to define a starting point for the turbine design were made with the SPDS, developed starting from the specifications obtained from the performance simulation results for the two-spool case (see Section 4.1).

The SPDS relied on several hypotheses:

- Constant axial velocity through the turbine
- Constant mass flow through the turbine
- Stage efficiency estimated through Smith chart ([15], p. 4.26)
- 50% reaction for each stage
- Free-vortex design
- Constant work done factor Ω
- Inter-stage walls parallel to the rotation axis

The chosen handles for the stage design were the following:

- Exit hub diameter
- Stage loading ΔH
- Stage loading coefficient $\Delta H/U^2$

Once the input and the handle parameters had been given, the SPDS was capable of calculating the turbine geometry and all the required parameters to be checked for an acceptable design according with Ref. [15], hence:

- Axial Mach
- NGV leaving angle α_0
- Rotor exit swirl
- Rotor and stator gas deflections

- Rotor root acceleration
- NGV tip acceleration
- Blade tip speed for DP and max rpm
- Blade root speed
- Hub/tip ratio
- Stage flow coefficient
- AN^2 parameter

The SPDS was also capable of estimating the turbine length, based on the blade aspect ratio correlation from Ref. [19] and the component gap estimations from Ref. [20]. An annulus distribution plot was available, as shown for example in *Figure 3.1* for a three-stage case study.

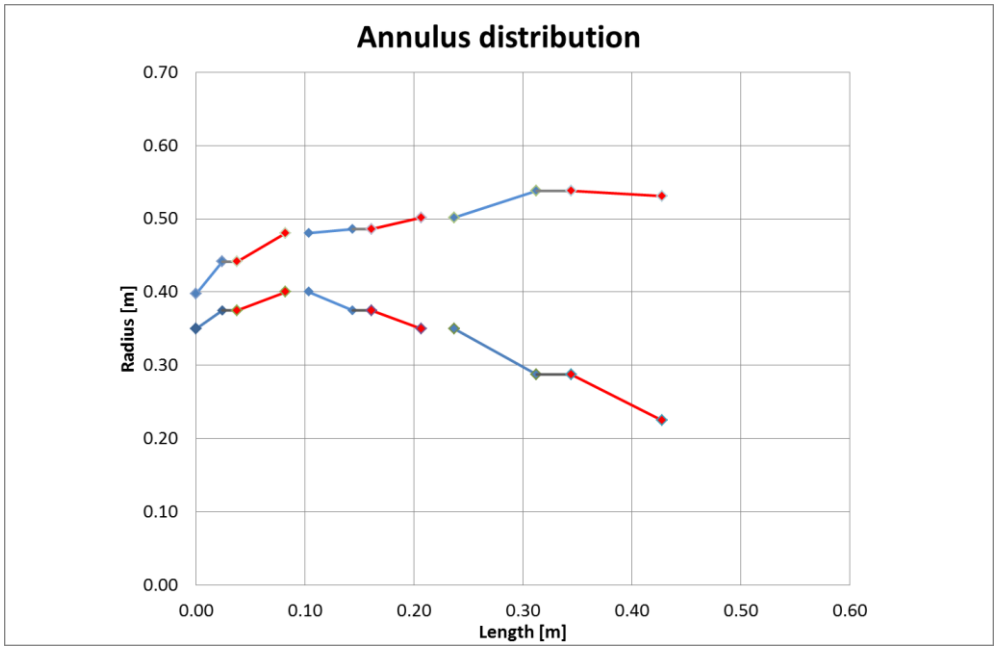

Figure 3.1 - Preliminary design spreadsheet output example

The SPDS allowed a preliminary turbine design determination, but the numerous hypotheses it was based on, coupled with the need to manually read from the Smith chart the stage efficiencies when a modification was introduced, limited its potentialities to perform a turbine parametric study with several parameters

variations. The need to perform this task led to the choice of the Preliminary Design Tool, described in Section 3.3.

As introduced in Section 3.1, a design of the same turbine configuration with the SPDS and the PDT was made in order to check the reliability of both the systems. The considered case was a three-stage turbine, having all the input parameters of the LEMCOTEC engine, plus the SPDS handles arbitrarily fixed. The results obtained were consistent, with most of the errors below 5% for the first two stages. Some higher discrepancies were noticed in the last stage, due to a difference in the stage geometry obtained with the automated PDT calculation. The differences mainly concerned the third stage exit tangential velocity, which resulted lower in the SPDS (3.5 against 12 m/s at blade mean height), thus implying a lower calculated exit swirl (1 against 3 degrees at BMH). The last stage stator deflection resulted about 10 degrees higher at BMH in the SPDS due to a higher stage inlet angle, while the differences in rotor deflections were always below 5% in all the stages and at each blade height considered. The tabulated results are reported in Appendix A.

3.3 Preliminary Design Tool

3.3.1 Introduction

The Turbomachinery Preliminary Design Tool (PDT) is a program developed within Cranfield University to help students and researchers designing axial-flow compressors and turbines. The tool aims to provide an intuitive interface through which the user can modify the design parameters, in order to obtain the desired geometry and performance characteristics. The PDT has been validated through the comparison of its results with different existing design data, proving to be reliable for turbine preliminary design [21]. The tool resulted useful in the preliminary design and parametric study of the low-pressure turbine for this thesis project. The aim of the following sections is to present the general characteristics of the program, its limitations and the information obtained from the results of its validation which proved to be relevant in the LEMCOTEC turbine design.

The development of the Preliminary Design Tool started from an existing Excel design tool, created by Dr K. W. Ramsden in Cranfield University for educational purpose and described in Ref. [22]. The original system was helpful to complete the preliminary design of compressors and turbines, determining the annulus geometry and the velocity triangles, as well as the turbine loading chart. It was useful for both separate and combined design, providing the tools for improvements in the performance and geometry characteristics. However, the simplicity of the program did not allow for producing complex geometries or multi-stage designs. The main improvements introduced by the new tool aimed in fact at multi-stage design and gave the possibility to control the geometry of each stage, thus overcoming the constant mean line limitation [21].

3.3.2 Program Features

The new Preliminary Design Tool presents a graphical user interface composed of three main panels: data input, data output and graphic output. Once the desired design has been selected (e.g. multi-spool or single design), the user can specify the preliminary design parameters such as power output, turbine mass flow, inlet total pressure, inlet total temperature and inlet diameter. The input interface is divided in three subpanels, as shown in the following screenshots.

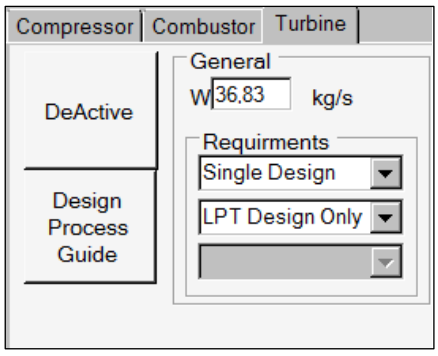

Figure 3.2 - PDT spool selection panel

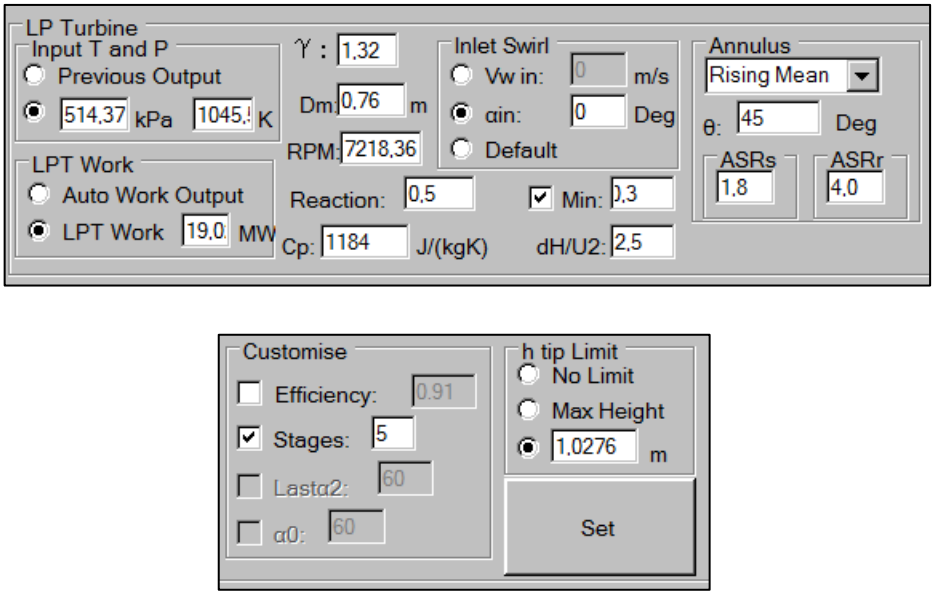

Figure 3.3 - PDT main input panel

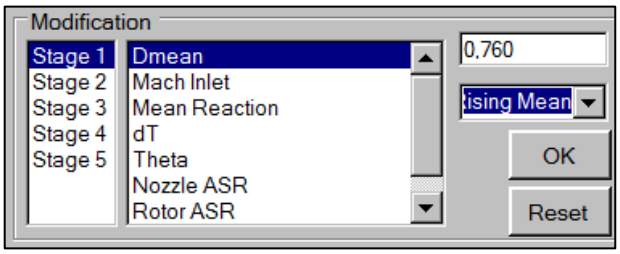

Figure 3.4 - PDT modification panel

The first panel defines the design choice, either single or multi-spool design, plus the component to be designed, in this case an LP turbine. The mass flow input is required in this section.

The second panel receives the main inputs, hence inlet flow conditions, required power output, rotational speed, gas properties, maximum stage loading and annulus geometry, including the blade aspect ratios. The number of stages can be set to be determined automatically according with the stage loading limit or it can be selected manually. For LPT designs it is finally possible to choose a maximum diameter limit, in order to respect the constraints set by the external bypass air duct. Once the inputs in this main section have been given, the calculation process can be launched.

The third panel can be used once the first run of the program has been completed. This part allows in fact modifying independently for each stage several flow and geometry parameters, such as the inlet Mach number, the stage reaction or the mean diameter. Through this window it is also possible to change the temperature distribution, hence the loading, among the different stages.

The calculation results are shown in the data output panel, shown in *Figure 3.5*. The results are divided in different sections: a group of three windows on the left gives in output the inlet and outlet geometries for each stage, plus an estimation of the isentropic efficiencies and stage power. Other three windows on the bottom of the panel display the velocities, the velocity angles, the Mach numbers and the reactions for the blade root, mean height and tip respectively.

On the right of the output panel there are the commands for the graphical output section. The program has in fact an in-built graphical visualizer, capable of showing for each stage the velocity triangles at blade hub, mid-height and tip, plus the turbine annulus diagram, the stage efficiencies on a Smith chart and plots of the trends of Mach numbers and flow angles on the whole turbine. Two screenshots of the graphic visualizer are shown in *Figure 3.6* and *Figure 3.7*.

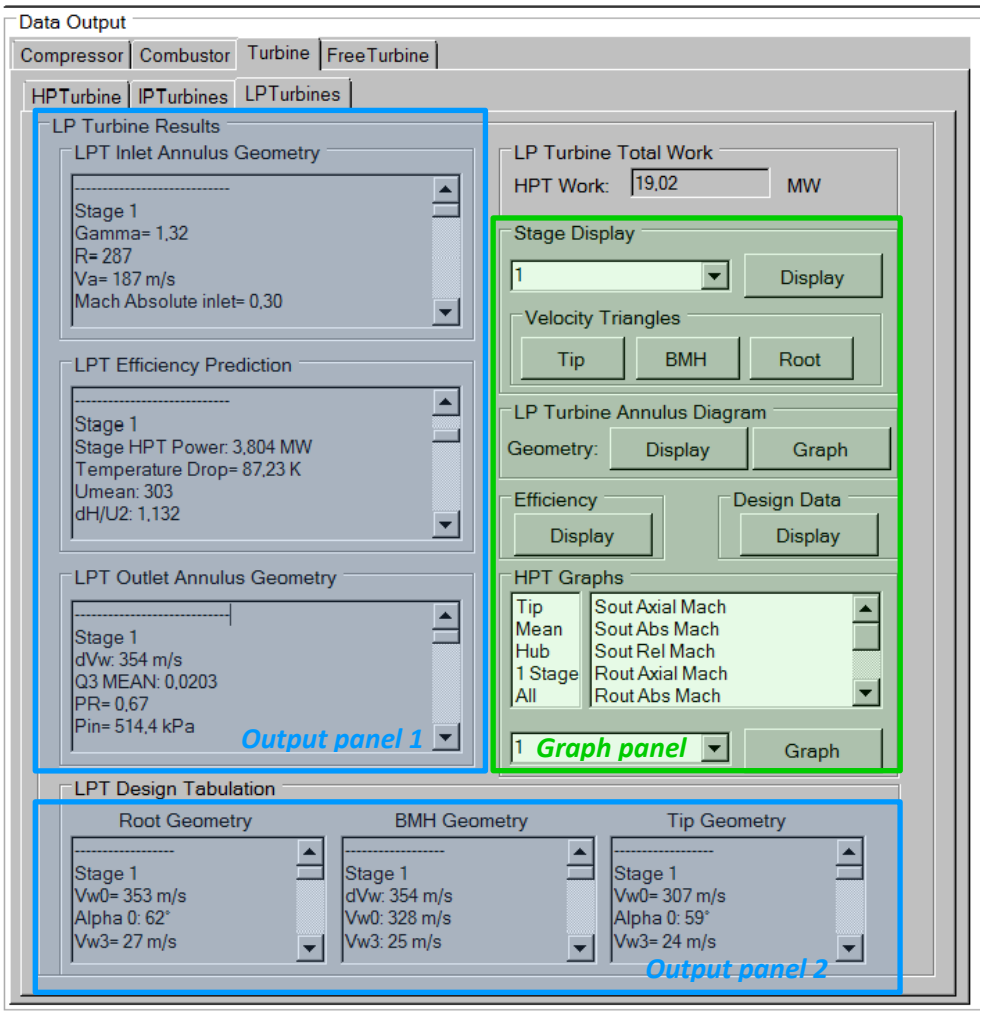

Figure 3.5 - PDT data output panel

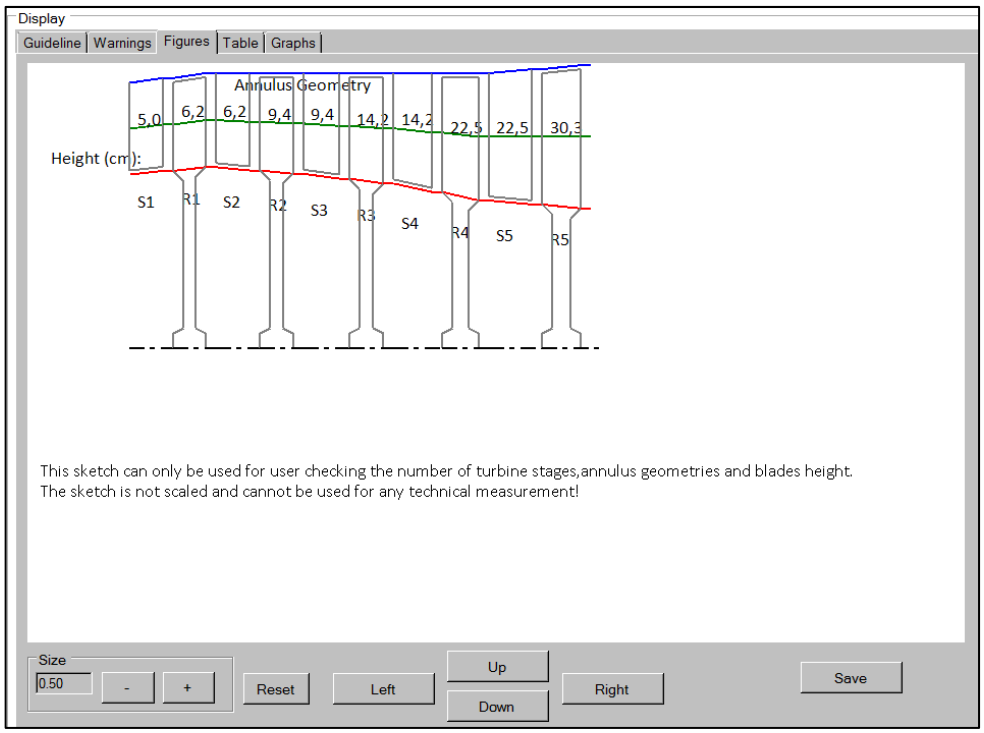

Figure 3.6 - PDT graphic visualizer, annulus diagram

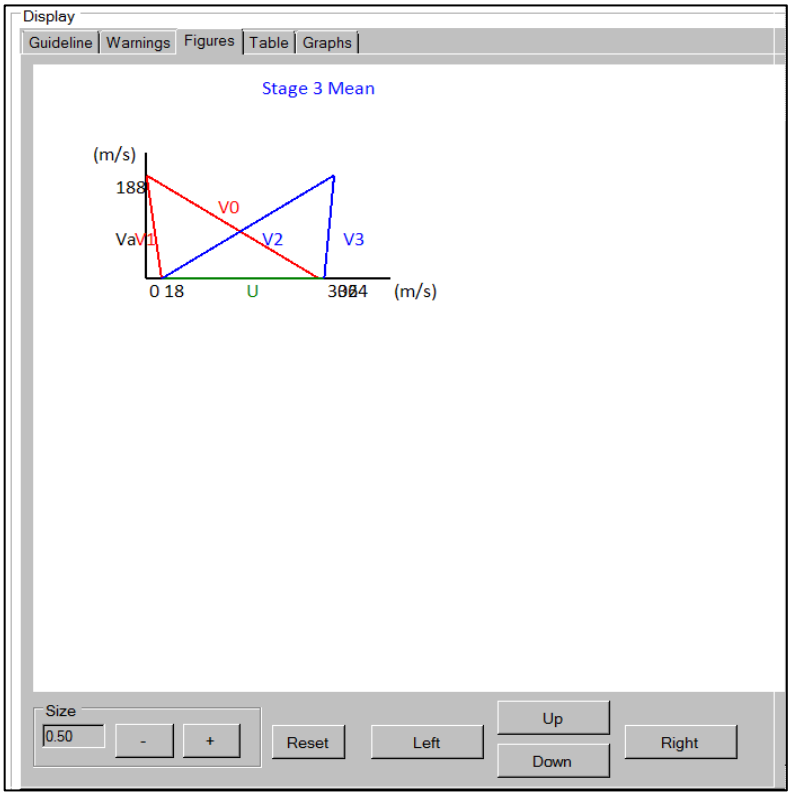

Figure 3.7 - PDT graphic visualizer, velocity triangles

3.3.3 Design Loop

The approach adopted in the Preliminary Design Tool for a single turbine design is illustrated in the following scheme. It can be observed that the program adopts a closed loop, hence allowing for modifications without restarting the whole process.

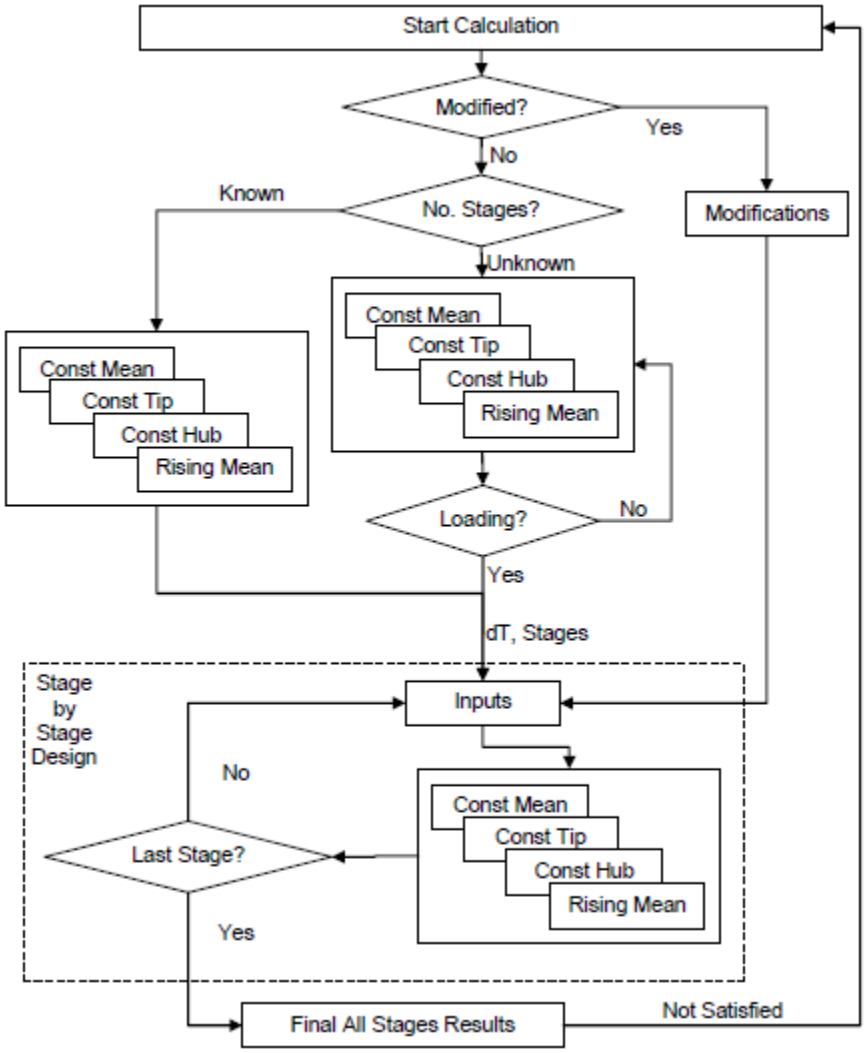

Figure 3.8 - Single spool design loop diagram **[21]**

The program requires a limited number of iterations (<100) to obtain the turbine design, hence the calculation process is fast. If convergence is not reached, an error message is displayed in the 'warnings' tab of the graphic visualizer. A convergence plot

is also available in the 'graphs' tab, where convergence is checked through the difference between the blade tangential speeds at the current and previous iteration.

3.3.4 Program Limitations

Due to its preliminary design purpose, the tool introduces some simplifications that need to be considered when evaluating the results:

- The program assumes a constant axial velocity through the stage, implying that a design for rising or falling axial velocity cannot be adopted. In the case of a fast-rotating LP turbine, a rising axial velocity through the stage would be useful to contain the blade height, thus reducing the blade and disc loads. The axial velocity is also assumed to be constant across the whole blade span, therefore introducing design inaccuracy.
- The maximum blade height is not limited. In the case of maximum tip diameter set, this can lead to excessively low hub diameters, thus giving unrealistic disc sizes.
- The design is based on the free-vortex flow hypothesis, hence with $rv_\theta = const$. Although this is the typical approach for preliminary design, in some cases a more accurate control of the flow tangential velocity is required in order to minimize the exit swirl.
- The flow used in the solution is one-dimensional: its characteristics are considered only at blade mean height, while the velocity triangles for the hub and tip are obtained from the free-vortex flow hypothesis.
- The blade profile is not taken into account in the program; hence it has no influence in the flow path.
- The mass flow remains constant through the whole turbine length. This means that cooling and sealing flows cannot be taken into account.
- The program does not provide automatic corrections or warnings for negative reactions at the blade hub. This aspect needs to be carefully considered, in order to avoid having turbine stages partially operating as compressors at their root.

3.3.5 Program Validation

This section presents the results obtained in the PDT validation process adopted by the program developer and reported in Ref. [21]. These results highlighted some characteristics of the program that needed to be taken into account in the LEMCOTEC design, such as the efficiency estimation model or the effects of the program limitations on the approximation of actual designs.

The Preliminary Design Tool was tested at first by simulating the same case study of the former Excel spreadsheet described in Ref. [22]. The turbine in this case was a twin spool single stage HPT-LPT combination. The design with the new tool proved to be very accurate for the HPT, giving errors below 1% for the exit total temperature, total pressure, absolute Mach number and axial Mach number. The LPT case produced as well acceptable results with errors below 5%, apart from the exit axial Mach number which resulted 6.2% higher [21]. This was probably due to error propagation from the input data, since the program used as LP turbine inputs the HP turbine calculation outputs, already containing a small error. As it could be observed successively, slight variations in the inlet Mach number deeply influence the stage design. Hence, the difference in axial Mach number at the LP turbine exit results justified.

After the successful completion of the first validation, the program was used by the developer to simulate real axial HP and LP turbine designs, in order to evaluate its reliability for multi-stage design. All the turbines used for the comparison were part of the NASA/GE/P&W Energy Efficient Engine program, as all their design parameters were of public domain. Two HPT and two LPT designs were used for the validation. Considering the LP turbine cases, the references were both high-efficiency, highly loaded, uncooled turbines with active clearance control. The models were the 5-staged NASA/GE CF6-50C LPT and the 4-staged NASA/P&W JT9D-7A LPT.

Once the flow path geometry was reproduced based on the available data, the program proved to be enough accurate for preliminary design. *Figure 3.9* presents the annulus geometry of the NASA/GE 5-staged test LP turbine, compared with the one obtained with the preliminary design tool [21].

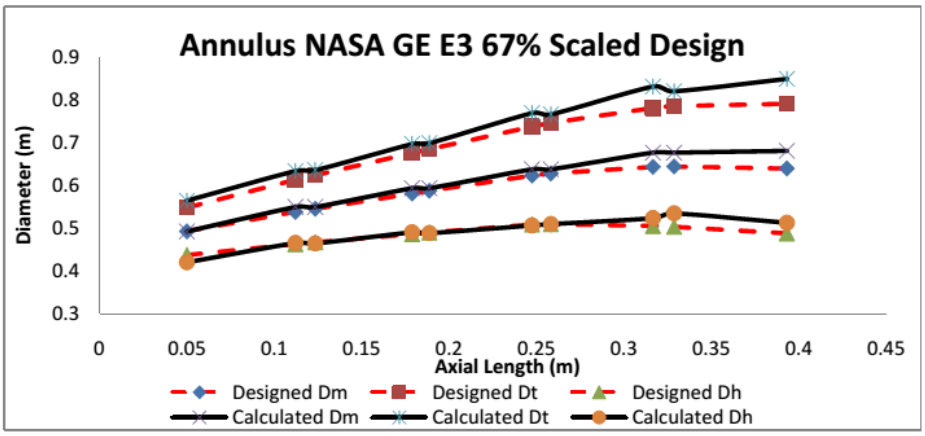

Figure 3.9 – EEE GE LP turbine flow path comparison **[21]**

The flow path reproduced with the PDT by stage to stage design is close to the original one in the first three stages, while in the last two the blade mean diameter is slightly higher than the design value, leading to a higher hub and tip diameter. This arrangement resulted necessary to obtain the same performance parameters from the program, such as stage loading coefficients and stage pressure ratios [21]. Moreover, as it can be observed from the annulus diagram of the simulated case, the flow needed to be accelerated in the inter-stage space by a reduction in annulus area, in order to compensate for a rising axial velocity design through the stage which cannot be achieved with the program (see 3.3.4 - Program Limitations). As a consequence, slight differences in annulus shape are justified.

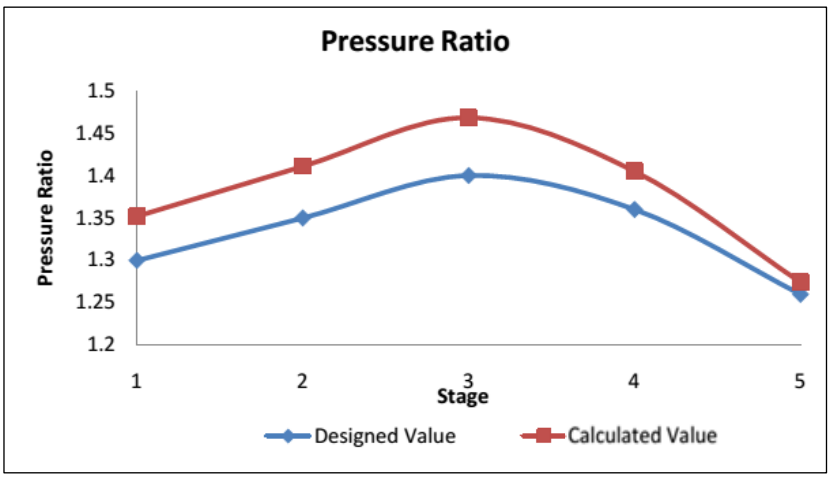

Figure 3.10 - EEE GE LP turbine pressure ratio comparison **[21]**

Following the input temperature drops through the stages, the program was capable of obtaining stage pressure ratios close to the design values, as shown in *Figure 3.10*. Other parameters such as the stage loading coefficient and the relative rotor exit Mach number at blade mean height resulted very close to the design values (*Figure 3.11* and *Figure 3.12*), thus confirming the validity of the program. However, the differences increased markedly moving far from the blade mean height, due to the weakness of the free-vortex flow hypothesis in the real turbine. In fact, the boundary effects in the wall proximity and the sealing flows are not considered in the program, leading to relevant differences in the results, as it can be observed in *Figure 3.13* for the blade tip Mach number.

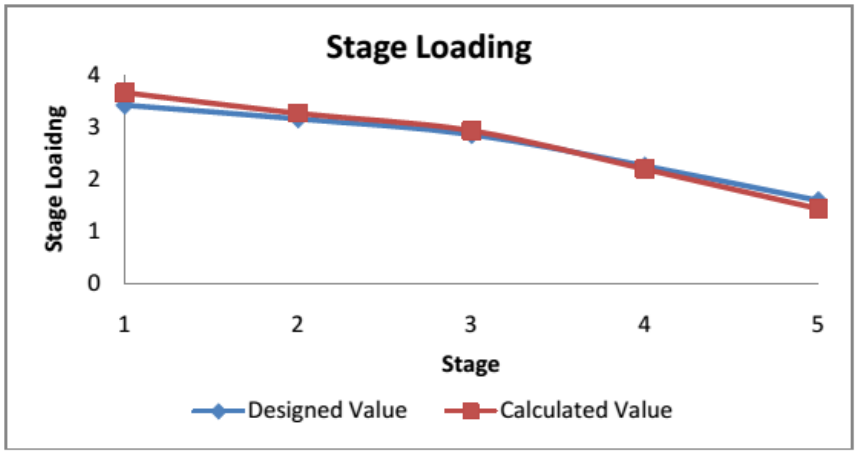

Figure 3.11 - EEE GE LP turbine stage loading coefficient comparison **[21]**

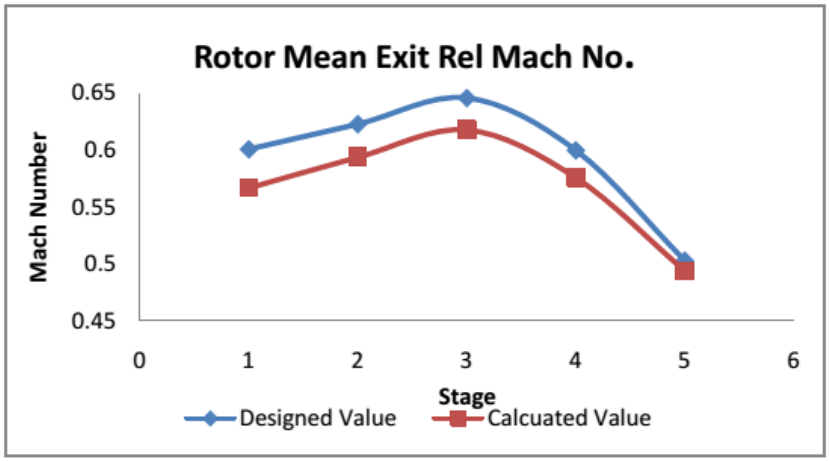

Figure 3.12 - EEE GE LP turbine exit relative Mach comparison at BMH **[21]**

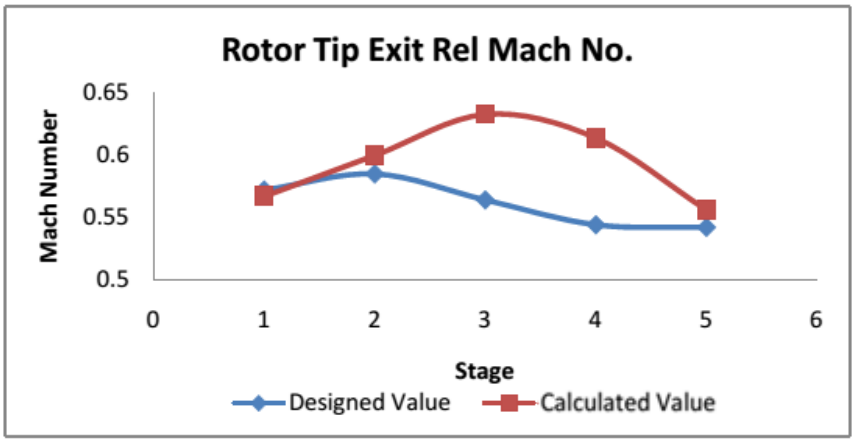

Figure 3.13 - EEE GE LP turbine exit relative Mach comparison at tip **[21]**

The stage isentropic efficiency estimations made with the program resulted always lower than the actual efficiencies, as shown in *Figure 3.14* for the 4-stage turbine. This was due to the fact that the program used a simple correlation based on experimental results for typical LP turbines, hence not highly loaded. The formula used was:

$$\eta_{is} = 0.98 - 0.0576\frac{\Delta H}{U^2} \qquad (3.1)$$

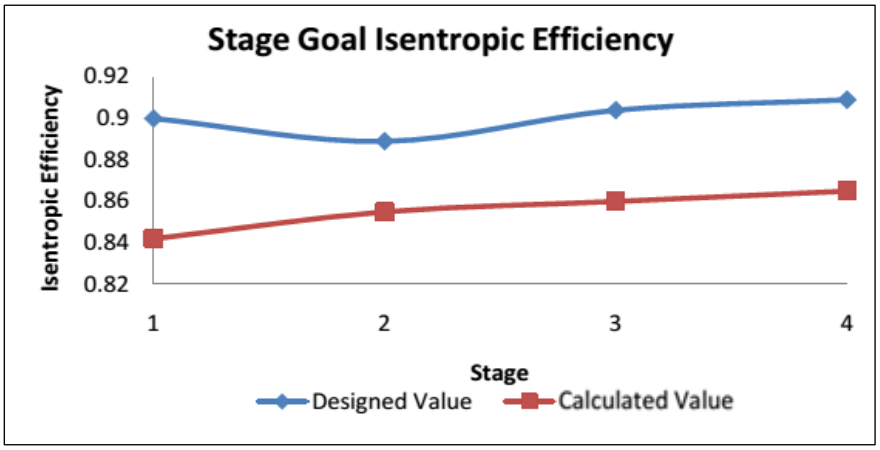

Figure 3.14 - EEE P&W LP turbine stage isentropic efficiency comparison **[21]**

Hence, the isentropic efficiency in the program was based only on the stage loading coefficient. In reality, also the flow coefficient $\frac{V_a}{U}$ needs to be taken into account, as well as the flow deflections at different blade heights and the friction losses. The formula however took into account the decrease in efficiency due to over-tip leakage, setting it to a 2% reduction [15].

The program limitations such as the lack of smooth geometry transitions across the stages, the simplified efficiency model and the impossibility to design and visualize the blading led to consider a more sophisticated program to obtain more information on the turbine geometry and performance. Another tool, T-AXI, presented the potentialities for performing this task, although it needed as starting point some input values which had to be obtained with a preliminary design study, such as the stage mean diameters and NGV exit angles [23]. The turbine design process was therefore divided in two steps: first of all obtain with the PDT a design capable of achieving the target parameters and respecting the given limitations; thereafter, use the produced data as an input for the T-AXI tool, thus generating a new design with a smooth flow path and more accurate efficiency estimation. Moreover, the latter suite presented some additional features such as disc design and rotor mass estimation, useful to extend the knowledge of the turbine stages characteristics.

3.4 T-AXI Suite

3.4.1 Introduction

The Turbomachinery Axisymmetric Design System (T-AXI) is a set of open source programs developed by the Department of Aerospace Engineering at the University of Cincinnati, USA. T-AXI was created for axial compressor and turbine design, mainly for educational purposes. However, it is claimed to be enough complete to produce actual designs, as reported in Ref. [23]. The program was validated by comparing its results with existing design data, both for the compressor and turbine code. The compressor code validation was based on a NASA single stage compressor test rig and on the

NASA/GE EEE engine ten stage HP compressor. The turbine code used instead as reference the 5-stage LP turbine of the latter engine.

3.4.2 Program Structure

The program is divided into different sub-programs, which perform the various steps of the turbomachinery design. A schematic of the suite is provided in *Figure 3.15*. The turbine design code is named T-T_DES. It requires in input an initialization file (init.xxx) which specifies the units, the unknown variables, the number of stages, the inlet flow conditions, the gas properties and the tip clearance for both the stator and the rotor. Moreover, it is possible to define at this step the shape and size of the turbine inlet duct. In addition to the initialization file, T-T_DES requires in input a file defining for each stage the flow conditions (stage.xxx). This file requires information provided by a preliminary design analysis, such as the NGV exit angle and Mach number, the stage exit total temperature, the stator and rotor Zweifel numbers, the stator and rotor loss coefficients, the blade aspect ratios, the row spacing, the stator and rotor mean radii and the rotor velocity ratios (hence allowing for rising or falling axial velocity design). An optional file can be used to include the outlet guide vanes in the turbine design (ogv.xxx).

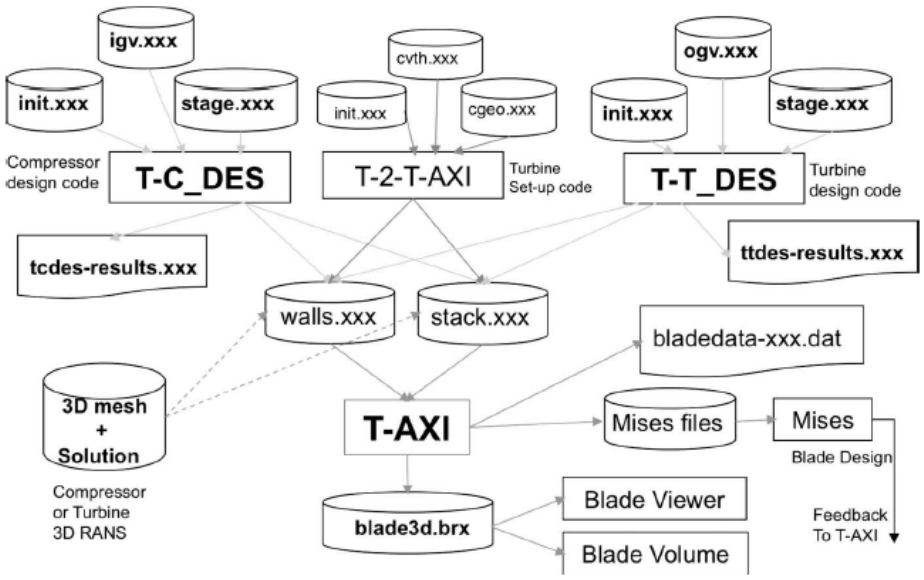

Figure 3.15 - T-AXI design system schematic **[23]**

Once T-T_DES has been run, a file of preliminary results is produced (ttdes-results.xxx). This file contains the information on the flow conditions (total and static pressure and temperature, Mach numbers, velocity components), the efficiency, the degree of reaction and the number of blades. Two additional files containing non-dimensional information on the wall and blading geometry/losses are written (walls.xxx and stack.xxx respectively). The latter files are used as input for the T-AXI solver, which produces as output a table of the aerodynamic quantities at each blade leading and trailing edge, plus data on the blade row performance such as loading coefficients and isentropic/polytropic efficiencies. T-AXI is a non-dimensional solver, hence all the input and output data are relative to a specified dimension. For example in the case of the lengths, the reference value is the first stage rotor leading edge tip radius. The blades result divided in a chosen number of nodes along their span (the default value is 20 nodes), thus providing a detailed resolution of the distribution of the quantities. Having defined a maximum thickness to chord ratio at the hub and tip, T-AXI can create a blade shape in five different sections of the span [23]. Through an in-built visualizer (blade3d.brx, t-viz in the current version), the three-dimensional blading can then be viewed.

3.4.3 Additional Features

The results obtained with T-AXI can be used as input in MISES, a program used in industry for blade profile optimization, described in Ref. [24]. The output from MISES can then be fed again into T-AXI by updating the losses and flow turning in the 'stack' file. A blading optimization loop can be therefore created.

More features to the suite of programs were added successively by the developers. Of particular interest results the disc optimization code 'T-AXI disk'. Once the blading has been defined, this code allows the design and stress analysis of gas turbine discs [25]. The main features of the code are the possibility to adopt four different disc shapes or to define the shape arbitrarily, a temperature dependent material database available, an automatic weight estimation tool, a mass optimization loop and detailed plots for the stress analysis. Although this program is a low fidelity

design tool, it can be helpful to preliminarily determine the disc sizes and weights for the considered fast-rotating LP turbines. As explained in Section 2.3, the disc design for this kind of turbine is a challenging task. Hence, a preliminary indication of the size magnitude would result useful. Moreover, once the disc sizing is obtained, a preliminary definition of the shaft diameters can be reached.

3.4.4 Program Validation

Considering the turbine case, the validation process adopted by the developers used two different approaches. A first solution was calculated after recreating the same flow path geometry, in order to evaluate the reliability of the T-AXI flow solver. A second solution was then calculated without preliminarily defining the flow path, thus using the in-built turbine design code to validate its capability of determining a suitable annulus diagram.

For the first approach, the walls and stack files were created by the developers using the setup code T-2-T-AXI, using the initial data presented in the EEE LP turbine report [26]. In this way, the flow path obtained was the same of the original turbine. The work split was chosen according with the report, although some adjustments were necessary to obtain the same overall temperature difference [23].

In the second approach, the published turbine inlet conditions and stage data were used by the program developers to create the inputs of T-T_DES (see Section 3.4.2). By tuning the input parameters, the code produced a geometry very similar to the original turbine, as it can be observed in *Figure 3.16*.

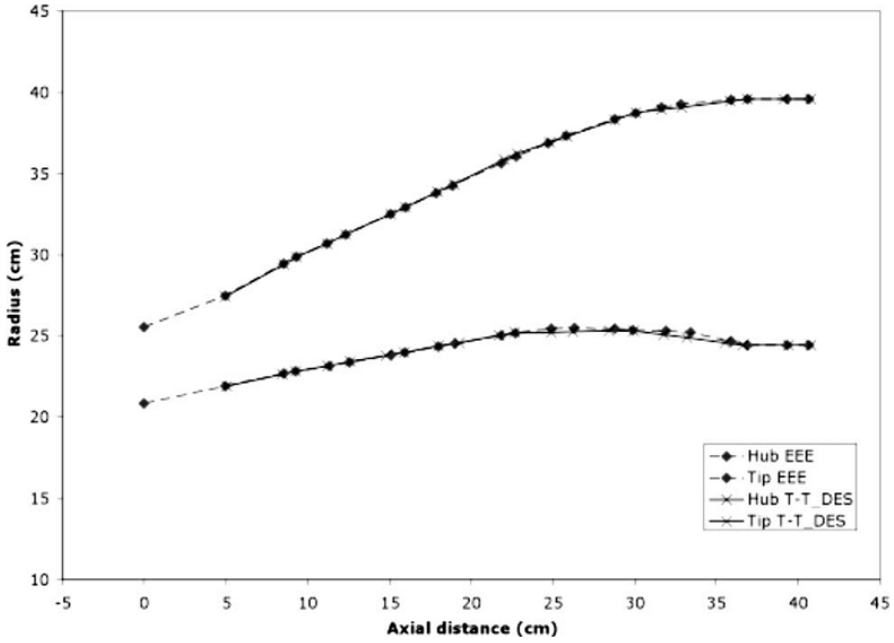

Figure 3.16 - Comparison between the flow path produced with the turbine design code and the actual EEE turbine **[23]**

The comparison of the results is published in *Table 3.1*. It can be noticed that both the approaches described yielded performances very close to the measured one.

Table 3.1 - Comparison of the EEE performance data with T-AXI results **[23]**

	Measurement reading 503	T-AXI calculation EEE flowpath	T-AXI calculation (T-T_DES design)
Pressure ratio	4.409	4.351	4.326
Temperature ratio	1.468	1.464	1.463
Efficiency	92.05	92.85	92.91

3.4.5 Differences with the Preliminary Design Tool

T-AXI introduces some additional features which can be used to refine the turbine design once some starting data have been obtained. Although T-AXI is a preliminary design tool, some specific data such as the NGV exit angles and Mach numbers are in fact required; an initial shape for the turbine needs to be defined as well by means of the stator and rotor mean radii for each stage. Therefore, it is better

to obtain a starting design with the Preliminary Design Tool described in Section 3.3 and then modify it with T-AXI, taking advantage of its additional features to improve the design characteristics.

The main capacities which overcome some of the limitations of the previously mentioned PDT are the following:

- Variable axial velocity through the stage
- Forced vortex flow design available
- Account for tip clearance losses
- In-built loss model
- Automatic determination of the blade profiles
- 3D blading visualization
- Output ready for CFD simulation

T-AXI results therefore useful to better characterize the turbine, thus increasing the level of detail and providing additional information on the modifications that should be adopted to produce a feasible and efficient design.

4 PRELIMINARY DESIGN PROCESS

4.1 Design data

4.1.1 Overview

The turbine was designed for a mixed exhaust engine case, at cruise condition, according with the input data obtained from the previous engine performance simulations performed by the two PhD advisors [18]. The input data provided for the two turbine design cases are summarized in the following tables.

Table 4.1 - Flight Conditions

Altitude	10668 m
Atmospheric Conditions	ISA
Operative Condition	Maximum Cruise Range
Flight Mach Number	0.82

Table 4.2 - Turbine Design Parameters

	2-spool	**3-spool IPT/LPT**	
	LPT	**IPT**	**LPT**
Required Power Output (MW)	19.063	13.703	6.112
Rotational Speed (rpm)	7218	9022	7049
Max Rotational Speed (rpm) *	7991	10023	7983
Inlet Total Pressure (kPa)	514.37	676.10	131.79
Inlet Total Temperature (K)	1045	1129	772
Mass Flow (kg/s)	36.83	33.58	34.77

* Highest value between TOC and T/O conditions in the performance simulation results [18]

The design point was chosen at the 'Maximum Cruise Range' operative condition of the performance simulation results of Ref. [18], since the considered LEMCOTEC engine is to be fitted on a long range aircraft. The development of the turbine was therefore based on its longest operative condition, in order to gain the maximum benefit in terms of fuel consumption over the whole mission.

4.1.2 Power Requirements

According with the mentioned performance simulation results, in the 2-spool case the fan power requirement is 13.325 MW, while the IP compressor requires 5.319 MW. The mechanical losses were set to 2% of the needed power, hence adding 0.373 MW to the LP turbine power output requirement. In the 3-spool case, the IPT drives the fan, connected through the gearbox to its shaft. The fan power requirement is in this case 13.310 MW, while the mechanical losses including the gearbox were assumed by the developers to be about 2.95% of the fan power, hence adding 0.393 MW to the IPT power output. In this case the mechanical losses were assumed to be higher because of the shaft higher rotational speed. The LP turbine of the 3-spool case directly drives the IP compressor, which requires 6.082 MW. Since there is no gearbox for this spool, the mechanical losses are lower; for this reason in the performance simulation they were assumed to be 0.5% of the IP compressor power, hence 0.030 MW.

4.1.3 Rotational Speeds

The rotational speed for the LPT is similar for both the two- and three-spool cases, being about 7000 rpm. Considering the IPT in the latter case however, the rotational speed was chosen in the performance calculation to be higher, taking advantage from the lack of IPC rotational speed constraints. This resulted in about 9000 rpm, thus allowing for a high blade speed with a lower turbine diameter.

In the turbine design process, the maximum rotational speed was taken into account as well, in order to preserve the mechanical integrity of the turbine at off-design conditions. From the performance simulation data, the maximum shaft rotational speed was reached either at take-off or top-of-climb condition. The chosen value was therefore the highest among the two, according with the component: in the 2-spool case the LPT had its maximum rotational speed at take-off, as well as the IPT in the 3-spool case, while the 3-spool engine LPT reached its maximum rpm at TOC condition. This difference should be motivated by the higher IPC pressure ratio

requirement for the 3-spool engine at TOC, which was 5.00 against the 3.50 of the two-spool engine.

4.1.4 Flow Conditions

The mass flow through the turbine was assumed to be constant, although in the reference performance simulation data it was increasing due to the introduction of sealing flows. For the preliminary design the inlet value was chosen, since a low mass flow was the most demanding condition in achieving the required power output.

The turbine inlet Mach number was set for the first calculations to 0.32, corresponding to an inlet axial velocity of 200 m/s; a parametric study on the effects of its variation above and below this value was successively performed. The typical range, according with the studies for novel large turbofan engine concepts reported in Ref. [27], is 0.28-0.46. The LPT inlet Mach choice is in fact a trade-off between the need to keep the lowest possible value, hence minimizing the pressure losses in the upstream s-duct, and the limitation of the LPT exit area, the latter having benefit from high Mach numbers, with an upper limit of 0.5 at the exit [15]. The latter requirement would imply either to adopt a high inlet Mach number or to design the turbine for rising axial velocity through the stages.

4.2 Objectives

The main objective of the turbine design was the achievement of an estimated stage isentropic efficiency above 90%, consistently with the high thermal efficiency target of the LEMCOTEC engine. The turbine integration with its upstream and downstream components was considered as well, thus aiming at an inlet mean diameter as close as possible to the HPT outlet value and at low exit blade height to limit the cross-sectional area of the exhaust cross-over duct. The design process had also the objective of producing turbines as compact as possible, in order to facilitate their integration in the engine arrangement and to contain the overall engine mass and size.

4.3 Constraints

The main limitations impacting on the turbine design were given by the high tangential speed of the blades, particularly in the exit stages. According with Ref. [15], the recommended value of the tip speed for an acceptable mechanical design is 430 m/s. The tip speed limitation set the maximum allowable diameter of the turbines, which resulted for the LPT about 1.03 m for both the two- and three-spool engine configurations. The turbines respecting the latter value can operate at their maximum rotational speed without exceeding the tip speed limit. The IPT maximum diameter limit was instead 0.82 m.

A second important limitation in the turbine design was the maximum blade height: the LP turbine blades for aero engines have values typically below 30 cm, as reported in Ref. [28]. The latter value should not be exceeded in order to achieve a feasible blade mechanical design and to have a compact exhaust duct. In the reverse-flow core engine presented in this study, the compactness of the latter is particularly relevant to maintain an acceptable core diameter.

Other limitations concerned the turbine performance, such as the need for exit swirl minimization and the requirement to maintain the gas accelerations above the value of 1.15, both for the stators and the rotors. The latter task resulted particularly challenging in the design of the turbine exit stage, because of the low blade root speeds related with a low hub diameter. An extensive discussion of this aspect is presented in the performance results of the turbines in Chapter 5, along with the complete report of the performance parameters considered.

4.4 Parametric Study with Preliminary Design Tool

4.4.1 Introduction

The three-stage baseline configuration analysed with the SPDS and the PDT resulted to give excessive stage loading coefficients ($\Delta H/U^2 > 3$). Moreover, the turbine had excessively low rotor root acceleration in the final stage, due to a too low blade hub speed; this was consequent to a too high annulus exit area, yielding a low hub

diameter having fixed the blade tip diameter. It was therefore decided to design a four-stage turbine, hence perform a parametric study based on this case to evaluate the influence of the design parameters on the performance and geometry, in order to understand the modifications to introduce for an acceptable configuration. The evaluation of the trends was the main purpose of this parametric study, hence the values presented in this section should be considered only as an illustration of how the design methodology was set up. The results of the designs capable of achieving the target performance and geometry while respecting the constraints set are reported in Chapter 5.

The geometry adopted for the turbine was a rising mean line design, with tip diameter limited to 1.03 m to respect the max tip speed constraint (see Section 4.3).

The design parameters modified in this parametric study were the following:

- Stage reactions
- Stage ΔT distribution
- Stage mean line diameters
- Inlet Mach number

Their individual effect was evaluated on the parameters critical in the turbine design, hence those which proved to be the most difficult in respecting the given constraints. The critical parameters were:

- Last stage rotor hub acceleration
- Last stage hub and mean exit swirl
- Last stage blade height
- Max tip diameter

The effect on stage efficiency was considered as well, since a high stage efficiency (η_{is} >90%) was one of the objectives of the turbine design.

4.4.2 Reaction Variations

The stage reactions were the first parameter investigated, since the last stage hub reaction resulted negative after the first design study. According with Ref. [15] and with the model adopted in the PDT, the stage reaction is defined as the ratio between the static pressure change across the rotor and across the whole stage:

$$R = \frac{\Delta p_{rotor}}{\Delta p_{stage}} \qquad (4.1)$$

The rotor acceleration is instead the ratio between the rotor inlet and outlet relative flow velocities. A value below 1 indicates that the flow is decelerating, hence being compressed. Consequently, the stage reaction will be negative. This situation is likely to happen at blade hub in the last stages of the LP turbine, when the aircraft is cruising at high altitudes and the turbine inlet pressure is relatively low, as in the case of the chosen design point. In the first case study, the last stage rotor hub acceleration resulted below 1, therefore the stage reaction needed to be modified.

Starting from the ideal value of 50%, the reactions of the four stages of the turbine were varied individually while reporting the corresponding last stage rotor hub acceleration, hub exit swirl and exit blade height. The results obtained indicated that an increase in stage reaction at blade mean height positively affects the hub reaction, as well as the hub acceleration, allowing their increase to acceptable values. On the other hand, larger values of stage reaction implied high exit swirls, due to the high exit velocity related with the increased flow acceleration in the rotor. The exit blade height resulted slightly increased, with a variation of 8 mm (36.2 to 37.0 cm) for an increase in reaction by 10%. The plot of the results is presented in *Figure 4.1*.

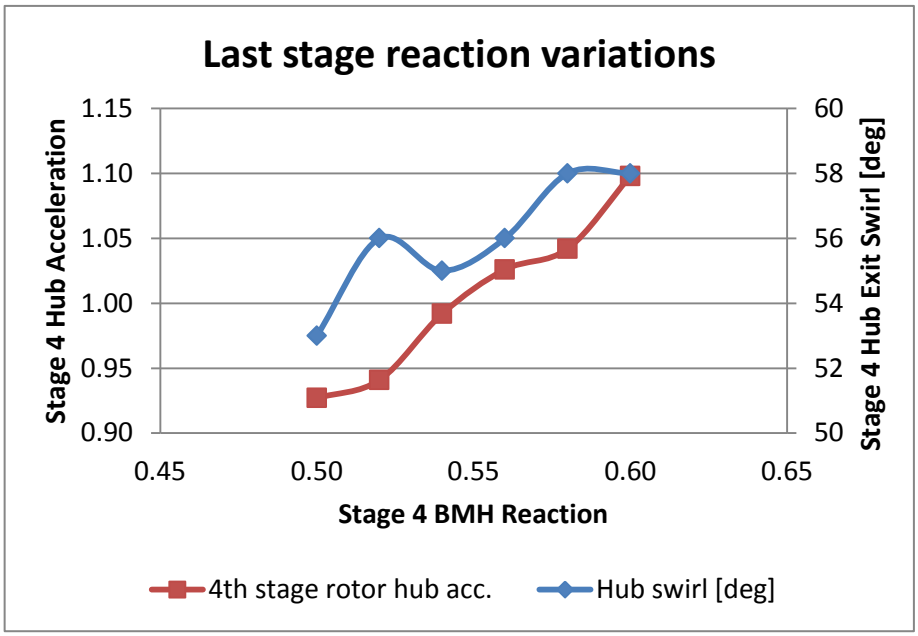

Figure 4.1 - Effect of stage reaction variations

It can be observed in the plot that increases in last stage reaction improve the hub acceleration but increase the exit swirl. Considering instead the third stage, reductions in its reaction proved to increase the last stage hub acceleration. In fact, a reaction decrease has as consequence the reduction in the third stage exit flow angle, implying less flow turning in the fourth stage NGV and thus allowing for a higher acceleration in its rotor. Modifications in the reactions of the stages upstream of the third gave instead negligible effects on the last stage reaction, with variations on the order of 0.1%.

The conclusions drawn from this analysis led to a turbine design with reaction increased above 50% at BMH in the last stage and reduced in the stage immediately upstream, in order to achieve an acceptable rotor hub acceleration. The reactions of the remaining stages were instead maintained at 50%.

4.4.3 Temperature Distribution Variations

Temperature distribution was the second parameter modified in the study. Starting from the temperature drop of 436 K equally split across the stages, hence 109

K per stage, modifications in the distribution were introduced in order to evaluate the effect on the critical parameters previously listed (see 4.4.1). The method adopted consisted in varying the temperature drop between couples of stages, hence increasing the ΔT on one stage while reducing it on the other to maintain the overall drop unchanged. The corresponding changes in last stage rotor hub acceleration, hub and mean exit swirl, blade height, maximum tip diameter and stage efficiencies were therefore reported and evaluated. Indicating with 1 the turbine entry stage and 4 the last stage, the combinations analysed to determine the temperature distribution across the turbine were: 1-2, 3-4, 1-4, 2-3. The plot of the trends obtained for the combination of the last two stages is reported in *Figure 4.2*. The plot represents in the x-axis the difference in temperature drop across the stages 3-4 (e.g. a zero value meaning an equal temperature drop in the two stages), while the y-axis reports the last stage hub acceleration and exit swirl.

The complete results for this case study are reported in Appendix B.

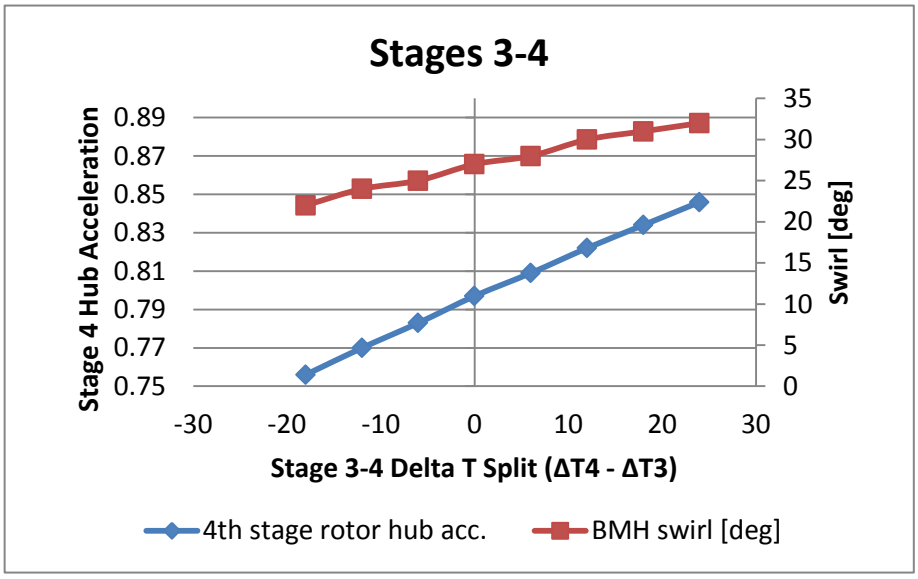

Figure 4.2 - Effect of temperature distribution variations

The trends obtained indicated that the highest energy extraction (hence the highest ΔT drop) for the considered four-stage turbine should be in the fourth stage, followed in order by the first, the second and the third stage. The choice was the result

of the trade-off between the increase in exit hub acceleration and the need to maintain a low exit swirl. The stage isentropic efficiencies resulted to decrease as the temperature drop was increased, according with the efficiency correlation adopted in the program (Equation (3.1)). Since the stage isentropic efficiency was inversely proportional to $\Delta H/U^2$, an increase in ΔH in the last stage without excessive reductions in efficiency was possible, thanks to the higher blade tangential velocity.

Although the temperature distribution obtained applies to the specific case considered, the methodology here developed could be used to analyse other turbine configurations.

4.4.4 Stage Mean Line Diameter Variations

The purpose of this section of the study was to understand the effect of changes in stage mean line diameters on the critical parameters. The first part considered the turbine inlet mean diameter variations (hence the first stage mean diameter); once chosen its value, modifications on the remaining stage diameters were introduced.

One of the limitations to the stage design is given by the maximum blade hub to tip ratio allowed. This limitation is provided to avoid excessively high tip clearance to blade height ratios, which would lead to excessive flow losses over the tip, and is typically set to 0.9. Starting from the maximum allowable tip radius of 1.03 m and taking into account both the hub to tip ratio limit and the inlet flow area, the corresponding hub diameter was therefore determined, thus giving a maximum mean inlet diameter of 0.823 m. The hub to tip limit proved to be always respected, given the relatively high inlet area. The parametric study was therefore performed starting from the maximum inlet mean diameter and reducing its value.

The results obtained proved that higher stage mean diameters yield higher isentropic efficiencies, thanks to the increase in blade tangential speed. This in fact reduces the stage loading coefficient $\Delta H/U^2$, hence improving the stage efficiency.

The parametric study in this case needed to be divided into two sections: the first was based on a ‘rising mean line’ setting in the PDT and was used for the highest

inlet mean diameters (0.640-0.823 m), whilst the second was based on a 'constant hub' setting for the lowest diameters (0.500-0.640 m). The division proved to be necessary, since the program could not respect all the constraints respectively below the diameter of 0.640 m in the first case and above 0.660 m in the second, becoming unable to reach convergence. Moreover, in the case of the highest inlet mean diameters the program converged on very different designs, thus giving an irregular correlation between the input parameters and the output. However, this fact was verified only for very high values, hence outside of the interval of interest, defined by the need to match the LPT inlet with the low HPT exit diameter (about 0.4 m). The study therefore concentrated in the region of inlet diameters between 0.50 and 0.64 m.

As shown in *Figure 4.3*, the turbine inlet diameter needs to be sufficiently high to have acceptable first stage efficiency. It can be observed that the efficiencies of the downstream stages are increasingly higher, because of the larger mean diameters related with the rising mean line profile. The first stage efficiency resulted therefore the main driver for the inlet diameter choice. A value of 0.64 m was chosen as a trade-off between efficiency and matching with the HPT and was used for the successive sections of the study.

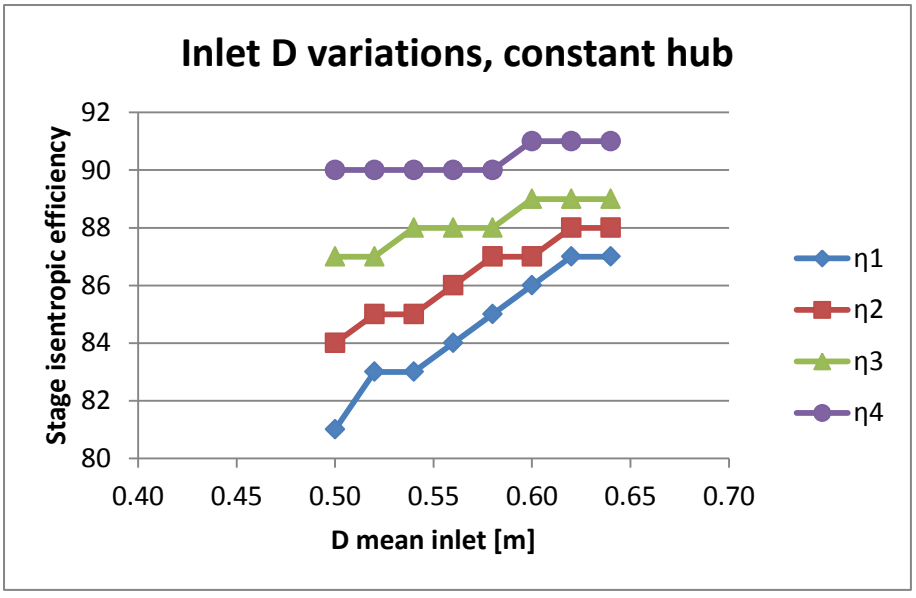

Figure 4.3 - Effect of inlet diameter variations on stage efficiencies

Once fixed the turbine inlet diameter and obtained the starting design, the remaining stage diameters were increased in order to take the maximum advantage from high blade tangential speeds. The results in terms of hub acceleration, exit swirl, stage efficiencies and reduction in blade height positively confirmed the concept of increasing as rapidly as possible the stage diameter through the turbine, thus leading to the definition of the annulus profile: this should be characterized by a steep rising mean line in the early stages, followed by a constant tip design imposed by the tip speed constraint.

Figure 4.4 shows the benefits of stage mean line diameter increase on the turbine exit swirl and on the maximum blade height. The complete results are reported in Appendix B.2.

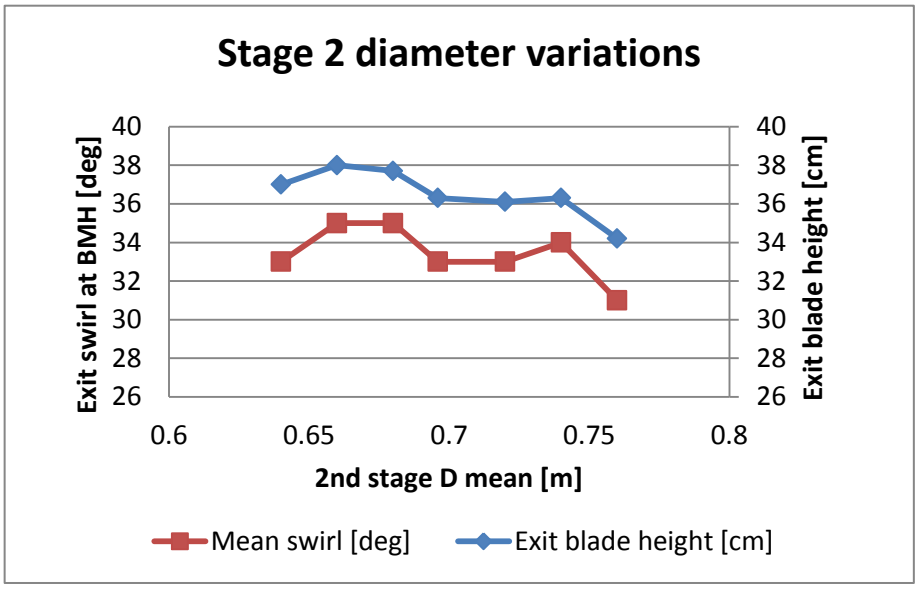

Figure 4.4 - Effect of stage mean diameter variation on blade height and exit swirl

4.4.5 Inlet Mach number Variations

This part of the parametric study evaluated the effect of changes in inlet Mach number on the turbine layout, with particular attention to the exit blade height and rotor hub acceleration. High axial Mach numbers correspond in fact to high axial velocities, implying from the principle of conservation of mass ($W = \rho A v$) low flow

areas, once the mass flow and density have been fixed. The benefit of having high Mach numbers in the last stage is a reduction in blade height, which results to decrease as the flow area is reduced. However, the friction losses increase with the flow velocity, hence reducing the stage efficiency, and the LPT inlet Mach number should be kept as low as possible to avoid excessive losses in the upstream s-duct [29]. A trade-off between containment of the blade height and high Mach number disadvantages needed therefore to be reached. As a limit, the maximum acceptable axial exit Mach number was set to 0.5, according with the indications from Ref. [15].

Although the relevant effect was on the exit section of the turbine, the handle chosen for the parametric study was the inlet Mach number. In fact, variations in its value directly affected the exit Mach number. Moreover, the individual stage inlet Mach numbers could be modified only slightly without altering the matching between the rotor exit area and the downstream stator inlet area, because of the stage constant axial velocity design limitation of the program (see 3.3.4 – Program Limitations). Individual stage inlet Mach modifications may in fact lead the program to insert converging ducts between the stages, hence producing an unrealistic turbine design.

Starting from M=0.20, the LPT inlet Mach was progressively increased up to M=0.40, which yielded an LPT exit axial Mach exceeding the value of 0.50 and was therefore considered the upper Mach limit.

The study showed that for the lowest inlet Mach numbers the last stage rotor hub acceleration results very low, due to the low blade hub velocity consequent to a large exit annulus area. The blade height also resulted excessively high and the program could not respect the maximum tip diameter constraint to achieve convergence. As the inlet Mach was progressively augmented, the hub acceleration increased thanks to the larger diameter giving a higher blade velocity, while the blade height decreased and the maximum tip diameter reduced to more acceptable values. The calculated hub and mean exit swirls remained instead almost constant, with variations on the order of one degree except for the lowest and highest inlet Mach

numbers, where designs very different among them gave respectively lower and higher swirl values. The stage isentropic efficiencies remained almost unvaried, since the model adopted by the program did not take into account the correlation between flow velocity and friction losses.

The relevant results are shown in the following *Figure 4.5* and *Figure 4.6*, while the complete results are reported in Appendix B.3.

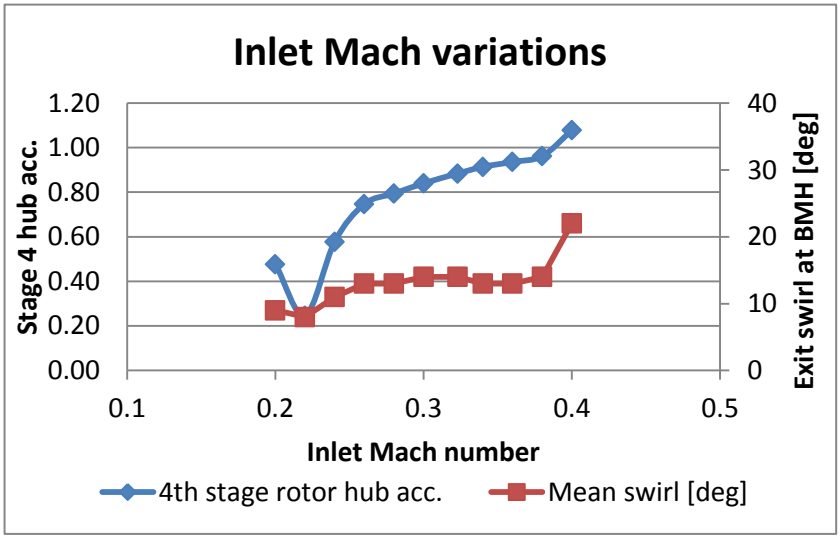

Figure 4.5 - Effect of inlet Mach variations on rotor hub acceleration and exit swirl

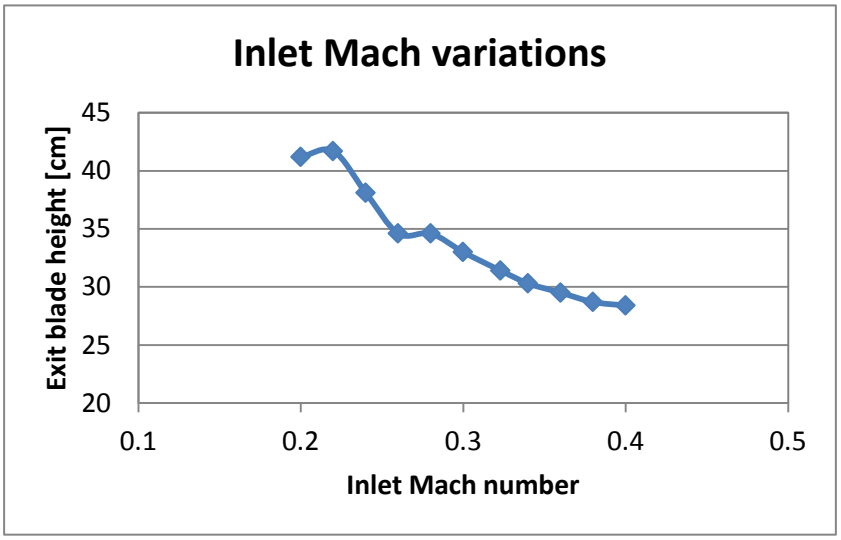

Figure 4.6 - Effect of inlet Mach on maximum blade height

The results obtained for the lowest and highest Mach number values presented a lack of continuity with the values comprised between M=0.26 and M=0.38. The reason for this trend was the impossibility of the program to converge on similar designs outside of this range. After an evaluation of the trends of the critical parameters, the final value chosen for the inlet Mach number was 0.32, which allowed obtaining an LPT exit blade height compatible with the current manufacturing technology and was lower than the maximum entry limit of 0.4, thus providing a margin for the containment of pressure losses.

4.4.6 Conclusions

The parametric study performed allowed understanding the changes in the relevant performance parameters according with the variations in the design input values. Through the development of the study, a design methodology could be established. The method consisted in varying individually the design parameters, evaluate their impact on the performance and geometry values (e.g. efficiencies, reactions, blade height, diameters) and then combine all the variations together to achieve the target design, capable of satisfying both the objectives and the given constraints.

A complete four-stage turbine design was performed, based on the design data and combining all the modifications that had been individually evaluated in the study. The result proved however to be still unacceptable, since the turbine obtained had too low stage efficiencies (<90%) in order to respect all the remaining constraints. The stage isentropic efficiencies obtained were in fact 88/90/92/89% respectively from the entry to the exit stage.

The results obtained from the four-stage parametric study led therefore to split the turbine work across an increased number of stages to achieve the target efficiencies. A five-stage design was consequently chosen. The methodology set in this study could then prove its validity, leading to a quick determination of the desired design in the five-stage case and in the successive IPT/LPT preliminary designs.

5 PRELIMINARY DESIGN RESULTS

5.1 Introduction

Following the methodology defined in the parametric study (Section 4.4), the desired designs for both the two and three-spool case were obtained. The designs were capable of achieving the target performance while respecting the given constraints (Sections 4.2 and 4.3).

The first part of this chapter presents the resulting turbine designs and specifications for the two engine configurations, while the second part analyses the differences between the two arrangements and the potential advantages of one configuration over the other.

5.2 Design Assumptions

The following results were obtained with the Preliminary Design Tool, hence taking advantage of its features. The design assumptions are those adopted in the PDT, recalled here:

- Constant axial velocity through the stage
- Constant axial velocity across the blade span
- Free-vortex hypothesis: $rv_\theta = const$
- Constant mass flow through the turbine (no sealing flows)
- γ constant through the turbine

Moreover, for all the turbines the inlet flow was assumed axial, hence $\alpha_{in} = 0$ degrees.

5.3 Two-Spool Engine: 5-Stage LPT

5.3.1 Specifications

The five-stage turbine design followed the methodology defined in the parametric study, hence vary individually the design parameters in order to evaluate their influence on the turbine performance and geometry, then combine them

together to achieve the target efficiencies and satisfy all the constraints. The process was in this case much faster, since the effects of their variations had already been determined. Moreover, the inlet Mach number and mean diameter adopted were the same obtained in the previous study, since they were the result of trade-offs independent from the number of stages. The number of iterations followed to obtain an acceptable design was therefore limited.

Table 5.1 recalls the inlet conditions at design point for the two-spool engine LP turbine:

Table 5.1 - 2-Spool Engine LPT Inlet Conditions	
Inlet Total Pressure	514.37 kPa
Inlet Total Temperature	1045 K
Inlet Mach Number	0.32
Mass Flow	36.83 kg/s

Consequently to the dedicated parametric study, the optimal temperature drop distribution determined in the five-stage case was an equal split across the stages. This approach minimized the last stage exit swirl compared to other distributions, while allowing for a high isentropic efficiency in all the stages.

The turbine specifications are presented in the following table:

Table 5.2 - 2-Spool Engine LPT Specifications	
No. of stages	5
Turbine Power [MW]	19.063
Rotational Speed [rpm]	7218
Overall Pressure Ratio	11.422
Overall Temperature Ratio	1.712
Temperature Drop [K]	436
Stage Temperature Drop [K]	87
Overall Isentropic Efficiency [%]	93.0
Stage Isentropic Efficiencies [%]	90 / 92 / 92 / 92 / 91

Stage Reactions	0.50 / 0.50 / 0.50 / 0.50 / 0.64
Inlet Mean Diameter [m]	0.640
Outlet Mean Diameter [m]	0.763
Max Tip Diameter [m]	1.085
Max Blade Height [cm]	32.1
Max Hub/Tip Ratio	0.84
Estimated Length [m]	0.471
Estimated Weight [kg]	485.2
γ	1.32

The turbine presents a relatively high temperature drop due to the requirement of driving both the fan and the IP compressor. The overall isentropic efficiency was calculated from the knowledge of the inlet and outlet total pressures, the inlet total temperature and the turbine temperature drop with the following equation:

$$\eta_{is} = \frac{\Delta T}{T_{in}\left[1 - \left(\frac{P_{out}}{P_{in}}\right)^{\frac{\gamma-1}{\gamma}}\right]} \qquad (5.1)$$

A discrepancy between the overall isentropic efficiency and the individual stage efficiencies was noticed. The reason for the difference should be in the methods adopted to determine the efficiencies: in the first case, the calculation relied on the analytical equation (5.1), while the individual stage efficiencies were determined from the empirical correlation used in the Preliminary Design Tool, based on the Smith chart (Eq. (3.1)).

The stage reactions were set to 0.50 in the first four stages, since this value proved to be the optimal. The reaction in the last stage was instead increased to 0.64, in order to have acceptable rotor hub acceleration.

The inlet mean diameter chosen allowed a good matching with the HPT exit mean diameter (about 0.40 m, from the studies previously made by the two PhD advisors), while maintaining a blade speed sufficiently high to give an acceptable first stage efficiency of 90%. The maximum tip diameter was obtained at the last stage exit

and resulted slightly higher than the limit, set at 1.03 m. The limitation had in fact to be relaxed to allow the program reaching convergence. The maximum blade height resulted about 2 cm above the typical LPT values, discussed in Section 4.3, while the maximum hub to tip ratio, obtained at the turbine inlet, respected the maximum limit of 0.9 (see Paragraph 4.4.4).

5.3.2 Geometry

According with the information obtained in the parametric study, the design of the annulus shape aimed at reaching rapidly a high stage diameter, in order to have high blade tangential speeds. The purpose was achieved through a steep rising mean line design in the first two stages, followed by a constant mean line in the third stage and a constant tip setting in the latter stages. As explained in the previous paragraph, the program had to relax the maximum tip diameter constraint to respect all the remaining settings; hence the last stage resulted to have an increasing tip diameter. The annulus diagram obtained with the PDT is reported in *Figure 5.1*.

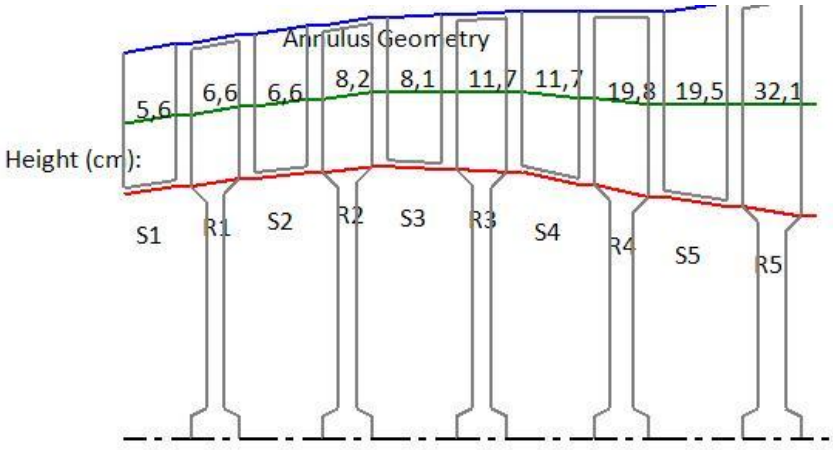

Figure 5.1 – LPT annulus diagram from PDT visualizer (not to scale)

The diagram produced by the program is not in scale. In fact, its purpose is limited to give quick indications on the blade heights and the mean line evolution. Another diagram was therefore created in a CAD Program (Autodesk® Inventor®) in order to visualize the turbine proportions, taking into account also the spacing across the stages and the actual axial chord lengths. The annulus diagram obtained is shown

in the following figures. The turbine is displayed with the same orientation it would have in the reverse-flow core engine, hence with the gas flowing frontwards.

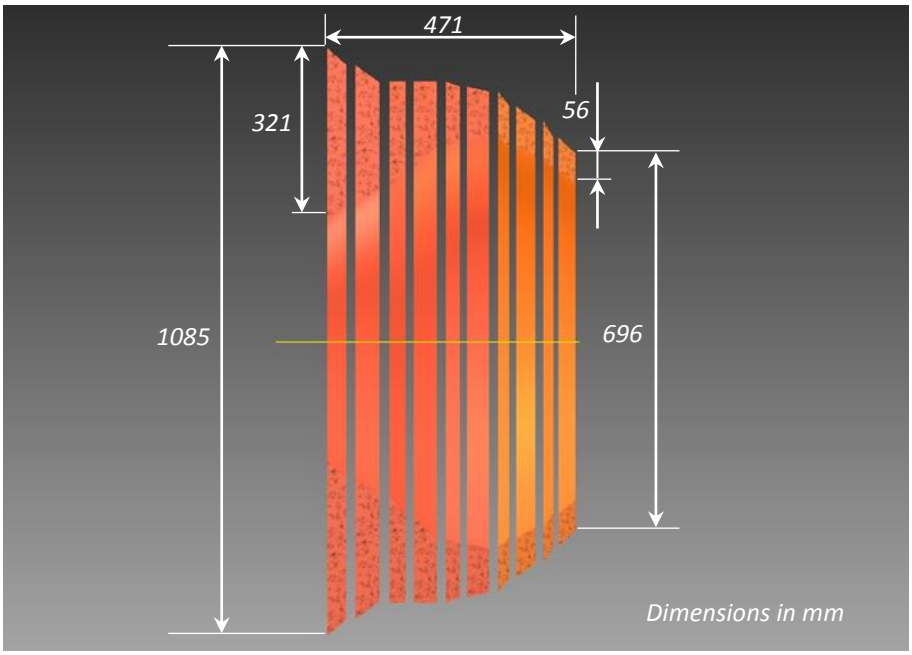

Figure 5.2 - LPT annulus section, side view (scale drawing)

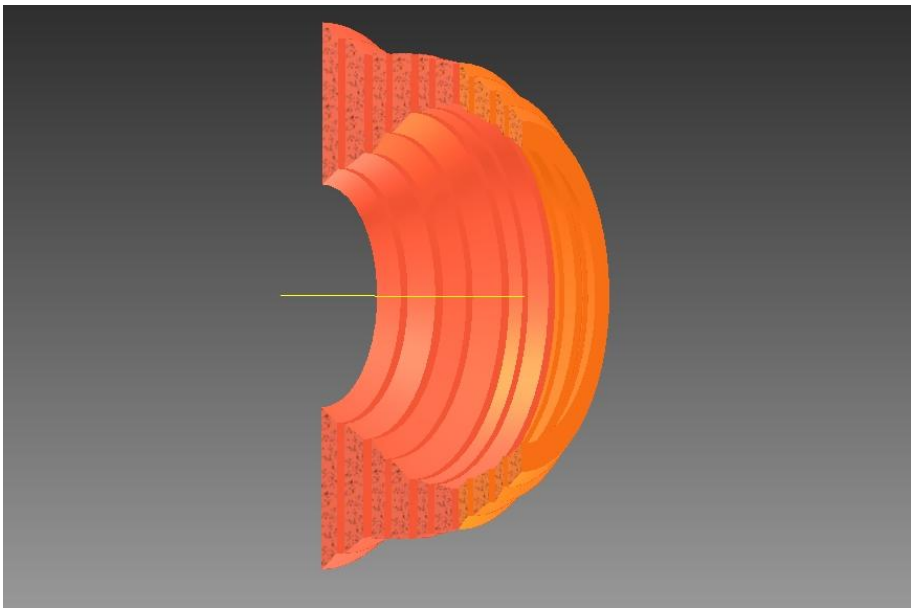

Figure 5.3 - LPT annulus section (scale drawing)

As shown in the annulus profile to scale, the last stage presents a large exit area and a steep increase in tip diameter. An increasing axial velocity for this stage would be beneficial to contain the turbine exit size. Although the turbine could respect all the performance parameters, the geometry results led in fact to successively improve the design with a more sophisticated design program, T-AXI. The results obtained with T-AXI will be presented in the following chapter.

The axial length of the stages was estimated from the knowledge of the blade height and blade aspect ratio, defined as the ratio between blade mean height and axial chord length at mid span. For the preliminary design the blades were assumed not tapered, hence the axial chord was constant across the span. The blade aspect ratio was estimated once determined the blade hub and tip diameters with the following correlations for LP turbines from Ref. [19]:

LPT stator:
$$AR = 10.95 - 10.9\frac{D_{hub}}{D_{tip}} \tag{5.2}$$

LPT rotor:
$$AR = 13.36 - 11.78\frac{D_{hub}}{D_{tip}} \tag{5.3}$$

From the definition of aspect ratio, the axial chord length was therefore determined:

$$C_a = \frac{h}{AR} \tag{5.4}$$

The stator-rotor and inter-stage spacing were determined following the indications in Ref. [20], which reported as typical stator-rotor gap and inter-stage gap respectively the 40% and 50% of the average axial chord lengths between the adjacent blade rows.

Table 5.3 and ***Table 5.4*** summarize the geometry of each turbine stage.

Table 5.3 - LPT Stage Radial Geometry Results

Stage inlet	Hub diameter [m]	Mean diameter [m]	Tip diameter [m]	Rotor blade mean height [cm]
1	0.584	0.640	0.696	6.4
2	0.685	0.751	0.817	7.8
3	0.763	0.844	0.924	10.8
4	0.727	0.844	0.961	17.8
5	0.568	0.763	0.958	29.0
Outlet	0.442	0.763	1.085	32.1

Table 5.4 - LPT Stage Axial Geometry Results

Stage	Stator axial chord length [cm]	Rotor axial chord length [cm]	Stator-rotor gap [cm]	Inter-stage gap [cm]
1	3.2	1.8	1.0	1.4
2	3.7	2.1	1.2	1.6
3	4.1	2.5	1.3	1.7
4	4.3	3.0	1.5	1.9
5	4.5	4.7	1.8	-

All the rotor aspect ratios resulted below the limit of 6 set in Sagerser, except for the last stage rotor which had from the correlation the value of 8.10. For calculated ARs exceeding the limit, the reference recommends to set the value to 6.0. A further investigation was however conducted to establish the state of the art values, in order to achieve a turbine weight and length reduction. According with the studies on future aero engine designs presented in Ref. [27], the LPT exit aspect ratio can be calculated with the following expression:

$$AR_{LPT,exit} = -36.10 + 0.0209 \cdot EIS \qquad (5.5)$$

where EIS is the engine expected entry into service year. For an EIS in 2020, the correlation gave an aspect ratio of 6.118, which was therefore chosen for the last stage rotor.

5.3.3 Velocity Triangles

The stage velocity triangles were determined using the in-built code and visualizer of the Preliminary Design Tool. The results for the entry and exit stage are reported below.

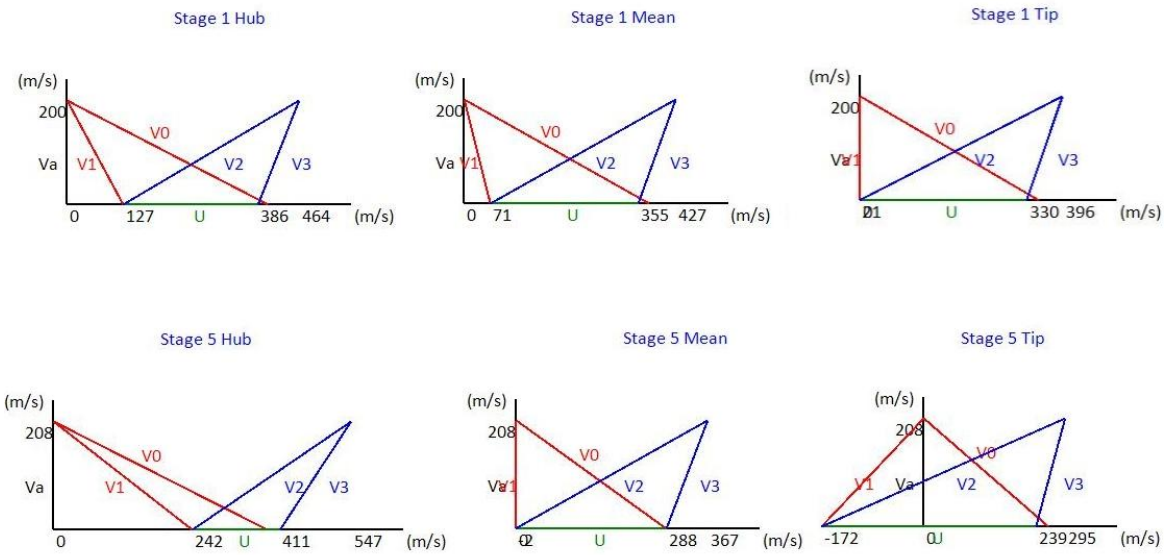

Figure 5.4 - Turbine inlet and outlet velocity triangles

It can be observed that the last stage blade speed at the hub is relatively low compared with the value at mean height, hence implying low rotor hub acceleration and a low value of reaction. The two values resulted in fact 1.15 and 0.18 respectively.

The complete results and velocity triangles data are reported in Appendix C.

5.3.4 Mass Estimation

The turbine mass estimation was based on the empirical correlation for cruise engines given by Ref. [19]:

$$WT = 7.9\ \overline{D}_M{}^{2.5} N_T \overline{U}_M{}^{0.6} \qquad (5.6)$$

Where $\overline{D}_M$ is the average of the mean inlet and outlet diameters, N_T the number of stages and $\overline{U}_M$ the average of the inlet and outlet mean blade speeds. The

correlation allowed taking into account the rotor discs, the rotor and stator blades, the seals and the casing.

The estimated mass resulted of 485.2 kg. The turbine is expected to have discs heavier than its conventional, ungeared equivalents, due to a high blade speed combined with high stage diameters. However, this disadvantage will be overweighed by the reduction in stage and blade count due to the higher efficiency [8]. Consequently to the high blade speed, the casing will result heavy as well to contain a possible blade-off, as explained in Section 2.3.

Further investigations were conducted with T-AXI in order to determine more precisely the blading and disc weights. The results obtained with this tool will be presented in the next chapter.

5.3.5 Blade Count Estimation

The estimation of the number of blades was made according with the expressions reported in Ref. [20], based on the Zweifel's loading coefficient method.

The Zweifel's loading coefficient is defined as follows:

Rotor:
$$\Psi_{Z,r} = \frac{2}{\sigma}\cos^2\alpha_2(\tan\alpha_1 - \tan\alpha_2) \tag{5.7}$$

Stator:
$$\Psi_{Z,s} = \frac{2}{\sigma}\cos^2\alpha_0(\tan\alpha_{in} - \tan\alpha_0) \tag{5.8}$$

The optimum value for Ψ_Z corresponds to the optimal spacing between the blades, minimizing the pressure loss due to flow separation and skin friction. According with the reference, the optimum Ψ_Z chosen was 0.8.

Once the Zweifel number had been fixed and the flow angles determined, the cascade solidity ratio σ was obtained from the previous equations. The solidity is defined as the ratio between the axial chord at mean line and the cascade spacing at mean line:

$$\sigma = \frac{C_a}{S_m} \tag{5.9}$$

Therefore, once estimated σ and knowing each cascade solidity, the spacing S_m could be calculated. From the knowledge of each cascade mean diameter, the blade count was then determined:

$$N_b = \frac{\pi D_m}{S_m} \tag{5.10}$$

The blade count results are presented in the following table.

Table 5.5 - 2-Spool Engine LPT Blade Count

Stage	Stator N_b	Rotor N_b	Stator σ	Rotor σ
1	73	160	1.104	1.274
2	89	139	1.345	1.159
3	78	121	1.210	1.148
4	70	101	1.148	1.220
5	69	71	1.280	1.060

From the calculations, the rotor blade number proved to be higher than the stator, particularly in the first stages. The result has to be addressed to the reduced rotor axial chord due to the higher aspect ratio, which yielded from Eq. (5.9) lower blade spacing.

5.3.6 Performance Parameters

The presented design was capable of respecting most of the limitations set in order to have acceptable turbine designs, while few limitations were slightly exceeded. The recommended values for the performance parameters limitations were obtained from the Ref. [15], except for the turbine exit swirl typical range which was obtained from Ref. [30].

The relevant results are presented in the following table.

Table 5.6 - Performance and Design Parameters

	Stage 1	Stage 5	Recommended
Stage loading coeff. $\Delta H/U^2$	1.50	1.24	< 3
Stage flow coeff. V_a/U	0.76	0.72	0.4 – 0.8
Tip speed at DP [m/s]	286.0	410.1	< 430
Tip speed at max rpm [m/s]	341.9	454.0	< 430
Min rotor hub acceleration	-	1.152	≥ 1.15
Min NGV tip acceleration	-	1.433	≥ 1.15
Turbine exit swirl at BMH [deg]	-	21	< 40, lowest possible
NGV max gas deflection [deg]	61 (hub)	73 (hub)	< 130
Rotor max gas deflection [deg]	92 (hub)	105 (hub)	< 130
Max NGV exit angle [deg]	61 (hub)	64 (hub)	≤ 72
Rotor axial exit Mach	0.33	0.44	< 0.5
NGV hub/tip ratio	0.84	0.59	< 0.9
Rotor hub/tip ratio	0.84	0.41	< 0.9
AN^2 at design point [$rpm^2\ m^2$]	$8.2 \cdot 10^6$	$40.2 \cdot 10^6$	$20 – 50 \cdot 10^6$

From the design calculations, the decision to split the turbine work into five stages instead of four resulted in a very low stage loading coefficient, largely respecting the limitation of a maximum value of 3. This implied a high stage efficiency, but with the disadvantage of an additional stage. Considering that the PDT tends to underestimate the stage efficiency, up to 4% as demonstrated in the P&W LPT validation section of Ref. [21], the choice of a five-stage turbine may result conservative once accurate efficiency calculations are made. Since the LPT is developed for an aero engine, the option of reducing the number of stages to four should be further investigated. Detailed calculations on the five-stage turbine design were performed with T-AXI in order to set the investigation; the related results are presented in the following chapter. The flow coefficients are instead in the range of the low pressure turbines, according with the Smith chart reported in [15].

As it can be observed in *Table 5.6*, the maximum blade tip speed respects the maximum limitation of 430 m/s at design point. However, if calculated for the

maximum turbine rotational speed, its value exceeds the limit by 24 m/s, hence by 5.6%. Although the latter is an off-design condition, a deeper analysis on the blade capability to withstand the increased mechanical load should be carried out.

The rotor hub acceleration was one of the most critical parameters in respecting the recommended value range ($V_2/V_1 \geq 1.15$). The reasons were the relatively low last stage rotor hub tangential speed, due to the low hub diameter, and the turbine operative condition, with a relatively low inlet pressure at design point. The final design presented in the results above respects the mentioned requirement.

The turbine exit swirl at blade mean height resulted within the typical range, although relatively high. The exit swirl represents in fact angular momentum of the flow which is not converted by the rotor into mechanical work, hence meaning a component of the flow energy which is lost [20]. Its value should be therefore reduced to the minimum possible value, indicatively below 10 degrees. The existence of a non-zero exit swirl also implies the need for turbine outlet guide vanes to redirect the flow axially through the engine exit.

The gas deflections both in the NGV and in the rotor largely respected the limitation of 130 degrees, consistently with the low stage loading coefficient: the low stage loading implied a limited flow turning; hence a potential margin for increased work extraction from the stages is still present.

The turbine exit axial Mach number was consistent with the choice made in the parametric study (Paragraph 4.4.5). The value resulted in fact below the limit of 0.5, although still giving a contained exit annulus area and therefore a limited blade height.

From the results presented in *Table 5.6*, the hub to tip ratios were acceptable for both the stator and the rotor. A further reduction in the first stage value would be however beneficial to contain the overtip leakage loss. This could be achieved either by reducing the inlet diameter or by reducing the inlet Mach number. The first choice would allow for an improved matching with the HPT exit, while the latter would imply an increasing axial velocity design to maintain the exit Mach number unvaried.

Finally, the blade centrifugal stress coefficient AN^2 resulted within the acceptable range, having a maximum value of $40.2 \cdot 10^6$, hence providing a feasible blade mechanical design.

5.4 Three-Spool Engine: 3-Stage IPT

5.4.1 Specifications

A work split between an intermediate pressure turbine driving the fan and a low pressure turbine driving the IP compressor represented the three-spool alternative to a two-spool engine configuration. The three-spool engine presents a geared, fast-rotating IP turbine, while the LP turbine is ungeared. The proposed turbine layout within the engine is shown in *Figure 5.5*.

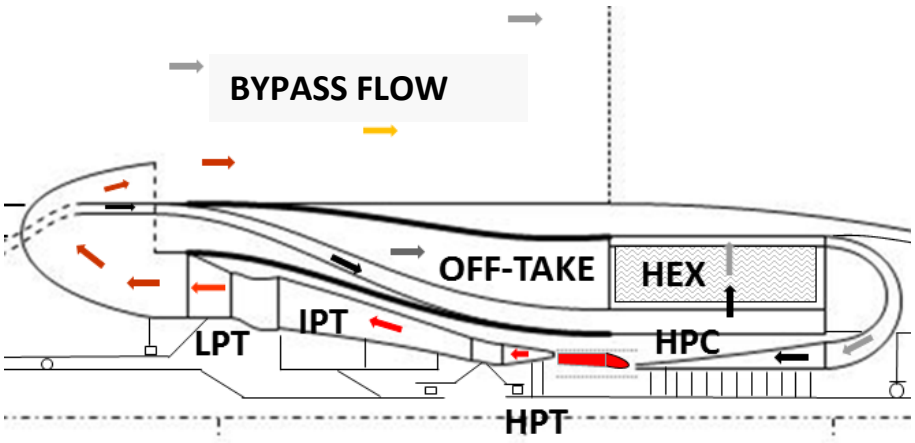

Figure 5.5 - 3-spool engine turbine arrangement (courtesy of E. Anselmi Palma)

The design process of the IP turbine followed the method set in the parametric study (Section 4.4): the design parameters were varied in order to evaluate the trends of the critical parameters, thus producing the desired configuration.

Table 5.7 reports the inlet conditions at design point for the three-spool engine IP turbine:

Table 5.7 - 3-Spool Engine IPT Inlet Conditions	
Inlet Total Pressure	676.10 kPa
Inlet Total Temperature	1129 K
Inlet Mach Number	0.24
Mass Flow	33.58 kg/s

The inlet Mach number was chosen consequently to the parametric study, as an opportunity for its reduction without affecting the LPT exit Mach was observed. The axial Mach reduction provided for a potential containment of the pressure losses due to skin-friction both in the s-duct connection with the HPT and within the LP turbine.

The temperature drop distribution was determined in the parametric study. In this case the distribution choice led to an increase of the work extraction in the last stage and a reduction in the first, realized through a variation in temperature drop of respectively +6 K and -6 K in these two stages. This allowed reducing the first stage loading coefficient, thus increasing its efficiency from the 89% of an equal temperature distribution to 90%. On the other hand, the third stage mean diameter was increased to maintain the same value of $\Delta H/U^2$, hence preserve its efficiency.

The turbine specifications are presented in *Table 5.8*:

Table 5.8 - 3-Spool Engine IPT Specifications	
No. of stages	3
Turbine Power [MW]	13.703
Rotational Speed [rpm]	9022
Overall Pressure Ratio	5.366
Overall Temperature Ratio	1.440
Temperature Drop [K]	346
Stage Temperature Drop [K]	109 / 115 / 121
Overall Isentropic Efficiency [%]	91.3
Stage Isentropic Efficiencies [%]	90 / 90 / 90
Stage Reactions	0.50 / 0.50 / 0.46
Inlet Mean Diameter [m]	0.580
Outlet Mean Diameter [m]	0.707

Max Tip Diameter [m]	0.881
Max Blade Height [cm]	17.4
Max Hub/Tip Ratio	0.82
Estimated Length [m]	0.224
Estimated Weight [kg]	249.6
γ	1.32

The turbine rotates at a higher speed than the corresponding LPT for the two-spool case, having a rotational speed about 1800 rpm higher. This allowed for a reduction in stage diameter without excessively reducing the blade tangential speed. The realization of a more compact turbine was therefore possible.

The turbine temperature drop proved to be a large fraction of the overall IPT-LPT assembly, about 70% of the total value, consistently with the large portion of work required by the fan (see 4.1.2 – Power Requirements). As in the 2-spool case, the calculated isentropic efficiency resulted higher than the stage efficiency estimations made by the program. In this case the difference was however less marked, 91.3% against an efficiency value of 90% in each stage. The reactions were maintained at 0.50 in the first two stages, while in the third a reduction to 0.46 proved beneficial to reduce the exit swirl.

Taking advantage from the increased rotational speed, the inlet mean diameter was reduced relatively to the two-spool case, in order to obtain a compact turbine design. This design choice allowed for a better matching with the HPT exit diameter (0.4 m at BMH, from the preliminary work conducted by the two PhD advisors). The outlet mean diameter was instead set to the same value of the downstream LPT inlet, in order to have a straight duct for the connection between the two components. The design of the LPT for the 3-spool engine will be presented in Section 5.5.

The maximum tip diameter allowed for an acceptable tip speed at design point. However, as in the 2-spool engine case, the off-design operation of the turbine exceeded the limitation of 430 m/s. The values obtained are reported in the following

Performance Parameters section (5.4.6). Both the blade height and maximum hub to tip ratio resulted instead well within the reference limits.

5.4.2 Geometry

As in the 2-spool engine case, the annulus design aimed at a low inlet mean diameter, with a rapid increase in stage diameter to take the maximum advantage from high blade tangential speeds. In the IPT case however there was a constraint on the exit blade height and mean diameter, given by the need to match the downstream LPT inlet. The objective was to obtain a straight connection duct with parallel walls, since this would imply minimizing the pressure losses and the turbine length. The latter would result in fact increased to allow for the flow curvature in the case of an s-duct, as well as the pressure losses would be higher due to the longer flow path and the more complex flow conditions [20]. In order to achieve the goal of a straight connection duct, the turbine outlet Mach number was controlled as well through variations in the inlet value, thus giving at the IPT exit the same annulus area of the LPT inlet.

The annulus diagram obtained with the PDT is reported in *Figure 5.6*.

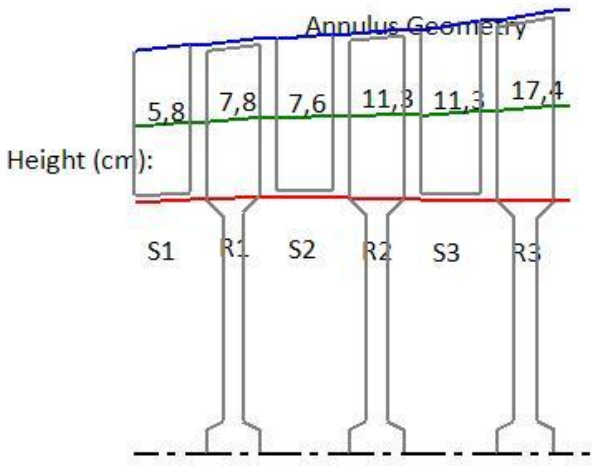

Figure 5.6 – IPT annulus diagram from PDT visualizer (not to scale)

In order to better visualize the turbine layout, a corresponding annulus diagram to scale was then realized; it is reported in *Figure 5.7* and *Figure 5.8*. The turbine is represented in this case with the orientation it would have in the engine, hence with the gas flowing frontwards.

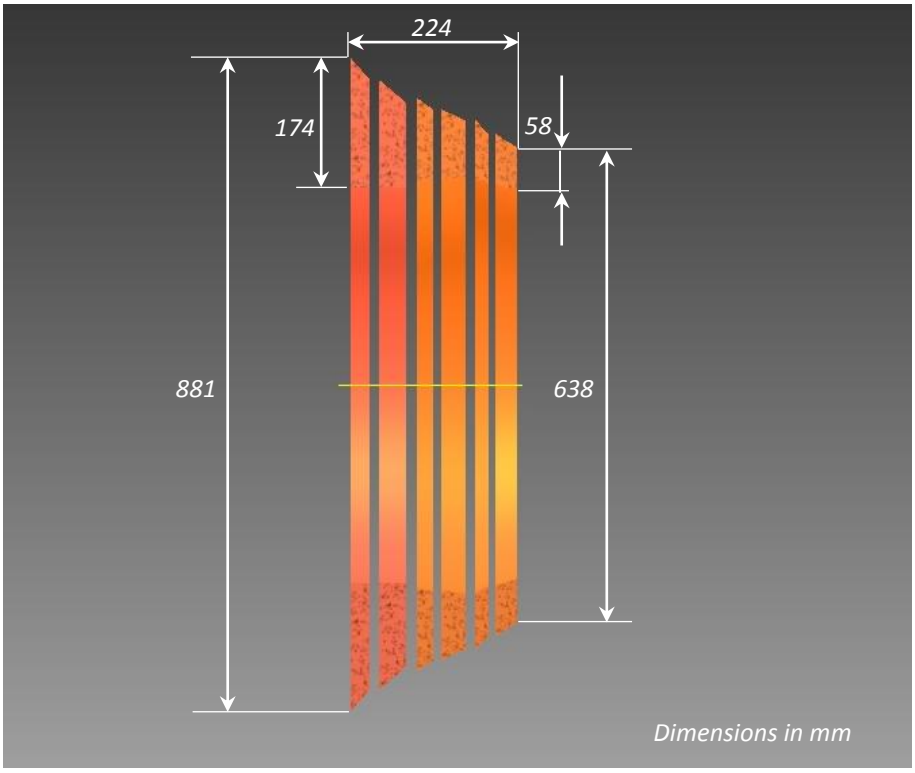

Figure 5.7 - IPT annulus section, side view (scale drawing)

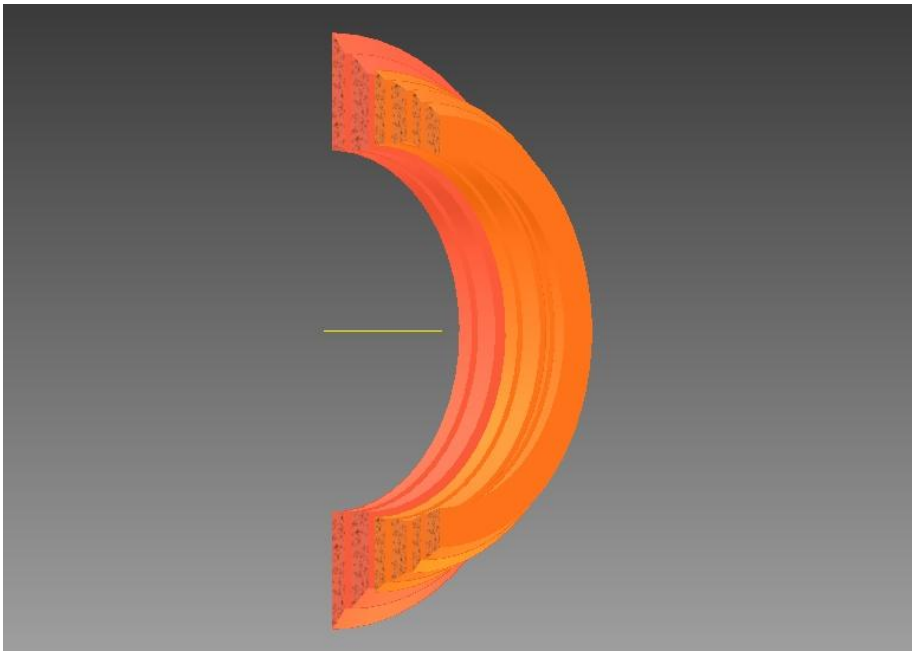

Figure 5.8 - IPT annulus section (scale drawing)

As it can be observed from the diagram, the turbine presents a rising mean line in all the stages, although the hub diameter slightly decreases in the second and third stage. The cascade axial lengths were estimated with the same correlations used for the LP turbine of the 2-spool engine case (Paragraph 5.3.2), hence with Equations (5.2) and (5.3) for the stator and rotor aspect ratios. Although different coefficients are proposed in reference [19] for IP turbines, the equations adopted were based on the correlation given for the LPT. The choice was based on the reason that the IPT stages actually exploit the function previously made by part of the LPT. This choice led to higher aspect ratios, thus reducing the turbine length.

The stage geometry obtained for the IPT is presented in the following tables:

Table 5.9 - IPT Stage Radial Geometry Results

Stage inlet	Hub diameter [m]	Mean diameter [m]	Tip diameter [m]	Rotor blade mean height [cm]
1	0.522	0.580	0.638	7.3
2	0.561	0.637	0.712	10.3
3	0.533	0.646	0.759	15.9
Outlet	0.533	0.707	0.881	17.4

Table 5.10 - IPT Stage Axial Geometry Results

Stage	Stator axial chord length [cm]	Rotor axial chord length [cm]	Stator-rotor gap [cm]	Inter-stage gap [cm]
1	2.9	1.8	1.0	1.3
2	3.3	2.2	1.1	1.4
3	3.6	2.7	1.3	-

5.4.3 Velocity Triangles

The stage velocity triangles were produced with the PDT in-built code and visualizer. The results for the entry and exit stage are presented in *Figure 5.9*.

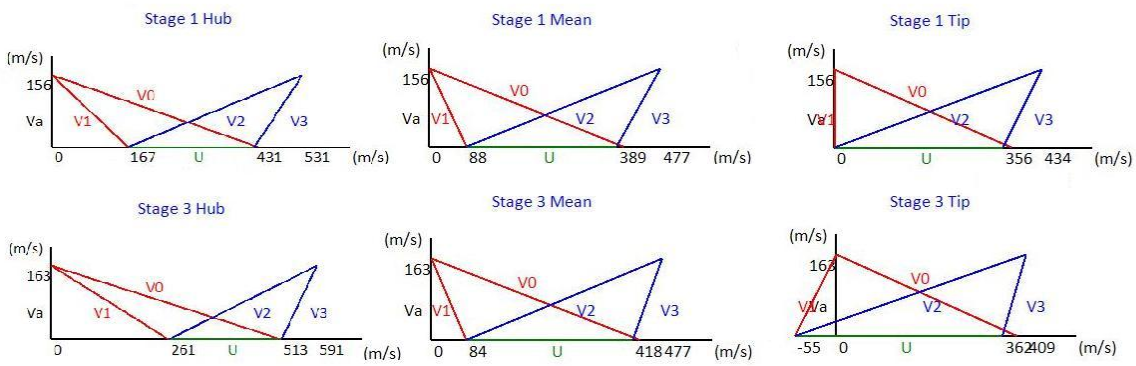

Figure 5.9 - Turbine inlet and outlet velocity triangles

The complete results and velocity triangles data are reported in C.2.

5.4.4 Mass Estimation

As for the 2-spool engine case, the turbine mass was calculated following the empirical expression for cruise engines (5.6), based on the inlet and outlet mean diameters and blade speeds. The result was a mass of 249.6 kg, accounting for the stator and rotor blade rows, rotor discs, seals and casing.

Compared with the two-spool engine LP turbine, the IPT had an inlet mean diameter 6 cm lower, while the blade speed at mean height in the first stage was 17 m/s higher. From equation (5.6), the estimated turbine mass is more sensitive to diameter than blade speed variations, since the first variable has an exponent of 2.5 and the latter of 0.6. In fact, although the blade speed had been increased, the lower inlet diameter proved to be beneficial for the weight of the IPT-LPT assembly, allowing for a reduction of about 26 kg compared with the two-spool LPT. The comparison of the differences between the two configurations is reported in Section 5.6.

5.4.5 Blade Count Estimation

The blade count estimation was based on the Zweifel coefficient's method, as in the 2-spool engine case (Paragraph 5.3.5). The results for the rotor and the stator, with the related blade row solidities, are reported in the following table:

Table 5.11 - 3-Spool Engine IPT Blade Count

Stage	Stator N_b	Rotor N_b	Stator σ	Rotor σ
1	57	116	0.899	1.063
2	69	103	1.111	1.077
3	60	89	1.032	1.094

Due to the rotor aspect ratio higher than the stator which implied a lower chord length, the spacing between the rotor blades resulted lower than the stator. Therefore the higher rotor blade count is justified.

5.4.6 Performance Parameters

The design obtained with the Preliminary Design Tool respected all the set objectives and constraints reported in Sections 4.2 and 4.3. Moreover, it was capable of matching the IPT exit with the LPT inlet, thus yielding the same annulus area and the same blade hub and tip radii. The relevant results and recommended values are presented in *Table 5.12*. As for the two-spool case, the recommended values refer to Ref. [15] and Ref. [30].

Table 5.12 - Performance and Design Parameters

	Stage 1	Stage 3	Recommended
Stage loading coeff. $\Delta H/U^2$	1.57	1.41	< 3
Stage flow coeff. V_a/U	0.54	0.51	0.4 – 0.8
Tip speed at DP [m/s]	337.3	416.2	< 430
Tip speed at max rpm [m/s]	374.7	462.4	< 430
Min rotor hub acceleration	1.195 (*stage 3*)		≥ 1.15
Min NGV tip acceleration	1.958 (*stage 2*)		≥ 1.15

Turbine exit swirl at BMH [deg]	-	20	< 40, lowest possible
NGV max gas deflection [deg]	70 (hub)	102 (hub)	< 130
Rotor max gas deflection [deg]	114 (hub)	122 (hub)	< 130
Max NGV exit angle [deg]	70 (hub)	72 (hub)	≤ 72
Rotor axial exit Mach	0.25	0.30	< 0.5
NGV hub/tip ratio	0.82	0.70	< 0.9
Rotor hub/tip ratio	0.78	0.60	< 0.9
AN^2 at design point [rpm^2 m^2]	$12.6 \cdot 10^6$	$31.5 \cdot 10^6$	$20 – 50 \cdot 10^6$

Evaluating the performance parameter results, the stage loading coefficients are well below the design limitation of 3, thus allowing for reaching the target isentropic efficiency of 90% in all the stages. Due to the tendency of the program to underestimate the stage isentropic efficiency, an increase in $\Delta H/U^2$ would be probably possible while maintaining the actual value above the goal limit. Further investigations on this aspect should therefore be conducted. The flow coefficients resulted as well within the design range. Their value was lower than that of the 2-spool engine LPT, falling in the range 0.5-0.6 instead of 0.7-0.8. This result was due to the combination of lower axial velocity and increased blade tangential speed. The effects were lower Mach numbers, increased flow turnings and larger annulus areas than the corresponding 2-spool LPT stages, leading to reduced blade count and chord lengths [15].

The maximum tip speed resulted below the recommended limit of 430 m/s at design point, while at the maximum rotational speed it reached the value of 462.4 m/s, hence exceeding the limit by 7.5%. Although the latter operative condition should last for a short time interval during the engine operation (e.g. at take-off), the turbine mechanical resistance capability in this condition should be further analysed.

Both the rotor hub and stator tip accelerations resulted above the minimum recommended value, as well as the exit swirl remained within the acceptable range. The latter value can be however reduced from the current 20 degrees by increasing the exit axial velocity or reducing the last stage reaction, in order to reduce the

component of the flow energy which is lost. The proposed design provides for outlet guide vanes downstream of the IPT, directing axially the flow in order to maintain for the LPT the same inlet angle condition independently from the operative point of the engine.

The gas deflections and NGV exit angles resulted higher than in the 2-spool LPT stages, according with the increased flow turning consequent to the lower axial velocity. The recommended limits were however respected.

The axial Mach was largely below the limit of 0.5, having a maximum value of 0.3 at the turbine exit. This implies a containment of the pressure loss related with the flow-blade friction, since its value increases with the gas velocity [15]. The hub to tip ratios resulted as well below the limitation both for the NGVs and the stators.

Finally, from the mechanical resistance point of view, the values of AN^2 resulted below the maximum limit of $50 \cdot 10^6$ rpm^2 m^2, thus indicating acceptable blade mechanical stress values.

5.5 Three-Spool Engine: 2-Stage LPT

5.5.1 Specifications

The LP turbine in the three-spool LEMCOTEC engine is designed to directly drive the IP compressor. Since the power requirement of the IPC is only the 30% of the global fan-IPC power (see Section 4.1.2), a two-stage LPT configuration resulted capable of satisfying the design requirements.

The ungeared configuration of the two-stage LPT represents the main difference with the turbines previously presented, although its rotational speed of about 7000 rpm makes it still comparable with the previous cases. The design considerations will therefore be the same of the fast-rotating LPTs presented in Section 2.3, such as the need for tapered rotor blades and heavy discs.

The preliminary design process followed the same procedure used for the turbines previously reported, hence evaluate the effect on performance and geometry

of individual design parameters modifications, then combine them together to obtain a design capable of achieving the set target efficiency and respecting the constraints.

The turbine inlet conditions adopted in the preliminary design are reported in *Table 5.13*. Since the priority in the preliminary design of the three-spool engine turbines had been given to the comparison of the exit diameters and swirl with the five-stage LPT, the 3-spool engine LPT was designed before the IPT. The inlet values for total pressure and total temperature were therefore obtained from the engine performance simulation results [18]. As it resulted from the successive IPT design, the Preliminary Design Tool estimated isentropic efficiency was lower than the value assumed in the performance simulation (91.4% against 93% of the latter), thus giving as output a lower IPT exit total pressure, 126.1 kPa against 131.7 kPa.

Table 5.13 - 3-Spool Engine LPT Inlet Conditions

Inlet Total Pressure	131.79 kPa
Inlet Total Temperature	772 K
Inlet Mach Number	0.30
Mass Flow	34.77 kg/s

Considering the inlet conditions reported in *Table 5.13*, the mass flow at the LPT entry is about 1 kg/s higher than the value used for the IPT, since it accounts for the addition of sealing flows in the IPT [18]. For this reason, the performance simulation yielded an IPT exit total temperature lower than the PDT results, 772 K against the 784 K of the latter. The inlet Mach number of 0.30 was chosen after the results of the related parametric study, since it proved to allow for acceptable blade heights while keeping a low turbine exit axial Mach value (0.33 against the limit of 0.50), thus providing the margin for the containment of pressure losses downstream of the turbine.

The temperature drop distribution was chosen after an evaluation of the results obtained in the related parametric study: the outcome was an equal temperature drop across the two stages, giving a good compromise between acceptable rotor hub acceleration and turbine exit swirl.

The turbine specifications are presented in the following table:

Table 5.14 - 3-Spool Engine LPT Specifications	
No. of stages	2
Turbine Power [MW]	6.112
Rotational Speed [rpm]	7049
Overall Pressure Ratio	2.631
Overall Temperature Ratio	1.237
Temperature Drop [K]	148
Stage Temperature Drop [K]	74 / 74
Overall Isentropic Efficiency [%]	91.4
Stage Isentropic Efficiencies [%]	91 / 92
Stage Reactions	0.56 / 0.58
Inlet Mean Diameter [m]	0.700
Outlet Mean Diameter [m]	0.757
Max Tip Diameter [m]	1.103
Max Blade Height [cm]	34.7
Max Hub/Tip Ratio	0.60
Estimated Length [m]	0.224
Estimated Weight [kg]	209.9
γ	1.32

As it can be observed in *Table 5.14*, the turbine required power output of 6.112 MW is less than 50% of the IPT power output (13.703 MW), according with the fact that the largest part of the work of the IPT-LPT assembly is absorbed by the fan. For this reason, the LP turbine temperature drop resulted much lower than the IPT, 148 K against 346 K.

In this case, the overall isentropic efficiency resulted comparable with the stage efficiencies, 91.4% against 91 and 92% respectively in the entry and exit stage. The reactions at blade mean height were set respectively to 0.56 and 0.58 in the first and second stage in order to achieve acceptable rotor hub accelerations.

The inlet mean diameter was set to 0.70 m; this allowed obtaining a maximum tip diameter of 1.10 m at the turbine outlet. The latter value was slightly higher than the 2-spool engine LPT (1.08 m), but the lower rotational speed compensated this variation, thus allowing for a slightly lower tip speed at design point (407 m/s against the 410 m/s of the 2-spool case). This aspect will be analysed in the Performance Parameters section (5.5.6). The exit blade height resulted as well about 2 cm higher than the 2-spool case, but it was still compatible with the acceptable manufacturing limitations (see Section 4.3 – Constraints). The maximum hub to tip ratio respected as well the limit of 0.9, thus avoiding excessive tip clearance to blade height ratios.

5.5.2 Geometry

One of the main challenges in the design of the LPT was the respect of the maximum tip speed constraint of 430 m/s through the containment of the turbine maximum diameter. The design of the annulus took therefore into account mainly this aspect, considering also that, once fixed the exit annulus area, the reductions in tip diameter would have been limited by excessive blade heights (namely above 35 cm). The geometry which produced the best results in terms of containment of the exit diameter and low blade height was a constant hub diameter for the first stage, followed by a constant mean diameter in the second stage. The large annulus exit area did not allow the program to respect the maximum tip diameter constraint set to 1.03 m; therefore, the stage mean diameters had to be modified manually in order to reduce the maximum turbine diameter as close as possible to the mentioned limit.

The annulus diagram obtained with the Preliminary Design Tool is reported in *Figure 5.10*:

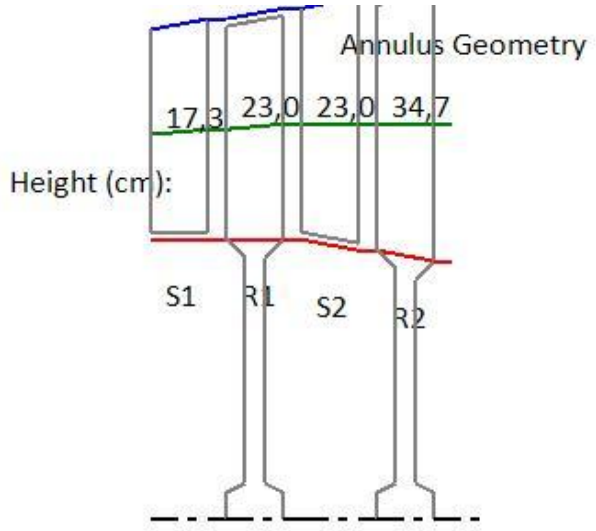

Figure 5.10 – LPT annulus diagram from PDT visualizer (not to scale)

In order to better visualize the turbine proportions, a second annulus diagram to scale based on the PDT results was realized, considering also the calculated stage axial chord lengths and the related spacing. The drawings obtained are reported in the following *Figure 5.11* and *Figure 5.12*.

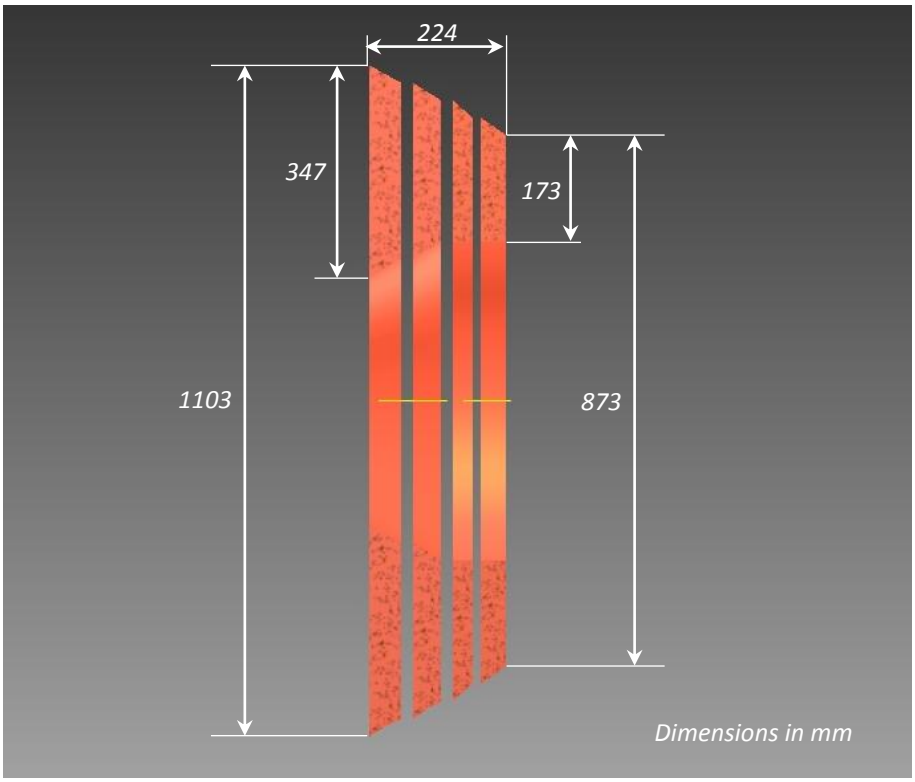

Figure 5.11 - LPT annulus section, side view (scale drawing)

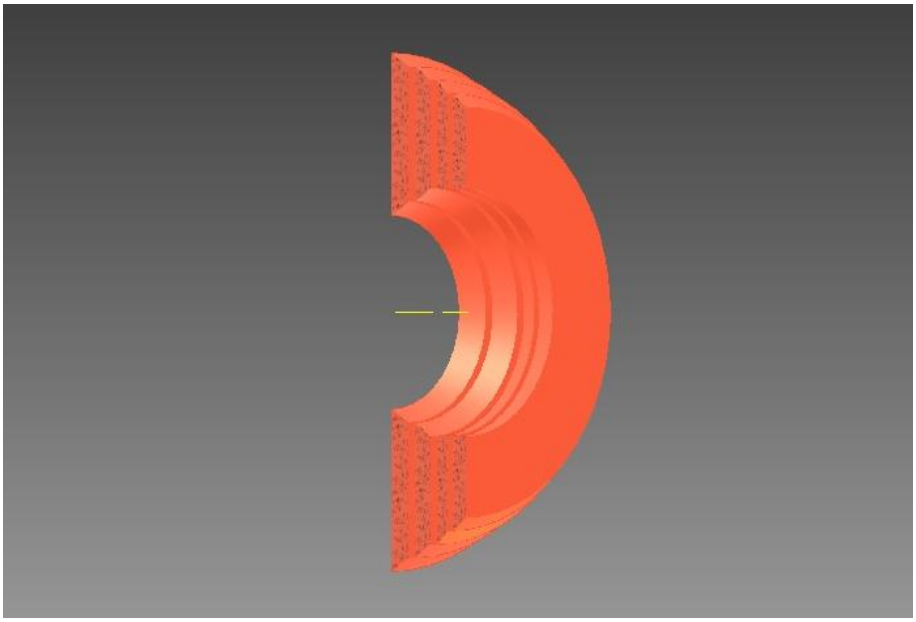

Figure 5.12 - LPT annulus section, side view (scale drawing)

As it can be observed in the annulus diagram to scale, the last stage blading covers a large portion of the turbine diameter. This may imply difficulties both in the integration of the turbine with the concentric spool layout and in the realization of the exhaust ducting. Therefore, a rising axial velocity design could be beneficial in order to reduce the exit annulus area.

The method adopted for the estimation of the turbine length is the same used for the turbines previously reported, based on the correlations (5.2) and (5.3) from Ref. [19] for the aspect ratios and on the procedure from Ref. [20] for the spacing across the stages. The aspect ratio limitation adopted for the last stage rotor, where the correlation adopted would have given a value exceeding the conventional design limit of 6, was obtained from the correlation from Ref. [27] based on the entry into service year of the engine (Eq. (5.5)). The aspect ratio for the last stage rotor, obtained for an engine entry into service in 2020, was therefore 6.118.

The following tables report the geometry of each turbine stage:

Table 5.15 - LPT Stage Radial Geometry Results

Stage inlet	Hub diameter [m]	Mean diameter [m]	Tip diameter [m]	Rotor blade mean height [cm]
1	0.527	0.700	0.873	21.6
2	0.527	0.757	0.987	31.7
Outlet	0.411	0.757	1.103	34.7

Table 5.16 - LPT Stage Axial Geometry Results

Stage	Stator axial chord length [cm]	Rotor axial chord length [cm]	Stator-rotor gap [cm]	Inter-stage gap [cm]
1	4.1	3.1	1.4	1.9
2	4.6	5.2	1.9	-

5.5.3 Velocity Triangles

The stage velocity triangles were produced with the PDT in-built code and visualizer. The results for both the stages are presented in *Figure 5.13*:

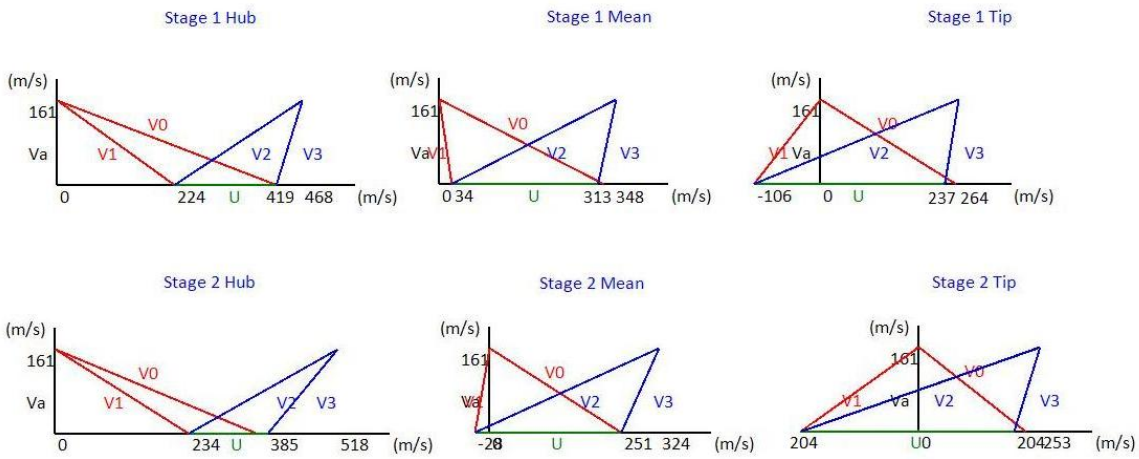

Figure 5.13 - Turbine inlet and outlet velocity triangles

From the velocity triangles it appears that the blade speed at the hub is very low compared with the ΔV_w required, particularly in the second stage (U_{hub}=151 m/s, ΔV_w=518 m/s). This fact implies in the latter stage a flow turning of 116 degrees, hence approaching the maximum limit of 130 degrees and giving a high root loading [15]. In order to decrease the flow turning, a design for increasing axial velocity through the stages would give the double advantage of raising V_a and allowing for a higher blade root speed, the latter due to the increase in hub diameter related with the reduction in annulus area.

The complete results and velocity triangles data are reported in C.3.

5.5.4 Mass Estimation

As in the previously reported cases, the turbine mass was estimated with Equation (5.6), thus using the inlet and outlet mean diameters and blade speeds. The estimated value was 209.9 kg, which summed with the mass of the IPT yielded an overall mass of 459.5 kg, thus lower than the 2-spool engine turbine (485.2 kg). However, the weight of the inter-turbine duct and the mass of the additional spool could not be taken into account in the IPT-LPT assembly; therefore the weight advantage might be overcome. Further considerations on the differences between the two turbines are reported in Section 5.6.

5.5.5 Blade Count Estimation

The blade count estimation was based on the Zweifel coefficient's method, as in the previous design cases (Equations (5.7), (5.8) and (5.9)). The results for the rotor and the stator are reported below:

Table 5.17 - 3-Spool Engine LPT Blade Count

Stage	Stator N_b	Rotor N_b	Stator σ	Rotor σ
1	57	83	1.036	1.121
2	67	48	1.300	1.036

The relatively low number of blades resulting for the last stage rotor is due to its long axial chord, which implied from equation (5.9) a large spacing between the blades (S_m=5 cm at mean diameter).

5.5.6 Performance Parameters

The design reported respected most of the performance parameters and constraints, although some limitations were slightly exceeded. As for the previously reported designs, the reference values were obtained from Ref. [15] and Ref. [30].

The relevant results obtained with the Preliminary Design Tool are reported in the following table:

Table 5.18 - Performance and Design Parameters

	Stage 1	**Stage 2**	**Recommended**
Stage loading coeff. $\Delta H/U^2$	1.22	1.12	< 3
Stage flow coeff. V_a/U	0.60	0.58	0.4 – 0.8
Tip speed at DP [m/s]	364.3	407.1	< 430
Tip speed at max rpm [m/s]	412.6	461.0	< 430
Min rotor hub acceleration	1.155 (*stage 2*)		≥ 1.15
Min NGV tip acceleration	1.469 (*stage 2*)		≥ 1.15
Turbine exit swirl at BMH [deg]	-	24	< 40, lowest possible
NGV max gas deflection [deg]	68 (hub)	93 (hub)	< 130
Rotor max gas deflection [deg]	110 (hub)	116 (hub)	< 130
Max NGV exit angle [deg]	68 (hub)	68 (hub)	≤ 72
Rotor axial exit Mach	0.31	0.33	< 0.5
NGV hub/tip ratio	0.60	0.53	< 0.9
Rotor hub/tip ratio	0.53	0.37	< 0.9
AN^2 at design point [$rpm^2\ m^2$]	$27.2 \cdot 10^6$	$40.9 \cdot 10^6$	$20 – 50 \cdot 10^6$

From the data obtained and reported in the table, the turbine stage loading coefficients resulted lower than those of the upstream IPT, according with the higher blade speeds and the lower enthalpy drop per stage (ΔH=87.85 kJ/kg against the

average 136.16 kJ/kg of the IPT). This allowed therefore for stage efficiencies higher than the values obtained for the IPT. The stage flow coefficients resulted within the recommended range.

The preliminary design led to a turbine with a maximum tip diameter above the limit of 1.03 m, which would have allowed for operation both at design and off-design conditions without exceeding the maximum tip speed limit of 430 m/s. The compromise was a turbine operating below this limit at design point, while reaching a maximum tip speed of 461 m/s at the maximum rotational speed, thus exceeding the limit by 7.2%. As observed in Paragraph 5.3.6 for the two-spool engine LPT, the latter condition should be further analysed to assess the mechanical resistance of the turbine.

From the analysis of the performance results, the rotor hub acceleration reached its minimum in the second stage of the turbine (V_2/V_1=1.155). The stage reaction at blade mean height was increased to 0.58 in order to achieve this value (see Paragraph 4.4.2 – Reaction Variations). The NGV tip acceleration resulted as well above the minimum recommended limit. However, the increase in stage reaction led to relatively high exit flow angles, with a value at blade mean height of 24 degrees, hence 3 degrees higher than the two-spool engine LPT. Some efforts to reduce this value in order to improve the turbine efficiency should therefore be undertaken, with an indicative exit swirl target of less than 10 degrees at blade mean height.

The calculated gas deflections reported in *Table 5.18* resulted in the rotor close to the limit of 130 degrees at blade hub, thus implying high root loadings [15]. The reason was the low hub diameter, which implied low blade tangential speeds, on the order of 150 m/s, with consequent high flow turnings to achieve the required ΔV_w (see velocity triangles in Paragraph 5.5.3).

Consequently to the inlet value chosen, the exit axial Mach value of 0.33 resulted well below the maximum limit of 0.5, thus implying the advantages discussed in Paragraph 5.5.1. In the annulus configuration considered, the blade hub to tip ratios respected the limitation imposed to avoid excessive fractions of tip leakage, as well as

the AN^2 parameter resulted within the design range, thus indicating the capacity of the turbine blades to withstand the stress values involved.

5.6 Comparison between Two-Spool and Three-Spool Configuration

After the completion of the preliminary design of the LP turbine for the two-spool engine and of the IP/LP turbines for the three-spool configuration, a comparison between the two layouts was made in order to evaluate the potential advantages of the two configurations. The relevant design parameters are summarized in *Table 5.19*:

Table 5.19 - Turbine configurations PDT results comparison

	2-spool	**3-spool**
Max diameter [m]	1.085	1.103
Estimated length [m]	0.471	0.447 + connect. duct
Estimated weight [kg]	485	459 + connect. duct
Max tip speed at DP/OD [m/s]	410 / 454	416 / 462 (IPT) 407 / 461 (LPT)
Max blade height [cm]	32.1	34.7
Stage is. efficiency [%]	90 / 92 / 92 / 92 / 91	90 / 90 / 90 / 91 / 92
Exit swirl at mean height [deg]	21	24
Inlet D mean [m]	0.640	0.580
Inlet Mach	0.32	0.24
Exit axial Mach	0.44	0.33
Max AN^2	$40.2 \cdot 10^6$	$40.9 \cdot 10^6$

Both the configurations resulted very similar in terms of size and mass: the maximum diameter differs by less than 2 cm between the two turbines, with the three-spool engine LP turbine slightly penalized by the larger exit annulus area (0.83 m^2 against the 0.77 m^2 of the two-spool design). The IPT/LPT assembly resulted about 2 cm shorter than the five-stage LPT, although the length of the inter-turbine duct was not considered in the tabulated value. Assuming still valid the correlation adopted to determine the inter-stage spacing, reported in Section 5.3.2, would yield a duct length of about 2 cm; however, taking into account also the IPT outlet guide vanes and assuming their axial chord length on the order of magnitude of the adjacent stages

would lead to an IPT/LPT configuration on the order of 3 to 4 cm longer than the two-spool engine LP turbine.

The estimated turbine weight resulted slightly lower for the three-spool engine, due to the lower inlet diameter leading to a more compact IPT. The advantage of this configuration was in fact the higher IPT rotational speed, which allowed the reduction of its entry diameter without compromising the blade tangential speed. However, the presence of the inter-turbine duct and the possible OGVs should be taken into account, since they contribute to the increase of the IPT/LPT mass. Moreover, the IPT/LPT configuration implies an additional spool with related bearings; hence the actual mass advantages over the two-spool engine configuration will be overweighed. A more accurate determination of the turbine masses including the spool weight estimations is therefore required to evaluate the actual weight advantage of one configuration over the other.

The tip speeds respected in all the cases the limitation of 430 m/s at design point, while at off-design the values exceeded the limit by percentages always below 8%. Although the blade tip speed excess is relatively low and should be withstand thanks to the safety margins adopted in the mechanical design, a better arrangement of the turbine annulus in both the cases would contribute to reduce the maximum tip diameter to safer values (namely below 1.03 m for all the turbines). A reduction in annulus areas would imply also a lower exit blade height, thus leading to lower blade mass and consequently lower disc loadings. Particularly, in the three-spool engine LPT the blade height resulted about 35 cm. As mentioned in the Section 5.5.6, the large exit annulus area would imply also a large cross-section of the exhaust duct, which may result challenging to produce and integrate within the reverse-flow core configuration. The blade height should therefore be reduced to a more acceptable value, namely about 30 cm.

The stage isentropic efficiencies resulted in both the cases above the set target of 90%, although a higher mean value was noticed in the 5-stage LPT configuration (91.4% against 90.6%). However, the simplified efficiency model adopted by the PDT

did not allow for accurate stage efficiency determination; therefore the actual values of this parameter should be more precisely calculated, taking into account also the pressure losses associated with the flow velocity which, according with its lower value, should move the balance in favour of the IPT/LPT arrangement.

The exit swirl is slightly higher in the three-spool engine configuration, thus implying a higher amount energy which cannot be converted into work by the turbine. The result is due to the lower axial velocity through the turbine in this configuration, with an exit value of 161 m/s against the 208 m/s of the 5-stage LP turbine. A design for rising axial velocity in the three-spool case is for this reason particularly recommended, since it would allow maintaining the advantages of a low turbine inlet Mach number while increasing the axial exit Mach, thus reducing the outlet swirl.

The main differences between the two configurations are the lower inlet Mach number and inlet diameter of the three-spool engine turbine assembly, giving the advantage of a better matching with the HPT exit diameter and lower pressure losses both in the HPT/IPT interconnection duct and in the IPT/LPT assembly. The exit axial velocity resulted lower as well for the three-spool configuration, with an axial Mach number of 0.33 against the 0.44 of the two-spool LPT, hence giving lower pressure losses in the exhaust ducting. Adopting a rising axial velocity design would partially reduce this advantage, but would lead to lower blade heights a more compact exhaust duct.

Finally, comparing the maximum disc loading parameters AN^2, the results for the two and three-spool case presented a very limited difference ($40.2 \cdot 10^6$ for the five-stage LPT, $40.9 \cdot 10^6$ for the two-stage LPT), since the larger annulus area of the latter case was compensated by the lower rotational speed. A reduction in the exit annulus area would further reduce the disc loading in both the cases, hence leading to a reduced disc mass and therefore weight saving.

The comparison of the two possible turbine configurations for the LEMCOTEC engine, based on the preliminary designs, highlighted some potential advantages of the three-spool engine over the two-spool from the turbine point of view. The

advantages are related with the faster rotational speed of the IPT, which allowed reducing the flow velocity and the inlet diameter while maintaining comparable sizes, weights and efficiencies. Although the primary scope of the thesis could be considered achieved, it appeared reasonable to conduct a more detailed study, with the aim of obtaining further information on the characteristics of the turbines and improve their design. The outcome is presented in the following chapter.

6 DESIGN IMPROVEMENT: T-AXI

6.1 Introduction

The results obtained with the Preliminary Design Tool proved the feasibility of the design of all the turbines. However, the program limitations left some design constraints which could not be fully satisfied, such as the turbine tip speed limit which resulted excessive at off-design operation, as reported in Section 5.6. A potential margin for improving the turbine design was identified in overcoming the assumption of constant axial velocity through the stage (see Paragraph 3.3.4 – Program Limitations), thus aiming at a design for rising axial velocity in order to reduce the annulus exit area. A second design was therefore implemented in T-AXI (see Section 3.4), starting from the stage mean diameters, NGV exit angles and NGV exit Mach numbers obtained with the PDT and modifying their values to generate a smooth turbine annulus shape. The performance and geometry results from T-AXI were then compared with those of the PDT. After this step, the rotor blading data were used to generate the input file for the disc calculator of the suite, thus allowing for a preliminary disc sizing and mass estimation.

6.2 5-Stage LP Turbine

6.2.1 Annulus Configuration

Starting from the mean diameters obtained with the Preliminary Design Tool and reported in Section 5.3, slight modifications in their value were introduced with the objective of smoothing the walls of the turbine annulus profile, generated by the turbine design code (T-T_DES, with reference to the program structure in *Figure 3.15*). The NGV outlet flow angles (α_0) and Mach numbers (M_0) were used as well as handle to control the stator-rotor annulus area: increases in α_0 imply a larger portion of the flow expansion in the stator, hence an increase in annulus area at the NGV-rotor interface, while variations in M_0 directly control the stage reaction. The axial velocity ratio was set to 1.1 in the last two stages, in order to obtain an exit annulus area lower than the PDT design, while in the first three stages it was maintained to 1 to prevent

excessive flow velocities (M_{exit} >0.5). All the remaining inputs were set to the same values of the corresponding PDT input file.

Figure 6.1 reports the annulus diagram obtained with the turbine design code and the related sizes.

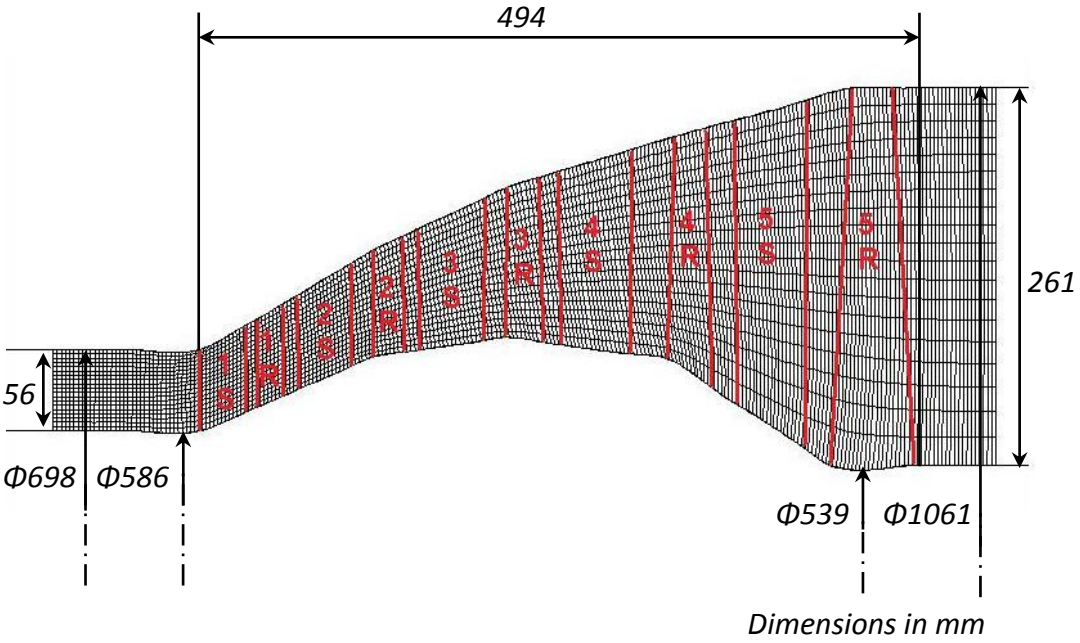

Figure 6.1 - T-AXI 5-stage LPT annulus diagram and dimensions

The main difference with the turbine configuration previously calculated with the Preliminary Design Tool can be noticed in the fifth stage: the constant tip configuration could be achieved with T-AXI, thanks to the reduced exit annulus area obtained with the increasing axial velocity design. The exit area was in fact reduced from the previous 0.77 m^2 to 0.66 m^2, thus yielding both a lower maximum blade height (26.1 cm against the former 32.1 cm) and a tip diameter of 1.06 m, implying a tip speed of 443.9 m/s at maximum rotational speed. The tip speed limitation therefore still could not be respected at off-design, but the excess was reduced from the previous 6% of the PDT to 3%.

6.2.2 Specifications and Performance

The relevant turbine specifications obtained from T-AXI are reported in the following *Table 6.1*. In order to evaluate the differences with the previous design approach, the Preliminary Design Tool results are recalled in the table.

Table 6.1 - 2-Spool Engine LPT Specifications Comparison

	T-AXI	PDT
Overall Pressure Ratio	10.364	11.422
Overall Temperature Ratio	1.711	1.712
Overall Isentropic Efficiency [%]	96.0	93.0
Stage Isentropic Efficiencies [%]	96 / 97 / 97 / 97 / 96	90 / 92 / 92 / 92 / 91
Stage Reactions at BMH [%]	46 / 48 / 49 / 51 / 64	50 / 50 / 50 / 50 / 64
Inlet Mean Diameter [m]	0.642	0.640
Outlet Mean Diameter [m]	0.800	0.763
Max Tip Diameter [m]	1.061	1.085
Max Blade Height [cm]	26.1	32.1
Estimated Length [m]	0.494	0.471

It can be observed that T-AXI calculations yielded stage and overall efficiencies higher than the PDT. The difference might rise from the simplified efficiency model adopted by the PDT, which had been proven to underestimate this parameter in other LPT designs (see Paragraph 3.3.5); conversely, the reference values used for the NGV and rotor blade loss coefficients in T-AXI were the same adopted by the developers to simulate the EEE engine 5-stage LPT presented in its validation report [23] and may be excessively low, thus leading to the very high calculated efficiencies. Further investigations on the choice of the loss coefficients in T-AXI should therefore be conducted before evaluating the possibility of a four-stage design.

Consequently to the higher turbine efficiency, the overall pressure ratio resulted lower, while the temperature ratio remained unvaried, as reported in ***Table 6.1***. The

latter result confirmed that, having fixed the mass flow and C_P, the turbine work output was the same both in T-AXI and the PDT.

Table 6.2 reports the comparison between the relevant performance parameters, obtained for the exit stage with the two programs:

Table 6.2 - Stage 5 Performance and Design Parameters Comparison

	T-AXI	PDT	Recommended
Stage loading coeff. $\Delta H/U^2$	1.13	1.24	< 3
Stage flow coeff. V_a/U	0.72	0.72	0.4 – 0.8
Tip speed at DP [m/s]	401.0	410.1	< 430
Tip speed at max rpm [m/s]	443.9	454.0	< 430
Rotor hub acceleration	1.206	1.152	≥ 1.15
NGV tip acceleration	1.405	1.433	≥ 1.15
Turbine exit swirl at BMH [deg]	12	21	< 40, lowest possible
Rotor axial exit Mach	0.48	0.44	< 0.5
AN^2 at design point [rpm^2 m^2]	$34.4 \cdot 10^6$	$40.2 \cdot 10^6$	$20 – 50 \cdot 10^6$

From the tabulated results, the calculated stage loading and flow coefficients resulted comparable between the two programs, with discrepancies due to the slightly different blade and axial flow velocities. As discussed in the previous section, the blade tip speed excess of the recommended value at off-design operation was reduced respectively to the PDT value, thanks to the lower maximum tip diameter. A better turbine performance was noticed also for the exit swirl at BMH, which was reduced to 12 degrees thanks to the increased exit axial Mach. The latter value resulted in fact higher than the PDT configuration and close to the maximum acceptable limit. Finally, thanks to the lower annulus exit area, the disc loading parameter AN^2 resulted decreased by about 15%, thus providing a margin for lighter disc realization.

6.2.3 Blading

Successively to the calculations which led to the definition of the turbine annulus, the data obtained were used to generate the blading. This task took

advantage of the calculation loop of T-AXI and the in-built blading visualizer. The blade spacing was calculated by the program with the Zweifel coefficient method, requiring in input its value. In the calculations performed, the latter was set to the optimal 0.8, as outlined in Paragraph 5.3.5.

The blade count estimation comparison is presented in the following table:

Table 6.3 - 2-Spool Engine LPT Blade Count

	T-AXI		PDT	
Stage	**Stator N_b**	**Rotor N_b**	**Stator N_b**	**Rotor N_b**
1	81	167	73	160
2	92	147	89	139
3	75	120	78	121
4	70	105	70	101
5	74	55	69	71

The outcome of the blading generator was a three-dimensional representation of the blade rows, which included the calculated chord lengths and the profile twisting. The following figures show the program output for the case considered.

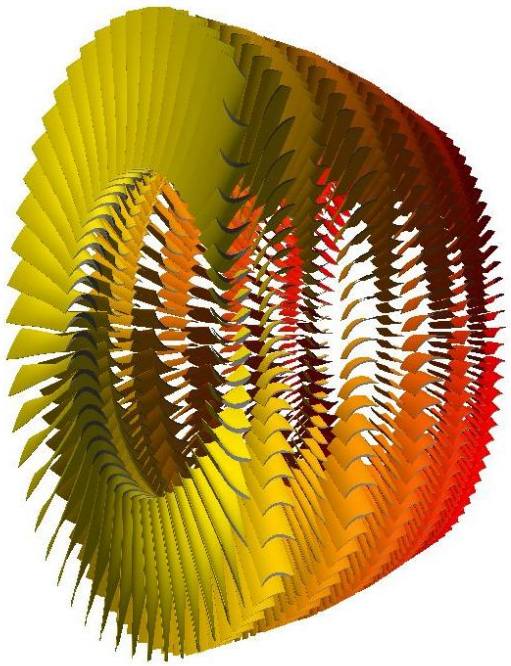

Figure 6.2 - T-AXI two-spool LPT blading, exit view

Figure 6.3 - T-AXI two-spool LPT blading, side view

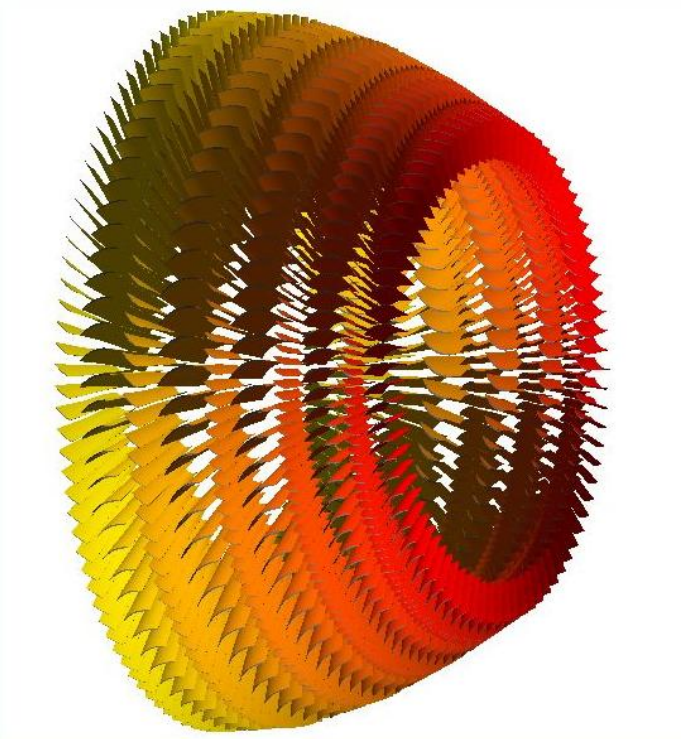

Figure 6.4 - T-AXI two-spool LPT blading, inlet view

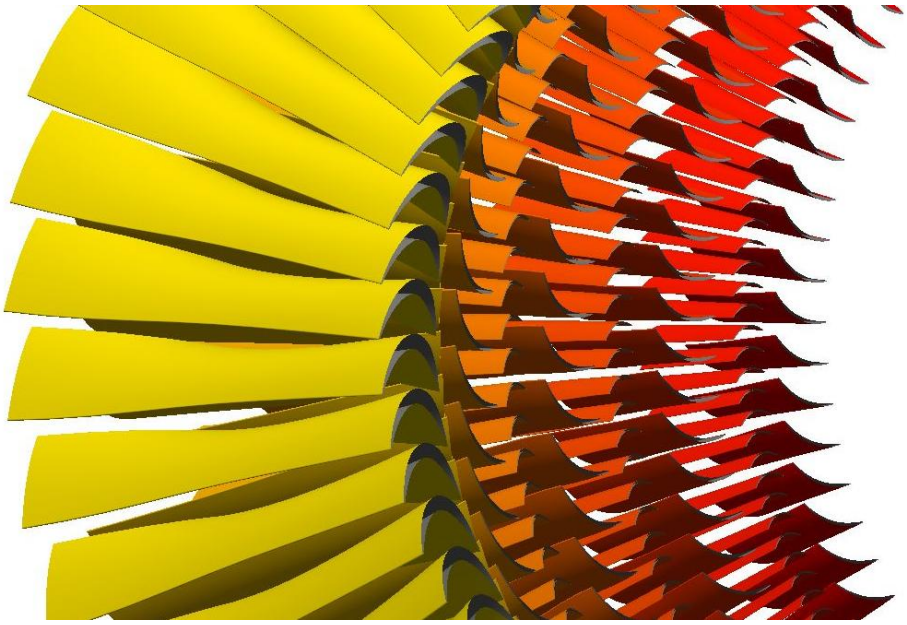

Figure 6.5 - Detail of the exit stages blading

From *Figure 6.5*, it can be observed how the airfoil shape in the blade changes from a configuration for low reaction at the hub, having a typical impulse blading shape with constant flow area, to a configuration for high reaction at the tip. This is consistent with the hypothesis of free-vortex flow adopted in the solution, which led to very twisted blades.

Starting from the data produced, further CFD investigations can be performed. This process was beyond the scope of the thesis; however, it was decided to generate the complete blade data files, which are now available for future work.

6.2.4 Preliminary Disc Mass Estimation

The information obtained from the main calculations in T-AXI was used as input for 'T-AXI disk', described in Paragraph 3.4.3. In order to preserve the disc integrity at off-design operation, the design was performed using as input the turbine maximum rotational speed and TET. The outcome was a preliminary sizing of the turbine discs respecting both the disc integrity constraint and the set 1.1 safety factor, with the related mass estimation of the disc and blading. The graphical results for the first and

fifth stage of the LPT are presented in the following figures. The complete results are tabulated at page 97.

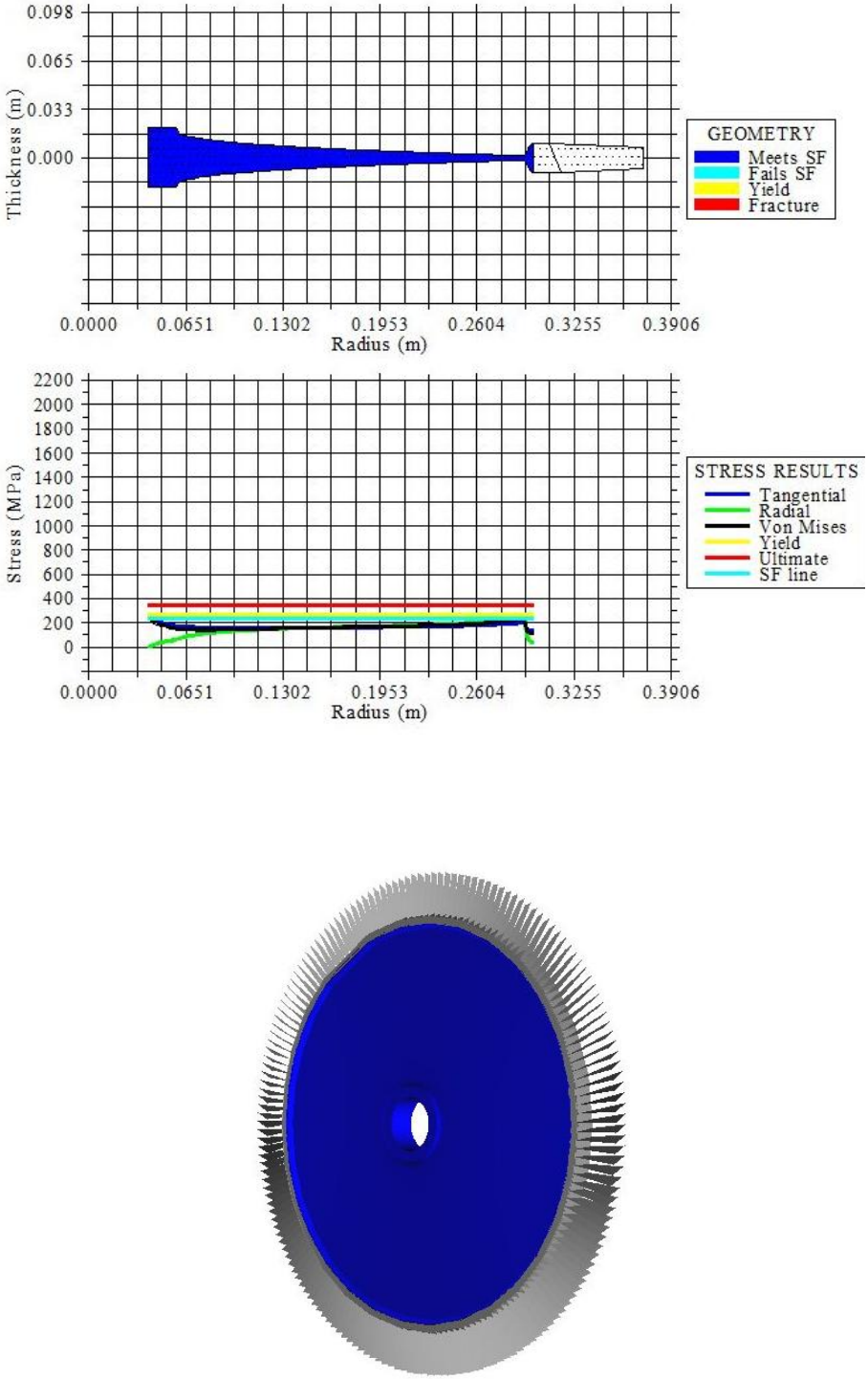

Figure 6.6 - Stage 1 disc graphical output

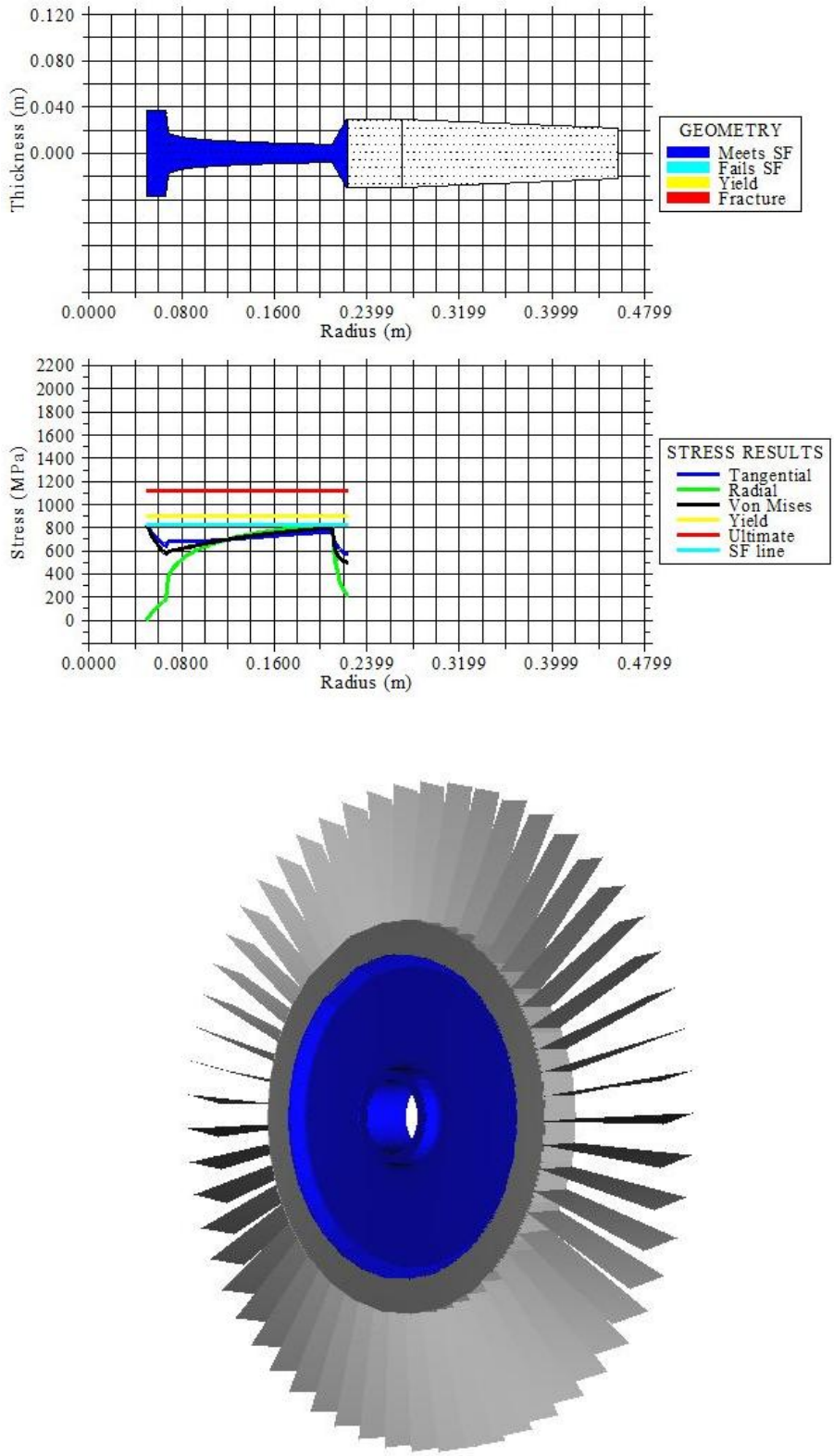

Figure 6.7 - Stage 5 disc graphical output

The disc output was the result of the optimization loop of the program, set to mass minimization while respecting the design safety factors. The disc shape chosen was a 'hyperbolic' setting, according with the arrangement indicated for geared LP turbines in Ref. [8]. The figures show how the program converged on a large bore size compared to the disc thickness. This result is consistent with the discussion about LP turbine disc sizing made in Section 2.3.

The material chosen for the discs was the René 41 alloy for the first and second stage, since it proved to be the only one in the program database capable of meeting the safety factors in the whole disc span. For the remaining three discs the less expensive Inconel 718 was instead adopted.

Table 6.4 reports the relevant results obtained from the disc optimization with T-AXI:

Table 6.4 - 2-Spool Engine LPT Disc Design Output

Stage	**1**	**2**	**3**	**4**	**5**
Material	René 41	René 41	Inco 718	Inco 718	Inco 718
Estimated disc mass [kg]	24.84	9.81	15.68	16.59	29.58
Estimated airfoil mass [kg]	0.012	0.016	0.035	0.124	1.014
Estimated total mass [kg] (disc+total dead weight)	30.62	17.47	27.81	40.61	112.17
Bore radius [m]	0.040	0.046	0.050	0.050	0.050
Total disc + blading mass [kg]	**228.68**				

The large mass of the last stage disc is mainly due to the blade weight, which as it can be observed is about 8 times the weight of the fourth stage airfoil. The fifth stage blade height is in fact higher than the fourth stage, thus implying a larger hub thickness to obtain a feasible blade mechanical design. The calculated blade thickness at hub was in fact 9.2 mm for the fifth stage, against the 2.3 mm of the fourth stage, hence motivating the large difference in airfoil mass. The tip thicknesses were instead 1.3 mm and 1.2 mm respectively for the fourth and fifth stage.

The calculated overall mass resulted much lower than the 486 kg of the previous overall turbine mass estimation performed in Paragraph 5.3.4. However, the value obtained with T-AXI accounted only for the turbine discs and their dead weight; hence it did not take into account the stator blades, the seals, the casing and the turbine accessories. The discrepancy should be therefore justified.

6.3 3-Stage IP Turbine

6.3.1 Annulus Configuration

The annulus design for the 3-spool engine intermediate pressure turbine aimed at obtaining at the outlet the same flow conditions used as input in the PDT for the downstream two-stage LPT. In order to achieve this purpose, it was necessary to match the turbine designed in T-AXI with the model adopted in the engine performance simulation by the two PhD advisors, task which could not be performed with the former PDT calculations (see Paragraph 5.5.1). The annulus development with T-AXI aimed also at having the same IPT exit mean diameter obtained with the Preliminary Design Tool, thus providing an LPT inlet geometry as close as possible to that adopted for the PDT design for comparison purpose.

With the objective of matching the IPT design with the aforementioned performance simulation results, the turbine isentropic efficiency was modified to obtain the given value of 93%. The handles adopted for this scope were the NGV and rotor loss coefficients, which were increased from the default values of the EEE LPT design to achieve the desired efficiency. In addition, starting from the PDT output values, variations in the mean diameters and in the NGV outlet Mach numbers and flow angles were introduced, in order to obtain a smooth profile of the annulus walls. All the remaining settings maintained the same values adopted in the PDT design.

The annulus diagram produced with the turbine design code of T-AXI and the related sizes are presented in *Figure 6.8*.

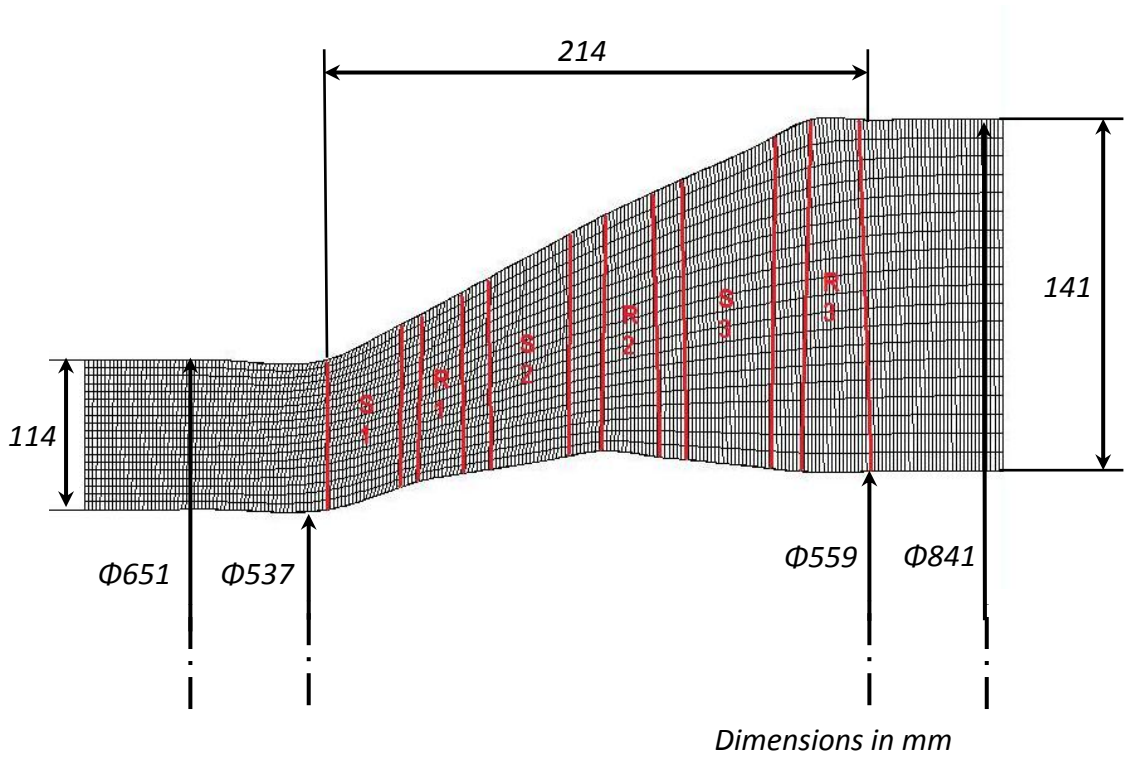

Figure 6.8 - T-AXI 3-stage IPT annulus diagram and dimensions

The annulus configuration obtained has a wall shape very similar to the outcome of the PDT (*Figure 5.7*) both for the inner and outer walls. Particularly, the outer wall presents a constant slope in both the designs. However, the exit annulus area resulted lower in T-AXI (0.31 m^2 against 0.39 m^2), due to the higher outlet pressure related with the higher turbine isentropic efficiency (93% against the former 91%) and the higher exit axial Mach number, 0.35 against the 0.30 of the PDT.

6.3.2 Specifications and Performance

The relevant specifications for the IP turbine obtained with T-AXI are reported in the following table. The PDT design outcome is recalled as well for comparison purpose.

Table 6.5 - 3-Spool Engine IPT Specifications Comparison

	T-AXI	PDT
Overall Pressure Ratio	4.934	5.366
Overall Temperature Ratio	1.440	1.440
Overall Isentropic Efficiency [%]	93.1	91.3
Stage Isentropic Efficiencies [%]	92 / 95 / 95	90 / 90 / 90
Stage Reactions at BMH [%]	47 / 47 / 42	50 / 50 / 46
Inlet Mean Diameter [m]	0.594	0.580
Outlet Mean Diameter [m]	0.700	0.707
Max Tip Diameter [m]	0.841	0.881
Max Blade Height [cm]	14.1	17.4
Estimated Length [m]	0.214	0.224

Comparing the outcome of the two tools, the turbine pressure ratio calculated with T-AXI resulted about 8% lower than the PDT, due to the higher estimated turbine isentropic efficiency. The temperature ratio has instead the same value, thus confirming that both the designs produce the same power output, having fixed the gas specific heat C_P and the mass flow. According with the lower exit annulus area, the maximum blade height resulted about 3 cm lower than the PDT value, thus allowing for a reduction in maximum tip diameter.

Table 6.6 presents the relevant performance parameters results for the IPT exit stage:

Table 6.6 - Stage 3 Performance and Design Parameters Comparison

	T-AXI	PDT	Recommended
Stage loading coeff. $\Delta H/U^2$	1.37	1.41	< 3
Stage flow coeff. V_a/U	0.52	0.51	0.4 – 0.8
Tip speed at DP [m/s]	397.4	416.2	< 430
Tip speed at max rpm [m/s]	441.5	462.4	< 430
Rotor hub acceleration	1.141	1.195	≥ 1.15
NGV tip acceleration	2.435	2.113	≥ 1.15

Turbine exit swirl at BMH [deg]	9	20	< 40, lowest possible
Rotor axial exit Mach	0.35	0.30	< 0.5
AN^2 at design point [rpm^2 m^2]	$25.2 \cdot 10^6$	$31.5 \cdot 10^6$	$20 – 50 \cdot 10^6$

Evaluating the performance results of the two programs, both the stage loading and stage flow coefficients presented only slight variations, related with the differences in turbine geometry and axial flow velocity. Although the maximum diameter was reduced, the tip speed limitation of 430 m/s was still unsatisfied at off-design operation. However, the excess was reduced from the 7.5% of the PDT to 2.6% of the T-AXI design. Conversely, the hub acceleration of the latter design resulted below the recommended value; a reduction in the NGV exit angle α_0 from the current 70 degrees to about 69 degrees would be recommended to raise V_2/V_1 above 1.15.

The turbine exit swirl resulted reduced from 20 to 9 degrees, thus indicating a lower amount of energy lost through the residual exit flow tangential velocity. Considering the disc loading parameter AN^2, its value resulted reduced by 20% due to the lower exit annulus area.

6.3.3 Blading

Following the approach adopted for the two-spool engine turbine design, the blade number and shape plot was obtained through the in-built features of T-AXI, setting the Zweifel coefficient to 0.8. The blade number estimation is presented in *Table 6.7*, while the graphical output is reported in the successive figures.

Table 6.7 - 3-Spool Engine IPT Blade Count

	T-AXI		**PDT**	
Stage	**Stator N_b**	**Rotor N_b**	**Stator N_b**	**Rotor N_b**
1	71	133	57	116
2	76	105	69	103
3	69	95	60	89

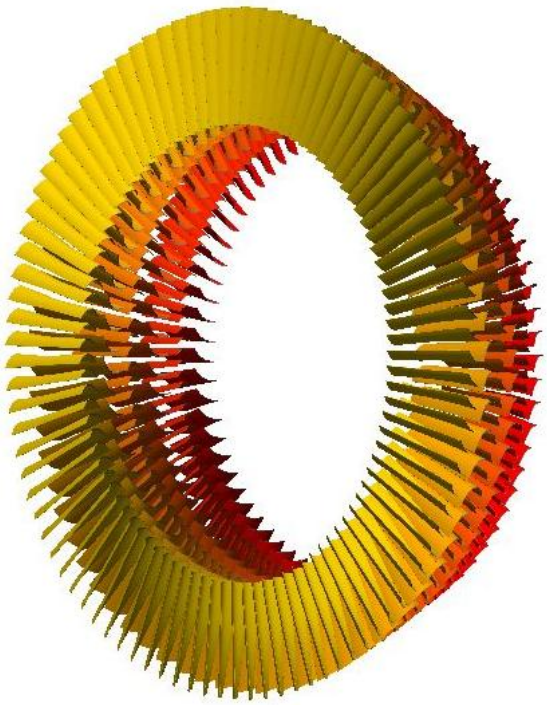

Figure 6.9 - T-AXI three-spool IPT blading, exit view

Figure 6.10 - T-AXI three-spool IPT blading, side view

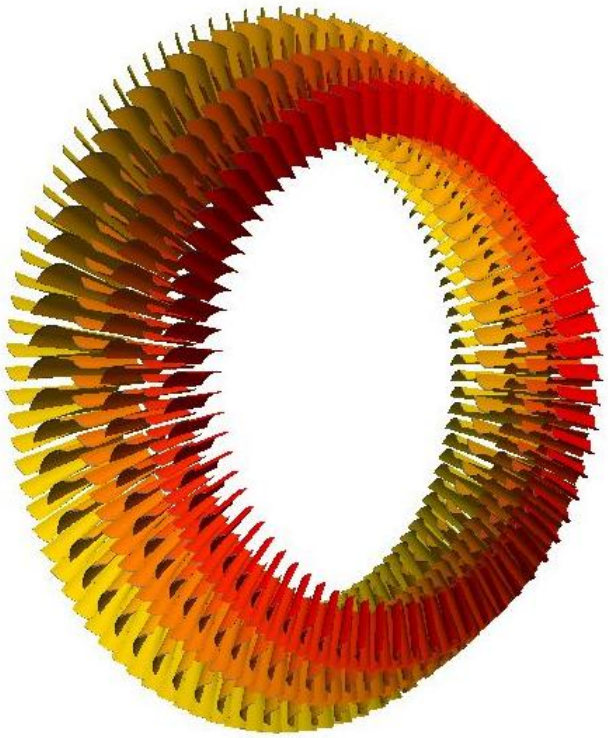

Figure 6.11 - T-AXI three-spool IPT blading, inlet view

Figure 6.12 - Detail of the entry stages blading

6.3.4 Preliminary Disc Mass Estimation

The blading results obtained with T-AXI were used to generate the IPT discs with the dedicated feature of the program, in order to obtain their preliminary mass and size estimation. The design approach adopted was the same of the two-spool engine LPT, hence use as inputs the turbine maximum rotational speed and TET to generate discs respecting the mechanical integrity and the 1.1 safety factor also at off-design operation. The IP turbine presented two main factors impacting on the disc design: the entry temperature was about 80 K higher than the 2-spool engine LPT, while the rotational speed was about 1800 rpm higher. The combination of these two factors implied the impossibility to obtain a feasible uncooled design for the first stage disc and led to the decision of adopting for it a cooled disc arrangement. The material chosen for the IPT discs was the René 41 alloy, since it proved to be the one from the T-AXI database capable of withstanding the highest stress and temperature combination.

The maximum rim allowable temperature for a feasible design of the first stage resulted with T-AXI about 1210 K, while the maximum off-design turbine entry temperature from the performance simulation data was 1312 K: the first stage disc rim needs therefore a cooling flow capable of maintaining the material temperature about 100 K below the TET at maximum rpm. Since the cooling requirement affects only the maximum rpm condition, an active cooling arrangement based on centrifugal forces such as the example presented in Ref. [31] should be an acceptable solution. The maximum first stage bore allowable temperature was instead about 980 K. A flow of cooling air should therefore be provided also for the disc bore. An example of possible arrangement is reported in Ref. [32].

The second disc did not require rim cooling, but an air flow to maintain the bore at a temperature below 1020 K was still needed. The IPT third disc could instead be realized without any cooling necessity. Although the material chosen for the design of the latter stage was René 41, a successive case study proved its feasibility with the less expensive Inconel 706, but with the penalty of an added disc weight of about 6 kg.

The graphical results for the first and the third stages are reported in the following figures, while the complete results are tabulated at page 107.

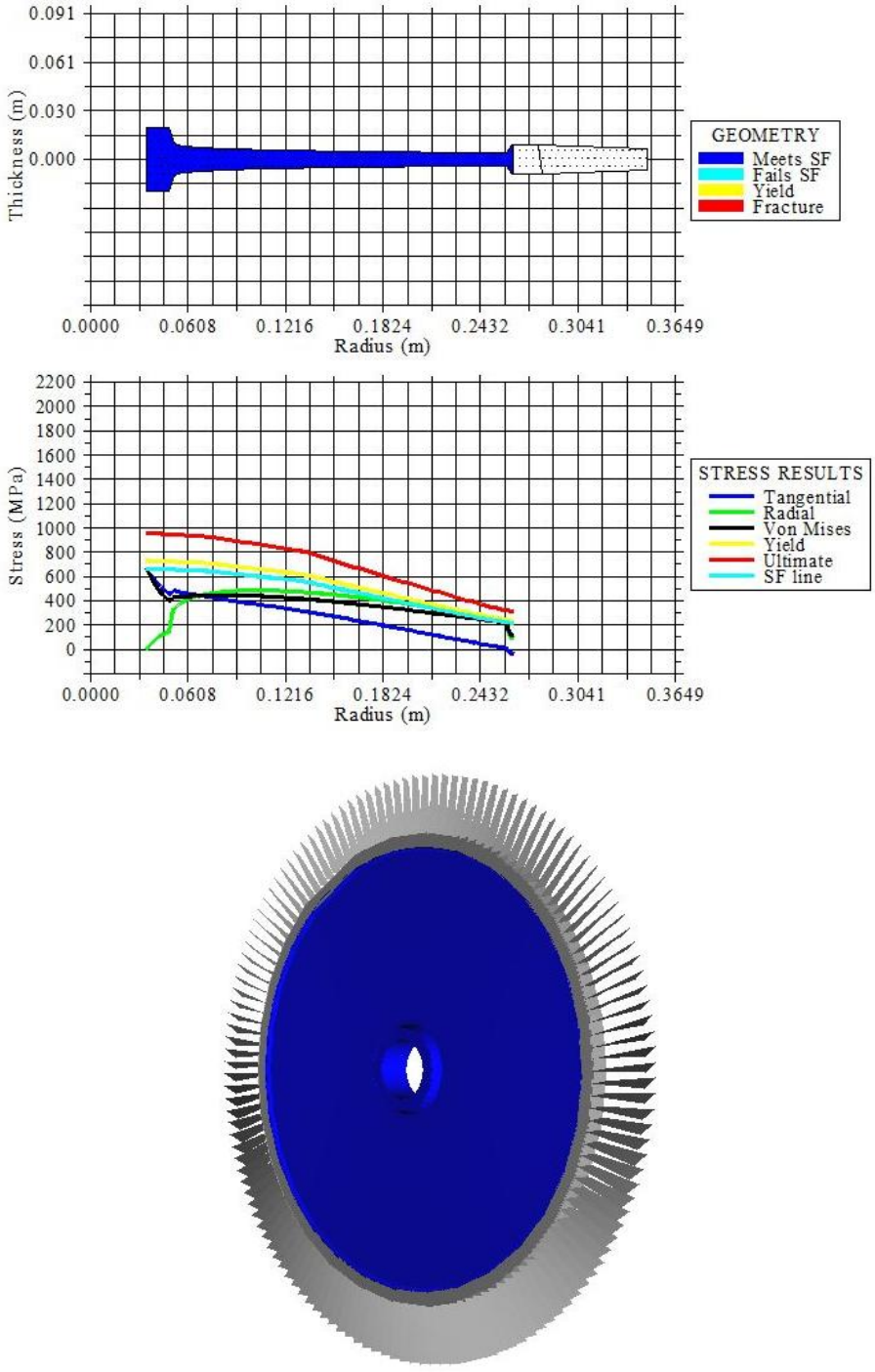

Figure 6.13 - Stage 1 disc graphical output

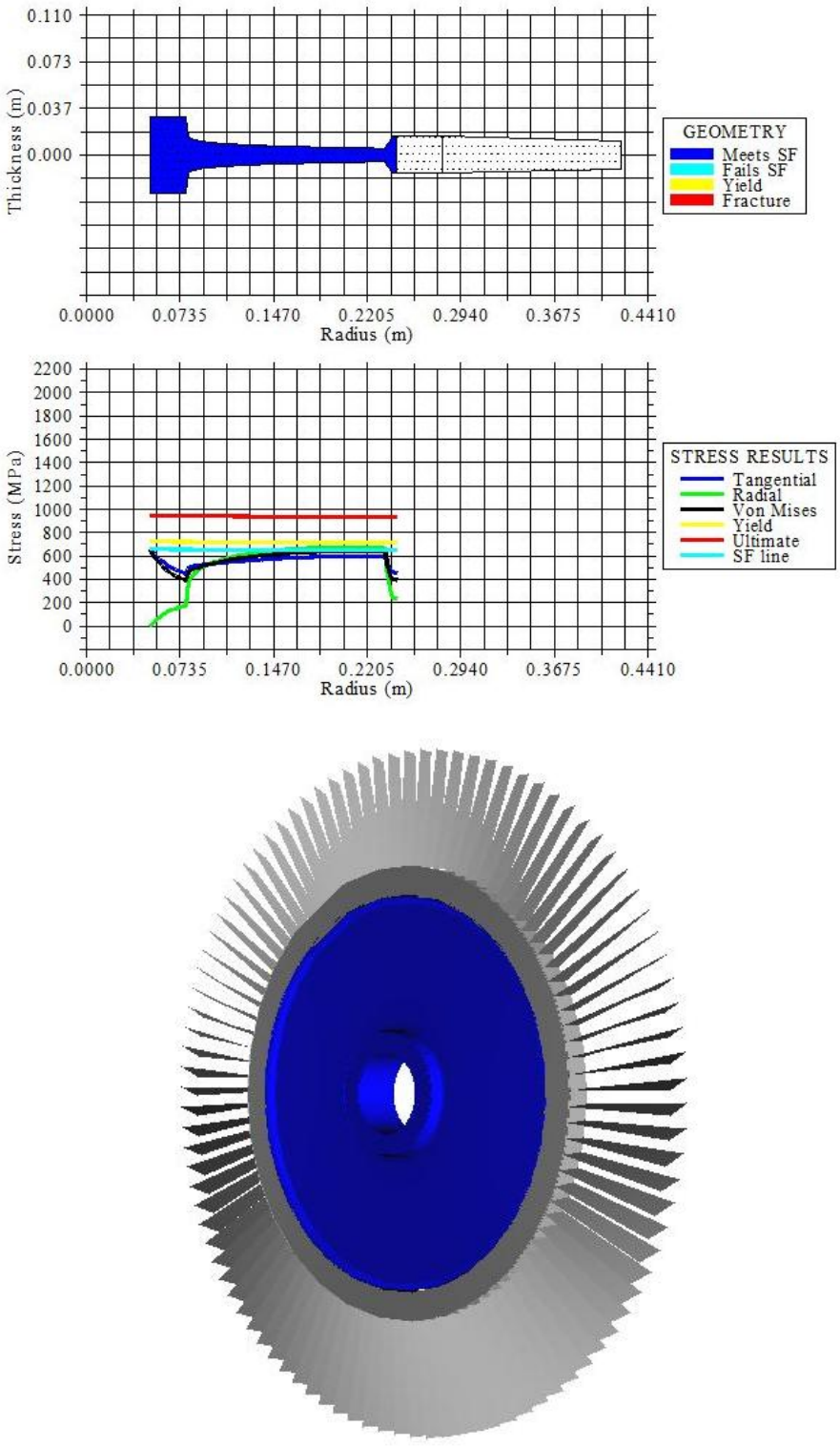

Figure 6.14 - Stage 3 disc graphical output

Table 6.8 - 3-Spool Engine IPT Disc Design Output

Stage	1	2	3
Material	René 41	René 41	René 41
Estimated disc mass [kg]	19.16	15.70	26.29
Estimated airfoil mass [kg]	0.037	0.055	0.226
Estimated total mass [kg] (disc+total dead weight)	28.28	27.54	56.36
Bore radius [m]	0.035	0.035	0.050
Total disc + blading mass [kg]	**112.18**		

Considering the results reported in *Table 6.8*, it should be noticed that the disc bore radius was set to low values to produce a feasible disc mechanical design. The current result implies an IP shaft maximum diameter of 70 mm. The evaluation of the suitability of this value for the shaft sizing was beyond the purpose of this thesis work; however, the shaft diameter requirement should be relatively low. In fact, the geared IPT rotational speed is higher than a conventional IPT, thus allowing a reduced torque transmission requirement for a given power. The adequacy of a maximum shaft diameter of 70 mm for the IPT spool will however need to be analysed in detail.

6.4 2-Stage LP turbine

6.4.1 Annulus Configuration

The annulus design of the 3-spool engine LP turbine was performed with the main objectives of matching the turbine entry with the IPT outlet geometry and minimizing the maximum tip diameter. The first objective was achieved by raising the turbine inlet Mach number from the IPT outlet value of 0.35 to 0.36, in order to compensate for the additional mass flow requirement of about 1 kg/s related with the IPT sealing flows (details in Paragraph 5.5.1 – Specifications). The LPT inlet blade height resulted therefore 6 mm larger than the IPT outlet.

The annulus diagram and the related sizes are reported in the following *Figure 6.15*.

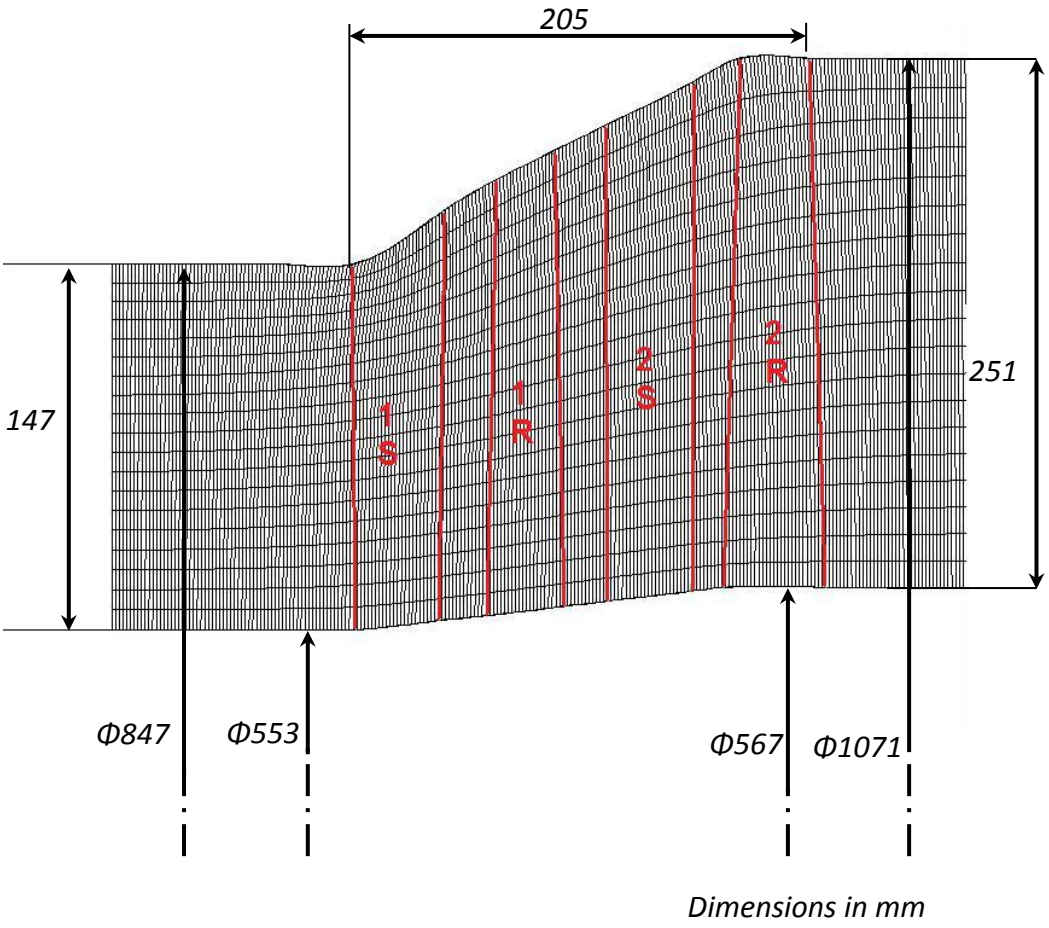

Figure 6.15 - T-AXI 2-stage LPT annulus diagram and dimensions

The exit blade height resulted lower than the 2-spool engine turbine outlet calculated with T-AXI, which was 26.1 cm. The difference is due to the lower mass flow for the three-spool engine case, which is for the LPT reduced by about 2 kg/s. The maximum tip diameter resulted instead 1 cm higher than the former case.

Considering the PDT previous results, the turbine walls presented a similar shape, but the exit blade height in the T-AXI results was reduced by about 9 cm, thanks to the rising axial velocity design adopted. The turbine length estimation performed with T-AXI yielded a value about 2 cm lower than the PDT.

The overall IPT-LPT assembly length calculated with T-AXI resulted 0.42 m without taking into account the IPT-LPT connection duct and the IPT outlet guide

vanes, while for the PDT this value was 0.44 m. Considering the additional length given by the two mentioned components, the results will be raised respectively to 0.48 and 0.50 m, thus approaching the 2-spool engine estimated LPT length.

6.4.2 Specifications and Performance

The relevant turbine specifications obtained from the calculations performed in T-AXI are reported in the following table, along with the results previously obtained with the PDT.

Table 6.9 - 3-Spool Engine LPT Specifications Comparison

	T-AXI	PDT
Overall Pressure Ratio	2.530	2.631
Overall Temperature Ratio	1.237	1.237
Overall Isentropic Efficiency [%]	95.1	91.4
Stage Isentropic Efficiencies [%]	95 / 97	91 / 92
Stage Reactions at BMH [%]	46 / 62	56 / 58
Inlet Mean Diameter [m]	0.700	0.700
Outlet Mean Diameter [m]	0.819	0.757
Max Tip Diameter [m]	1.071	1.103
Max Blade Height [cm]	25.1	34.7
Estimated Length [m]	0.205	0.224

Evaluating the outcome of the two programs, the turbine overall pressure ratio resulted about 4% lower in T-AXI, consistently with the higher estimated turbine isentropic efficiency. The reference pressure loss coefficients adopted in the program were the default values used by the developers of T-AXI for the EEE LPT design and may be excessively low. This factor, combined with the tendency of the PDT to underestimate the turbine efficiency, is the reason for the discrepancy between the two values. Further investigations on the choice of the NGV and rotor pressure loss coefficients should therefore be conducted, in order to increase the accuracy of the efficiency estimation. Once performed this task, if the calculated stage efficiency is still

very high, namely above 94%, the option of adopting a single-stage LPT should be considered.

The estimated turbine performance parameters for the turbine exit stage are reported in *Table 6.10*:

Table 6.10 - Stage 2 Performance and Design Parameters Comparison

	T-AXI	**PDT**	**Recommended**
Stage loading coeff. $\Delta H/U^2$	0.96	1.12	< 3
Stage flow coeff. V_a/U	0.68	0.58	0.4 – 0.8
Tip speed at DP [m/s]	395.3	407.1	< 430
Tip speed at max rpm [m/s]	447.7	461.0	< 430
Rotor hub acceleration	1.108	1.155	≥ 1.15
NGV tip acceleration	1.314	1.469	≥ 1.15
Turbine exit swirl at BMH [deg]	4	24	< 40, lowest possible
Rotor axial exit Mach	0.43	0.33	< 0.5
AN^2 at design point [rpm^2 m^2]	$32 \cdot 10^6$	$41 \cdot 10^6$	$20 – 50 \cdot 10^6$

Comparing the results of *Table 6.10*, the stage loading coefficient resulted lower with T-AXI, due to the higher exit mean blade diameter, while the stage flow coefficient resulted higher due to the increased exit axial velocity. Due to the rising axial velocity design, it was possible to achieve a maximum tip diameter lower than the PDT, thus allowing for a reduction of the maximum tip speed. The latter value resulted still exceeding the limitation of 430 m/s, but the excess was reduced from 7% of the PDT design to about 4%. The rotor hub acceleration obtained with T-AXI was lower than the recommended value, although still indicating flow expansion in this blade section. Some slight adjustments to the NGV exit angle and Mach number are however recommended to raise its value.

The exit swirl at blade mean height showed a large improvement in the turbine performance, giving an almost axial exit flow. The result was due to the increased turbine axial velocity in the T-AXI design. The reduction in exit annulus area was

beneficial also for the disc design, reducing the disc loading parameter AN^2 by about 22%.

6.4.3 Blading

The LPT blading was designed taking advantage of the in-built T-AXI blade generator loop and visualizer. As for the turbines previously designed, the Zweifel coefficient input was set to 0.8. The stator and rotor blade count is reported in the following table, while the graphical output is presented in the successive figures.

Table 6.11 - 3-Spool Engine LPT Blade Count

	T-AXI		PDT	
Stage	**Stator N_b**	**Rotor N_b**	**Stator N_b**	**Rotor N_b**
1	**90**	**109**	**57**	**83**
2	**101**	**56**	**67**	**48**

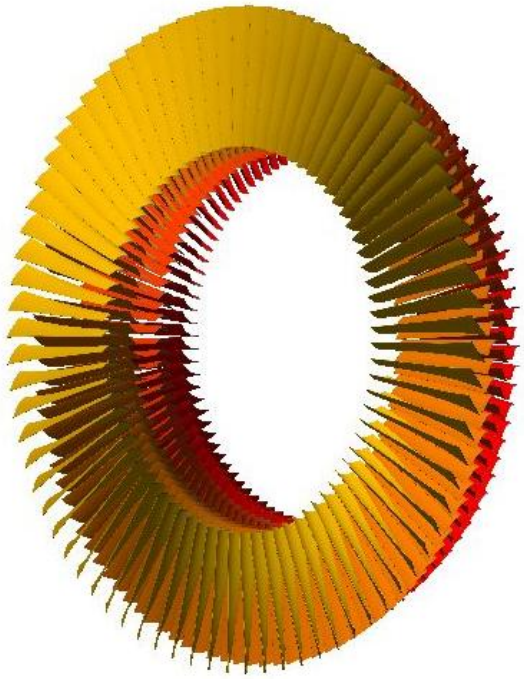

Figure 6.16 - T-AXI three-spool LPT blading, exit view

Figure 6.17 - T-AXI three-spool LPT blading, side view

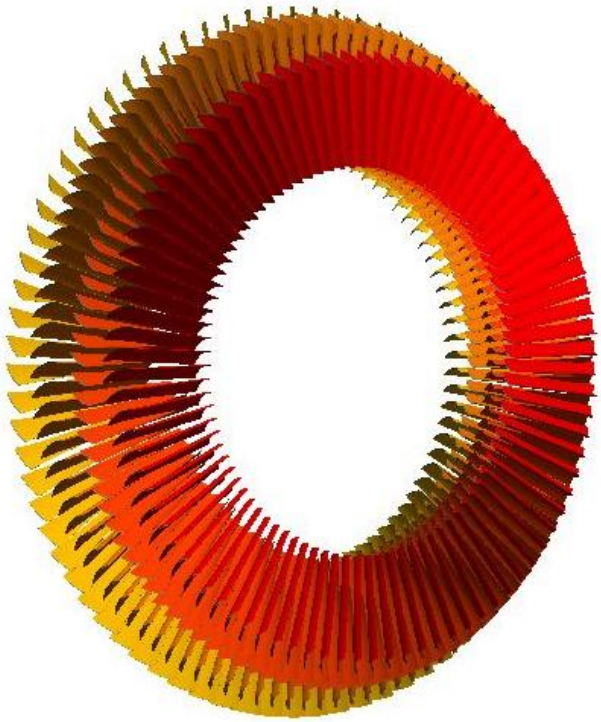

Figure 6.18 - T-AXI three-spool LPT blading, inlet view

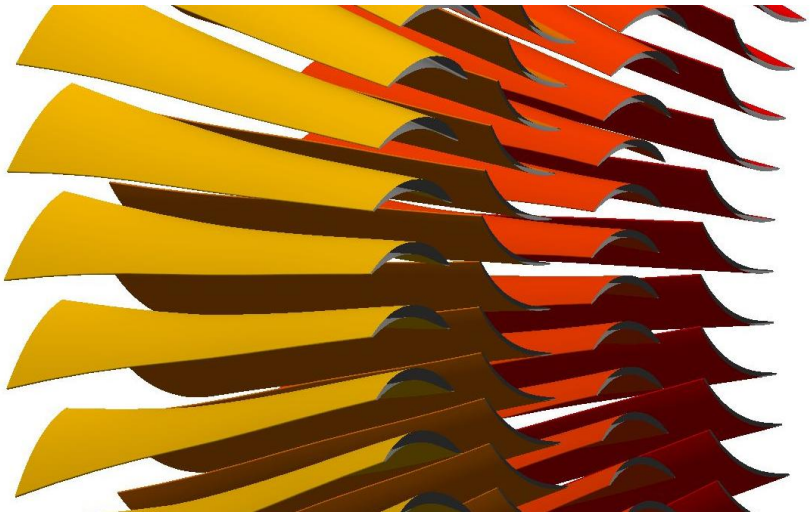

Figure 6.19 - Detail of the exit stages blading

6.4.4 Preliminary Disc Mass Estimation

The disc sizing process relied on the dedicated module of T-AXI. As for the previous cases, the process aimed at achieving a disc design capable of preserving the mechanical integrity and respecting the 1.1 safety factor at the maximum turbine rotational speed and entry temperature, the latter being about 130 K higher than the design point value. The material chosen for the two discs was the Inconel 718 alloy, which proved to be capable of withstanding the combination of stresses and temperatures involved.

The graphical output for the two turbine stages is reported in the following figures, while the numerical results are tabulated at page 116.

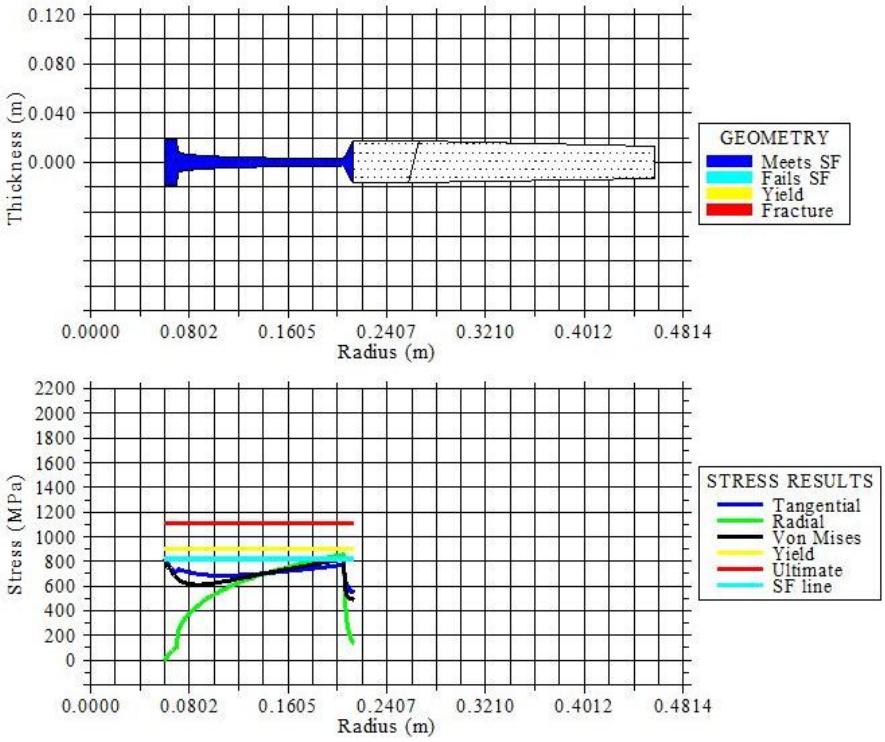

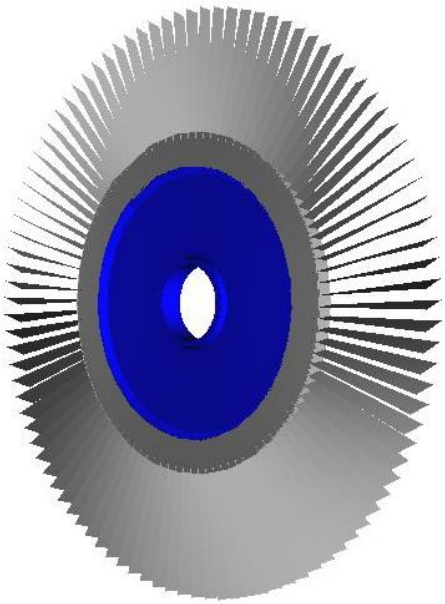

Figure 6.20 - Stage 1 disc graphical output

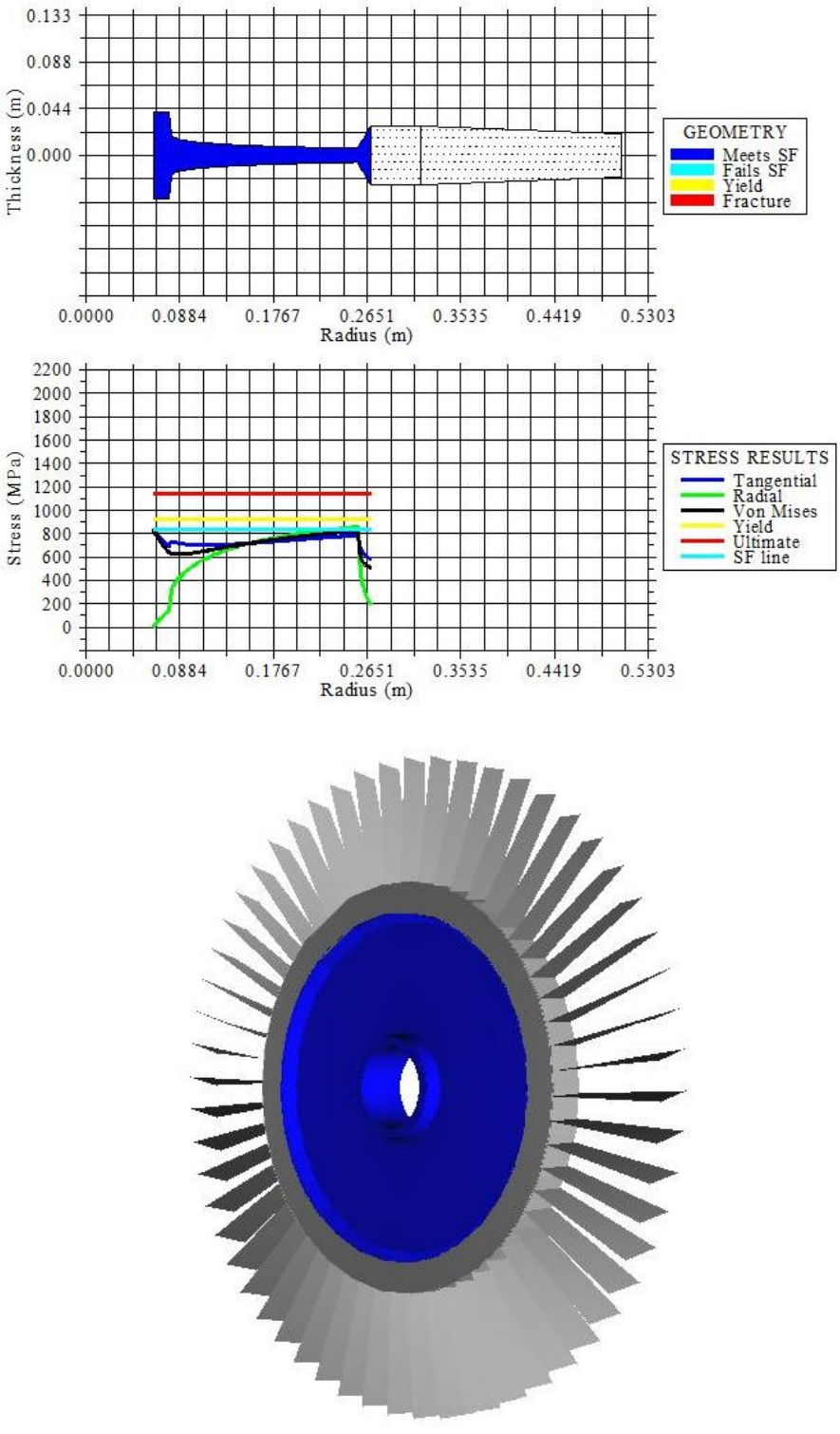

Figure 6.21 - Stage 2 disc graphical output

Table 6.12 - 3-Spool Engine LPT Disc Design Output

Stage	1	2
Material	Inco 718	Inco 718
Estimated disc mass [kg]	10.04	38.20
Estimated airfoil mass [kg]	0.139	0.816
Estimated total mass [kg] (disc+total dead weight)	23.70	115.21
Bore radius [m]	0.060	0.065
Total disc + blading mass [kg]	**138.91**	
Total IPT + LPT disc mass [kg]	**251.09**	

Evaluating the results reported, the second stage rotor of the turbine resulted about five times heavier than the first. The result is mainly due to the blade mass, which in the second stage was about six times higher than the first. The latter was the consequence of the feasibility of the blade mechanical design with the material chosen, which required a hub thickness set to 13% of the chord length for the second stage, while for the first stage this value could be maintained at the default 5%. The tip thicknesses instead were set respectively to 5% and 2.5% of the chord length for the first and second stage.

The overall mass of the IPT and LPT rotors in the three-spool configuration resulted about 22 kg higher than the two-spool engine LPT; the difference in weight between the two turbines is therefore moderate. However, as for the estimation made in Chapter 5, the evaluation of the mass advantage of one arrangement over the other is still conditioned by the need to calculate the additional mass implied by the third spool and relative bearings in the three-spool engine configuration.

7 CONCLUSIONS

From the evaluation of the outcome obtained with the Preliminary Design Tool and T-AXI, the realization of the IP/LP turbines for the LEMCOTEC engine results feasible both for the two- and three-spool configuration.

The baseline annulus shape has been defined for both the arrangements as a steep rising mean line design in the entry stages, followed by a constant tip diameter configuration. The result is the consequence of the choices adopted to achieve the design requirements at the turbine inlet and outlet. In fact, the main challenges related with the design of the entry stages are the need to maintain an inlet mean diameter sufficiently low to match the upstream HPT exit duct, thus avoiding excessive flow curvatures in the connection between the two components; secondly, the requirement to maintain the inlet Mach number as low as possible to minimize the blade friction losses within the turbine. The exit stage design is instead driven by the need to obtain a sufficiently low blade height while respecting the maximum tip speed constraint and while maintaining acceptable flow accelerations on the whole blade span.

All the designs developed respect the reference performance values and limitations recommended, with slight excesses only for the off-design maximum tip speed. Particularly, the additional work performed with T-AXI showed the possibility to improve the turbine design through a fine tuning of the parameters previously obtained with the PDT, such as NGV exit angles and Mach numbers. The modified design has in fact the maximum tip diameter further decreased from the PDT values, thanks to the stage rising axial velocity configuration adopted, and the exit blade heights result significantly reduced. The containment of the exit stage blade height is fundamental, both for the challenges involved in the integration of the turbine with its downstream exhaust duct and for the control of the blade mass. The latter in fact, as it could be observed from the disc design outcome, will tend to influence significantly the last stage weight.

The estimated stage isentropic efficiency is above the target value of 90% in all the designed turbines for both the programs adopted. The PDT calculated efficiencies proved to be always lower than the values obtained with T-AXI, mainly because of the simplified model adopted by the first program. However, due to the loss coefficient settings adopted in the calculations performed with T-AXI, an overestimation of the turbine efficiency by the latter tool may be possible. Further investigations on the appropriate choice of the stator and rotor pressure loss coefficients should therefore be conducted, performing CFD simulations starting from the blading obtained. If a more accurate estimation of the stage isentropic efficiency still yields high values, the option of reducing the two-spool engine LPT to a four-stage design and three-spool engine LPT to a single stage design should be considered, since in these two turbines the current stage loading coefficients are relatively low.

The two engine possible layouts do not outline significant differences in terms of size and mass between the five-stage LPT and the IPT/LPT configuration. In the current design, the five-stage LPT is in fact only 2 cm longer than its three-spool engine equivalent, since the advantage in compactness given by the faster rotating IPT is penalized by the additional IPT/LPT duct. The maximum tip diameter is comparable as well, with a final difference of 1 cm between the two configurations in the improved design achieved with T-AXI. Considering the overall turbine masses, their estimated values differ by about 30 kg in favour of the IPT/LPT configuration, but the difference will probably be overcome once the additional weight given by the third spool and relative bearings is taken into account.

Although from the evaluation of the size and mass outcomes the three-spool engine configuration may result equivalent to the two-spool from the turbine point of view, with the additional disadvantage of an increased complexity, some other factors should be considered. The IPT configuration is in fact better matched with the HPT exit diameter, thanks to its reduced inlet diameter allowed by the higher rotational speed; moreover, the inlet Mach number can be set to lower values than the equivalent 2-spool engine LPT, thus providing margins for reduced blade-friction pressure losses. On the other hand, the disc design showed that a cooling flow is required for the first and

second rotors of the IPT at the maximum rotational speed and TET, thus implying the need for active cooling and therefore contributing to the increased complexity of the three-spool configuration. For the aforementioned reasons, the choice of a three-spool layout will therefore need to be carefully evaluated, since the added complexity will tend to overweight the performance advantages given by the fast-rotating IPT.

The present work provided the essential geometry information for the LP turbine integration in the LEMCOTEC reverse-flow core engine, along with the flow conditions required for the sizing of the turbine inlet and the exhaust ducts. The design of the ducting connected with the LPT and its integration within the core will represent one of the next challenges for a successful development of the engine. In particular, the capacity of the downstream cross-over duct to achieve a 180-degrees flow turning with contained pressure losses will be one of the key elements to reach the goal of a significant improvement in overall engine efficiency, thus allowing the intercooled, reverse-flow core engine concept to set a step from its predecessors in terms of specific fuel consumption.

In addition to this thesis work, the blade geometry data obtained with T-AXI for all the designs are available to perform further CFD investigations, which are recommended to improve the assessment of the turbine efficiency. The disc geometry data are available as well in the ANSYS format to carry out high fidelity rotor stress analyses, in order to better characterize the turbine layout.

8 REFERENCES

[1] High Level Group on Aviation Research, Flightpath 2050 - Europe's Vision for Aviation, Publications Office of the European Union (2011).

[2] P. Pilidis and J. R. Palmer, *Gas Turbine Theory and Performance Course Notes*, Cranfield: Cranfield University Press (2012).

[3] European Union, *About LEMCOTEC*, LEMCOTEC (2012). (Online). Available: http://www.lemcotec.eu/page/about-lemcotec/objectives.php. (Accessed 26 June 2013).

[4] European Union, *About NEWAC*, NEWAC (2011). (Online). Available: http://www.newac.eu/16.0.html. (Accessed 26 June 2013).

[5] Avio Aero, *Markets and Applications - Trent 900*, Avio Aero (2012). (Online). Available: http://www.avioaero.com/en/catalog/civil/engines/trent_900. (Accessed 3 August 2013).

[6] J. Sieber, NEWAC Technologies - Highly Innovative Technologies for Future Aero Engines, NEWAC, Munich (DE) (2011).

[7] Rolls-Royce plc, *Trent 900 factsheet* (2013). (Online). Available: http://www.rolls-royce.com/civil/products/largeaircraft/trent_900/. (Accessed 26 June 2013).

[8] C. Riegler and C. Bichlmaier, The Geared Turbofan Technology - Opportunities, Challenges and Readiness Status, MTU Aero Engines GmbH, Munich, DE (2007).

[9] MTU Aero Engines, *PW 1000G Product Leaflet* (2013). (Online). Available: http://www.mtu.de/de/products_services/new_business_commercial/programs/pw1000g/PW1000G.pdf. (Accessed 30 June 2013).

[10] X. Zhao and T. Gronstedt, Report on Profiled Tubular Heat Exchanger Concept Study, Chalmers University of Technology, Goteborg, Sweden (2011).

[11] K. G. Kyprianidis and T. Grönstedt, Assessment of Future Aero-engine Designs with Intercooled and Intercooled Recuperated Cores, *Journal of Engineering for Gas Turbines and Power,* vol. 133, (January 2011).

[12] R. R. Van Nimwegen, Design Features of the Garrett ATF3 Turbofan Engine, Society of Automotive Engineers, Los Angeles, USA (1971).

[13] W. J. Calvert, E. Swain, M. Dempsey and U. Schmidt-Eisenlohr, Comparative Studies Of Alternative HPC Configurations For The NEWAC IRA Engine, *European Workshop on New Aero Engine Concepts*, Munich, DE (2010).

[14] W. Waschka, ATFI-HDV: Design of a new 7 stage innovative compressor for 10-18 klbf thrust, *ISABE,* no. 1266 (2005).

[15] K. W. Ramsden and D. MacManus, *Axial Turbine Design and Performance Course Notes*, Cranfield, UK: Cranfield University (2012).

[16] J. W. Norris et al., Reversed-flow Core for a Turbofan with a Fan Drive Gear System, US Patent 2011/0056208 A1 (10 March 2011).

[17] R. A. Cookson and A. S. Haslam, *Mechanical Design of Turbomachinery Course Notes*, Cranfield, UK, Cranfield University Press (2011), pp. 242-248.

[18] E. Anselmi Palma and W. Camilleri, 2-spool and 3-spool LEMCOTEC

Engine Performance Simulation Results Spreadsheet, Cranfield University, Cranfield, UK (January 2013).

[19] D. A. Sagerser et al., Empirical Expressions for Estimating Length and Weight of Axial-Flow Components of VTOL Powerplants, NASA, Washington D.C., USA (1971).

[20] E. A. Baskharone, Principles of Turbomachinery in Air-Breathing Engines, New York, USA, Cambridge University Press (2006).

[21] Z. Li, Preliminary Design System of Axial Flow Turbine Aerodynamics, Cranfield University, Cranfield, UK (2012).

[22] K. W. Ramsden and P. Pilidis, A Multimedia Computational Aid To Gas Turbine Design Teaching, Cranfield University, Cranfield, UK (1995).

[23] M. G. Turner, A. Merchant and D. Bruna, A Turbomachinery Design Tool for Teaching Design Concepts for Axial-Flow Fans, Compressors, and Turbines, *Journal of Turbomachinery,* vol. 133 (2011).

[24] M. Drela and M. B. Giles, Viscous-Inviscid Analysis of Transonic and Low Reynolds Number Airfoils, *AIAA Journal,* vol. 25, no. 10, pp. 1347-1355 (1987).

[25] D. Gutzwiller, T-Axi Disk V2.2 User's Guide and Tutorial, University of Cincinnati, USA, Cincinnati, OH (2009).

[26] D. G. Cherry et al., Energy Efficient Engine Low Pressure Turbine Test Hardware Detailed Design Report, NASA, Washington D.C., USA (1982).

[27] T. Grönstedt, Conceptual Aero Engine Design Modeling, Chalmers University of Technology, Chalmers, Sweden (2011).

[28] H. Koch, D. Kožulovic and M. Hoeger, Outlet Guide Vane Airfoil for Low

Pressure Turbine Configurations, *42nd AIAA Fluid Dynamics Conference and Exhibit*, New Orleans, USA (2012).

[29] A. D. Walker et al., Duct Aerodynamics for Intercooled Aero Gas Turbines: Constraints, Concepts and Design Methodology, *Proceedings of ASME Turbo Expo 2009: Power for Land, Sea and Air*, Orlando, FL, USA (2009).

[30] J. D. Mattingly, W. H. Heiser and D. T. Pratt, Aircraft Engine Design, Second Edition, Reston, VA, USA, AIAA (2002).

[31] S. M. Antonellis, Active Cooling of Turbine Rotor Assembly. US Patent 5,339,619 (23 August 1994).

[32] A. J. Quinones et al., "Turbine Disk Cooling System". US Patent 5,472,313 (5 December 1995).

[33] J. C. Evans, *The Garrett ATF3 Online Museum*, (2010). (Online). Available: http://www.atf3.org/ATF3_Engine.html (Accessed 4 July 2013).

[34] E. Anselmi Palma and W. Camilleri, LEMCOTEC Axial Turbine Layout Calculator Spreadsheets, Cranfield University, Cranfield (2012).

APPENDICES

Appendix A – Comparison Tables for Preliminary Design Spreadsheet and Preliminary Design Tool Results

These tables report all the velocity, angle and Mach number outputs produced for a three-stage turbine design with the Preliminary Design Tool (Section 3.3) compared with the data produced for the same case with the Preliminary Design Spreadsheet (Section 3.2). The results were obtained with both the programs for the blade mean height and then propagated at the blade hub and tip through the free-vortex hypothesis: $r\, v_\theta = const$.

This comparison was part of the assessment of the Excel spreadsheet capabilities and served as a check for the PDT compatibility with the LP turbine design considered.

Stage 1 root				
Design Tool			**Excel**	**Difference %**
Vw0	585	m/s	599.9	2.55
Vw3	287	m/s	284.7	-0.80
V3	351	m/s	347.9	-0.88
U INTER hub	246	m/s	245.7	-0.13
U EXIT hub	246	m/s	245.7	-0.13
V0	619	m/s	632.4	2.16
Vin	202	m/s	200.0	-0.99
V1	395	m/s	406.8	2.99
V2	570	m/s	566.8	-0.56
t3	821	K		
Alpha 0	71	°	71.6	0.79
Alpha 3	55	°	54.9	-0.16
Alpha inlet	0	°	0.0	
Alpha 1	59	°	60.6	2.63
Alpha 2	69	°	69.3	0.49
NGV Exit Gas Angle	71	°	71.6	0.79
Nozzle Deflection	71	°	71.6	0.79
Rotor Deflection	129	°	129.9	0.69
Nozzle Accel	2.537			
Rotor Accel	1.443		1.393	-3.45
Exit Swirl	55	°	54.9	-0.16
Reaction	0.394			
Stator axial Exit Mach	0.35			
Stator abs Exit Mach	1.07			
Stator rel Exit Mach	0.68			
Rotor axial Exit Mach	0.36		0.37	1.88
Rotor abs Exit Mach	0.63			
Rotor rel Exit Mach	1.02			

Stage 2 root Design Tool			Excel	Difference %
Vw0	597	m/s	623.4	4.43
Vw3	232	m/s	239.2	3.09
V3	306	m/s	311.8	1.89
U INTER hub	245	m/s	245.7	0.27
U EXIT hub	245	m/s	245.7	0.27
V0	630	m/s	654.7	3.92
Vin	350	m/s	347.9	-0.59
V1	405	m/s	427.4	5.54
V2	517	m/s	524.5	1.45
t3	669	K		
Alpha 0	71	°	72.2	1.71
Alpha 3	49	°	50.1	2.24
Alpha inlet	55	°	54.9	-0.16
Alpha 1	60	°	62.1	3.50
Alpha 2	67	°	67.6	0.87
NGV Exit Gas Angle	71	°	72.2	1.71
Nozzle Deflection	127	°	127.1	0.10
Rotor Deflection	128	°	129.7	1.32
Nozzle Accel	1.283			
Rotor Accel	1.278		1.227	-3.99
Exit Swirl	49	°	50.1	2.24
Reaction	0.255			
Stator axial Exit Mach	0.39			
Stator abs Exit Mach	1.22			
Stator rel Exit Mach	0.78			
Rotor axial Exit Mach	0.40		0.41	1.28
Rotor abs Exit Mach	0.61			
Rotor rel Exit Mach	1.03			

Stage 3 root Design Tool			Excel	Difference %
Vw0	458	m/s	472.9	3.26
Vw3	16	m/s	4.8	-70.14
V3	254	m/s	230.0	-9.43
U INTER hub	253	m/s	283.5	12.04
U EXIT hub	247	m/s	253.2	2.52
V0	523	m/s	525.9	0.55
Vin	335	m/s	358.5	7.03
V1	325	m/s	298.0	-8.31
V2	365	m/s	345.6	-5.30
t3	583	K		
Alpha 0	61	°	64.1	5.02
Alpha 3	4	°	1.2	-70.25
Alpha inlet	41	°	50.1	22.19
Alpha 1	39	°	39.5	1.23
Alpha 2	46	°	48.3	4.97
NGV Exit Gas Angle	61	°	64.1	5.02
Nozzle Deflection	102	°	114.2	11.92
Rotor Deflection	85	°	87.8	3.25
Nozzle Accel	1.122			
Rotor Accel	1.123		1.160	3.29

Exit Swirl	4	°	1.2	-70.25
Reaction	0.119			
Stator axial Exit Mach	0.53			
Stator abs Exit Mach	1.1			
Stator rel Exit Mach	0.69			
Rotor axial Exit Mach	0.54		0.50	-7.84
Rotor abs Exit Mach	0.54			
Rotor rel Exit Mach	0.78			

Stage 1 mean				
Design Tool			**Excel**	**Difference %**
dVw	768	m/s	766.2	-0.24
Vw0	521	m/s	519.6	-0.27
Vw3	246	m/s	246.6	0.23
Alpha 0	69	°	68.9	-0.08
Alpha 3	51	°	51.0	-0.09
V3	318	m/s	317.5	-0.16
U	286	m/s	278.3	-2.68
V0	559	m/s	556.8	-0.40
Alpha 1	51	°	51.0	-0.09
V2	570	m/s	566.7	-0.58
Alpha 2	69	°	69.3	0.48
NGV Exit Gas Angle	69	°	68.9	-0.08
Nozzle Deflection	69	°	68.9	-0.08
Rotor Deflection	120	°	120.3	0.24
Nozzle Accel	2.772			
Rotor Accel	1.792			
Exit Swirl	51	°	54.9	7.67
Reaction: 0.501	0.501		0.50	-0.20
V1= 318 m/s	318		317.5	-0.16
t3=	830	K		
Stator axial Exit Mach	0.34			
Stator abs Exit Mach	0.95			
Stator rel Exit Mach	0.54			
Rotor axial Exit Mach	0.36		0.37	1.88
Rotor abs Exit Mach	0.57			
Rotor rel Exit Mach	1.02			

Stage 2 mean				
Design Tool			**Excel**	**Difference %**
dVw	656	m/s	668.35	1.88
Vw0	481	m/s	483.03	0.42
Vw3	176	m/s	185.31	5.29
Alpha 0	67	°	67.51	0.76
Alpha 3	41	°	42.82	4.43
V3	266	m/s	272.66	2.50
U	324	m/s	307.39	-5.13
V0	521	m/s	522.80	0.35
Alpha 1	41	°	42.82	4.43
V2	538	m/s	540.73	0.51
Alpha 2	68	°	68.29	0.43

NGV Exit Gas Angle	67	°	67.51	0.76
Nozzle Deflection	118	°	118.46	0.39
Rotor Deflection	109	°	111.11	1.94
Nozzle Accel	1.640			
Rotor Accel	2.020			
Exit Swirl	41	°	42.8	4.43
Reaction	0.500		0.50	0.00
V1=	266	m/s	272.7	2.50
t3=	679	K		
Stator axial Exit Mach	0.37			
Stator abs Exit Mach	0.97			
Stator rel Exit Mach	0.5			
Rotor axial Exit Mach	0.39		0.41	3.88
Rotor abs Exit Mach	0.53			
Rotor rel Exit Mach	1.06			

Stage 3 mean				
Design Tool			**Excel**	**Difference %**
dVw	358	m/s	348.03	-2.78
Vw0	346	m/s	344.55	-0.42
Vw3	12	m/s	3.48	-71.00
Alpha 0	54	°	56.28	4.21
Alpha 3	3	°	0.87	-71.10
V3	253	m/s	230.03	-9.08
U	346	m/s	344.32	-0.48
V0	429	m/s	414.26	-3.44
Alpha 1	3	°	0.87	-71.10
V2	438	m/s	419.69	-4.18
Alpha 2	55	°	56.77	3.22
NGV Exit Gas Angle	54	°	56.28	4.21
Nozzle Deflection	89	°	99.09	11.34
Rotor Deflection	57	°	57.64	1.12
Nozzle Accel	1.392			
Rotor Accel	1.729			
Exit Swirl	3	°	0.9	-71.10
Reaction	0.500		0.50	0.00
V1=	253	m/s	230.0	-9.08
t3=	583	K		
Stator axial Exit Mach	0.52			
Stator abs Exit Mach	0.88			
Stator rel Exit Mach	0.52			
Rotor axial Exit Mach	0.54		0.50	-7.84
Rotor abs Exit Mach	0.54			
Rotor rel Exit Mach	0.93			

Stage 1 tip				
Design Tool			**Excel**	**Difference %**
Alpha 0	67	°	66.4	-0.87
Alpha 3	47	°	47.4	0.84
Alpha inlet	0	°	0.0	0.00
Alpha 1	39	°	38.3	-1.85

Alpha 2	70	°	69.6	-0.51
NGV Exit Gas Angle	67	°	66.4	-0.87
Nozzle Deflection	67	°	66.4	-0.87
Rotor Deflection	109	°	107.9	-0.99
Nozzle Accel	2.537		2.500	-1.46
Rotor Accel	2.224			
Exit Swirl	47	°	47.4	0.84
Reaction	0.578			
Vw0	470	m/s	458.2	-2.51
Vw3	216	m/s	217.4	0.67
V3	295	m/s	295.4	0.15
U INTER tip	306	m/s	300.4	-1.83
U EXIT tip	327	m/s	321.6	-1.64
V0	512	m/s	500.0	-2.35
Vin	202	m/s	200.0	-0.99
V1	260	m/s	254.8	-2.01
V2	579	m/s	575.0	-0.69
t3	836	K		
Stator axial Exit Mach	0.34			
Stator abs Exit Mach	0.86			
Stator rel Exit Mach	0.44			
Rotor axial Exit Mach	0.36		0.37	1.88
Rotor abs Exit Mach	0.52			
Rotor rel Exit Mach	1.03			

Stage 2 tip				
Design Tool			**Excel**	**Difference %**
Alpha 0	64	°	63.10	-1.40
Alpha 3	35	°	37.10	6.00
Alpha inlet	47	°	47.39	0.84
Alpha 1	11	°	12.54	14.00
Alpha 2	70	°	69.67	-0.48
NGV Exit Gas Angle	64	°	63.10	-1.40
Nozzle Deflection	111	°	110.49	-0.46
Rotor Deflection	80	°	82.21	2.76
Nozzle Accel	1.527		1.496	-2.01
Rotor Accel	2.842			
Exit Swirl	35	°	37.1	6.00
Reaction	0.629			
Vw0	402	m/s	394.3	-1.93
Vw3	141	m/s	151.3	7.27
V3	245	m/s	250.8	2.35
U INTER tip	365	m/s	349.8	-4.17
U EXIT tip	402	m/s	388.5	-3.37
V0	449	m/s	442.1	-1.54
Vin	294	m/s	295.4	0.49
V1	204	m/s	204.9	0.43
V2	579	m/s	575.6	-0.59
t3	683	K		
Stator axial Exit Mach	0.37			
Stator abs Exit Mach	0.82			
Stator rel Exit Mach	0.37			
Rotor axial Exit Mach	0.39		0.41	3.88

Rotor abs Exit Mach	0.48	
Rotor rel Exit Mach	1.14	

Stage 3 tip				
Design Tool			**Excel**	**Difference %**
Alpha 0	48	°	49.68	3.49
Alpha 3	2	°	0.68	-65.91
Alpha inlet	30	°	37.10	23.66
Alpha 1	29	°	29.04	0.13
Alpha 2	61	°	62.65	2.71
NGV Exit Gas Angle	48	°	49.68	3.49
Nozzle Deflection	78	°	86.78	11.25
Rotor Deflection	89	°	91.69	3.02
Nozzle Accel	1.287		1.233	-4.23
Rotor Accel	1.800			
Exit Swirl	2	°	0.7	-65.91
Reaction	0.355			
Vw0	278	m/s	271.0	-2.52
Vw3	9	m/s	2.7	-69.59
V3	253	m/s	230.0	-9.08
U INTER tip	416	m/s	398.7	-4.16
U EXIT tip	444	m/s	441.9	-0.47
V0	376	m/s	355.4	-5.47
Vin	292	m/s	288.4	-1.24
V1	288	m/s	263.1	-8.66
V2	519	m/s	500.6	-3.54
t3	583	K		
Stator axial Exit Mach	0.51			
Stator abs Exit Mach	0.76			
Stator rel Exit Mach	0.58			
Rotor axial Exit Mach	0.54		0.50	-7.84
Rotor abs Exit Mach	0.54			
Rotor rel Exit Mach	1.10			

Appendix B – Parametric Study Results

B.1 Temperature Distribution Variations

The following plots report the results obtained in the temperature distribution parametric study for a 4-stage LPT with the Preliminary Design Tool. The plots are complementary to those presented in Paragraph 4.4.3, hence the x-axis represents the difference between the two considered stage temperature drops (e.g. zero represents an equal temperature split across the two stages), while the y-axes report the last stage hub acceleration and exit swirl, both of which were critical in respecting the design constraints.

It should be noted that the values in last stage rotor hub acceleration and mean exit swirl are still not acceptable. However, the purpose of the study was only to evaluate their trends according with the temperature split variations.

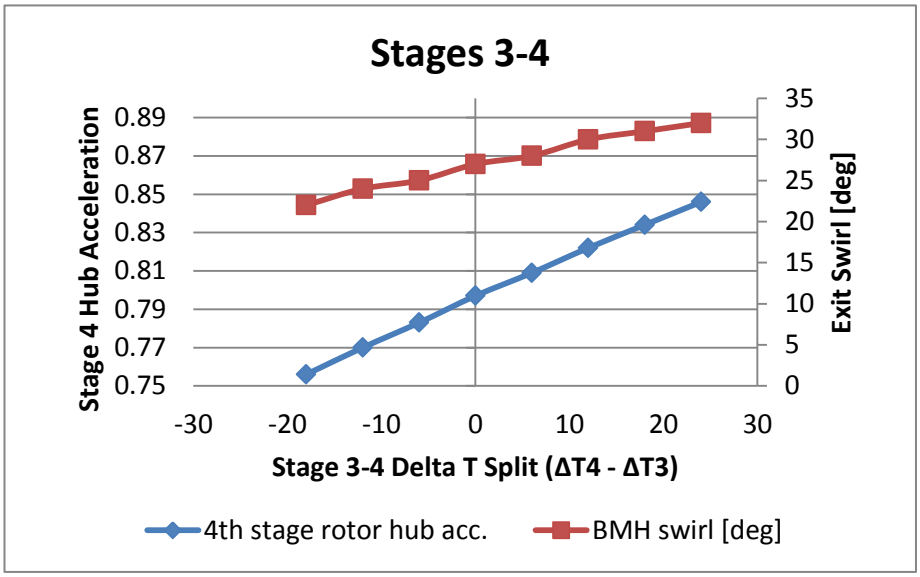

Figure 8.1 - Effects of temperature distribution variation, stages 3-4

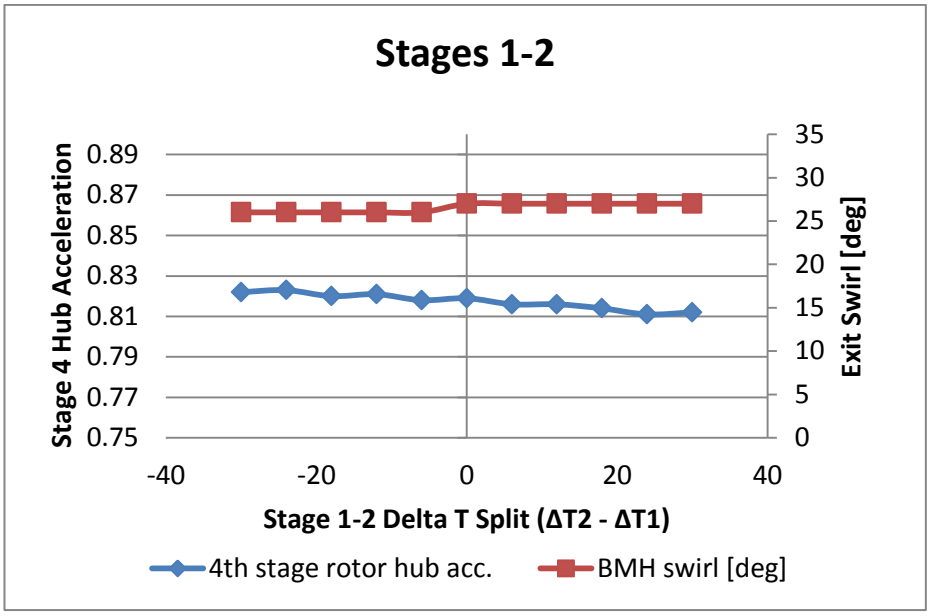

Figure 8.2 - Effects of temperature distribution variation, stages 1-2

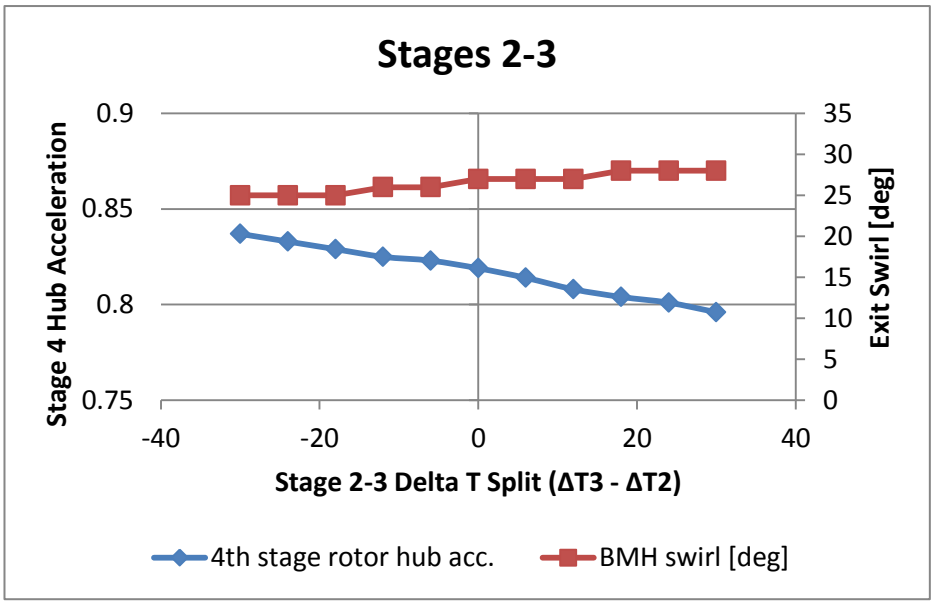

Figure 8.3 - Effects of temperature distribution variation, stages 2-3

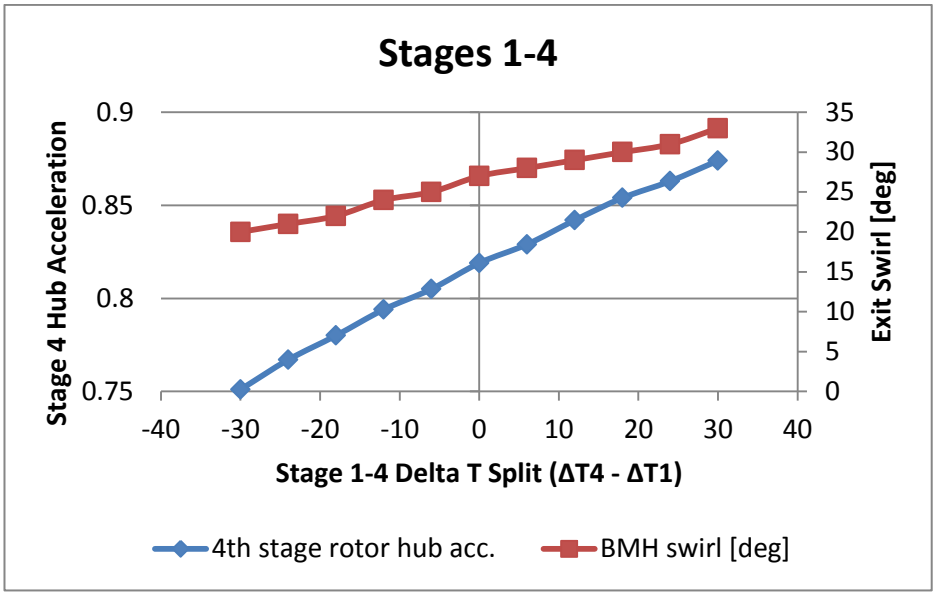

Figure 8.4 - Effects of temperature distribution variation, stages 1-4

B.2 Stage diameter variations

The following plots report the results obtained for the changes in stage mean diameters within the 4-stage LPT parametric study. These results are complementary to those presented in Paragraph 4.4.4.

It should be noted that for high diameters (*Figure 8.5*) the results are not regularly correlated, because the program could not converge on similar designs in this range. However, the diameters producing these results were out of the range of interest (0.50-0.64 m, see Paragraph 4.4.4).

The results presented here concern the modifications in the inlet (first stage) mean diameter and second stage mean diameter. The variations in the sizes of the remaining stages were consequent to the modifications introduced and were automatically calculated by the program. It should be noted that for the stage 2 diameter variations the efficiencies are different from those of the stage 1 study (Paragraph 4.4.4), since for the stage 2 parametric study a different temperature distribution with increased loading on the first and fourth stage was chosen. However, the effects on the trends were still useful for the parametric study, confirming the efficiency dependency on the stage diameter.

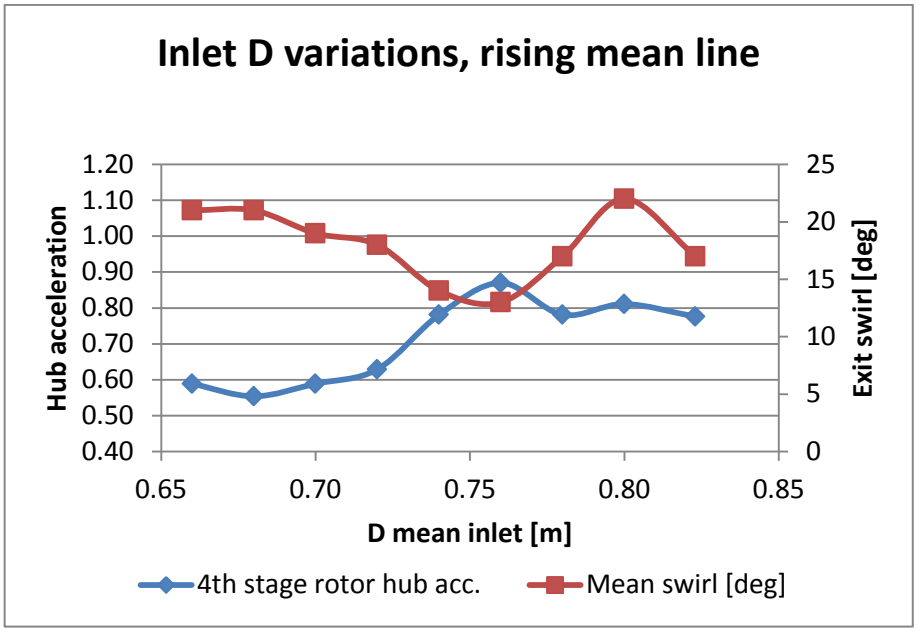

Figure 8.5 - Effect of inlet diameter variations, range 0.64-0.82 m

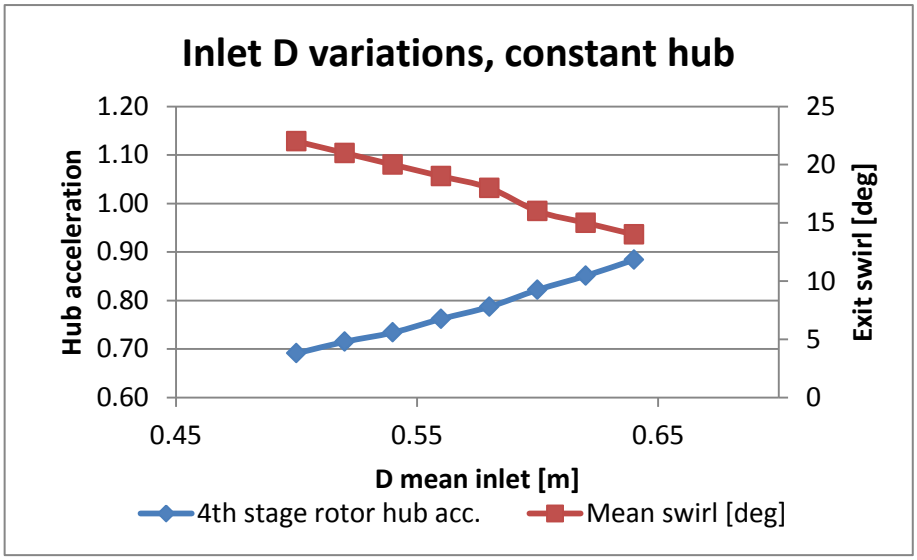

Figure 8.6 - ***Effect of inlet diameter variations, range 0.50-0.64 m***

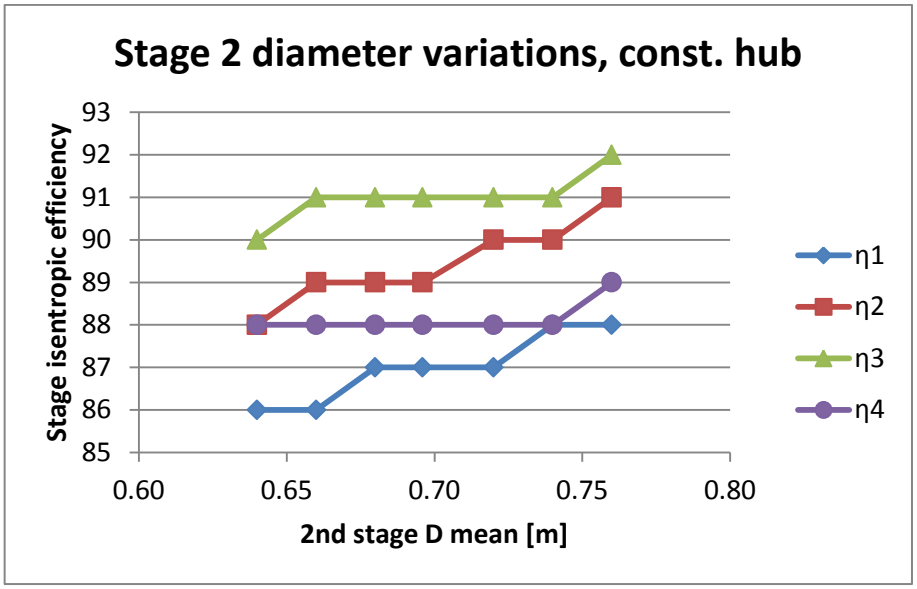

Figure 8.7 - Effect of 2nd stage diameter variation on stage efficiencies

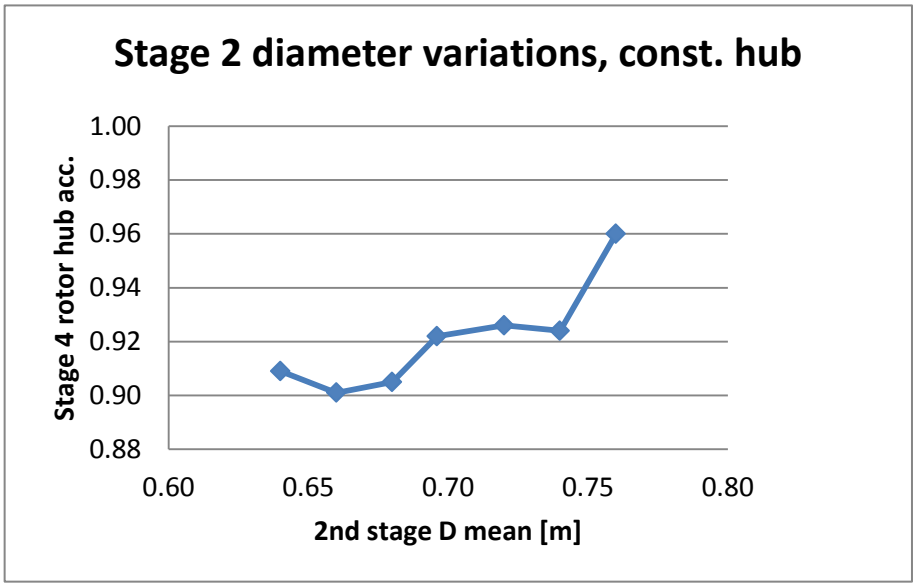

Figure 8.8 - Effect of 2nd stage diameter variation on last stage rotor hub acceleration

B.3 Inlet Mach variations

The following results report the effect of inlet Mach number variations on the turbine maximum tip diameter and on the stage isentropic efficiencies. The results are complementary to those presented in Paragraph 4.4.5.

It can be observed from the plot of *Figure 8.9* that the program could not respect the maximum tip diameter constraint which had been set to 1.03 m. However, it

appears that the increase in axial Mach allowed for a diameter reduction, apart for the first three cases where the program converged on very different designs. The second plot shows that, apart from the mentioned designs, the stage efficiencies remained almost unvaried, according with the model adopted by the program which could not take into account the dependency of the friction losses on the axial velocity.

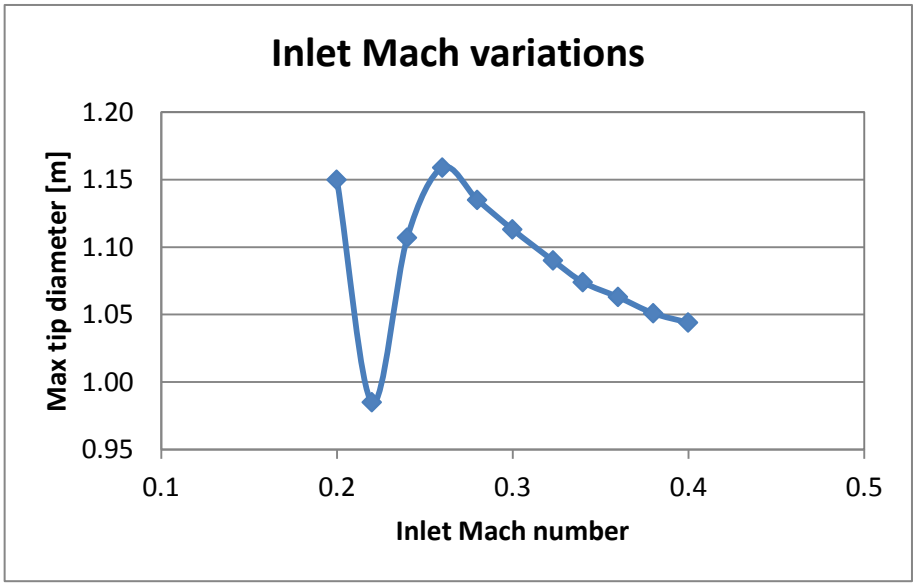

Figure 8.9 - Effect of inlet Mach number variations on turbine diameter

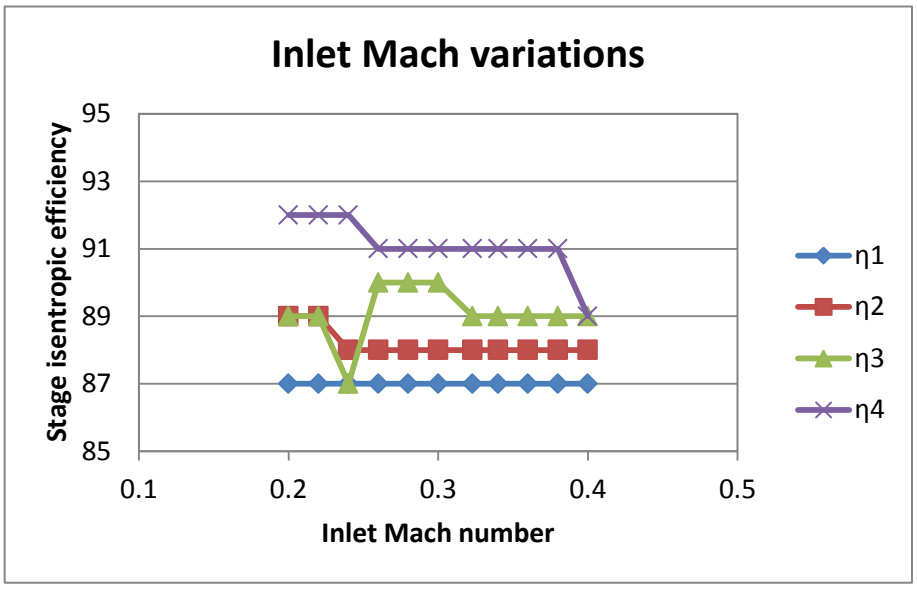

Figure 8.10 - Effect of inlet Mach number variations on stage efficiencies

Appendix C – Preliminary Design Tool Results

C.1 2-Spool LPT

This section reports the numerical results obtained with the PDT for the 5-stage LP turbine designed for the 2-spool LEMCOTEC engine. The results reported in the following table include stage pressures and temperatures, turbine geometry, blade and flow velocities, flow angles, Mach numbers and stage reactions. The data were derived also for the stage hub and tip, according with the free-vortex flow assumption.

Table 8.1 - 2-spool LPT preliminary design tool results

LPT INLET ANNULUS GEOMETRY	LPT OUTLET ANNULUS GEOMETRY
----------	----------
Stage 1	Stage 1
Gamma= 1,32	dVw: 405 m/s
R= 287	Q3 MEAN: 0,0224
Va= 200 m/s	PR= 0,67
Mach Absolute inlet= 0,32	Pin= 514,4 kPa
Vwin= 0 m/s	P3= 344,8 kPa
Alpha inlet= 0°	T3= 959
Vin= 200 m/s	P3= 345
Vin/Sqrt(T)= 6,178	A3= 0,147 m
Mach Relative inlet= 0,32	A3 annulus= 0,157 m
T/t inlet= 1,016	Theta= 50°
Q inlet= 0,0205	Stator Aspect Ratio= 1,80
TET= 1046	Rotor Aspect Ratio= 4,00
Pin= 514	Vw0 MEAN: 334 m/s
A= 0,113	Vw3 MEAN: 71 m/s
A annlus= 0,113	Alpha 0 MEAN: 59°
NGV Height= 0,056 m	Alpha 3 MEAN: 20°
NGV Tip Diameter= 0,696 m	V3 MEAN: 212 m/s
NGV Mean Diameter= 0,640 m	V3/Sqrt(T3) MEAN: 6,853
NGV Hub Diameter= 0,584 m	M3 Relative MEAN: 0,36
NGV Hub/Tip= 0,838	T3/t3 inlet= 1,020
	Rotor Height= 0,066 m
	Rotor Tip Diameter= 0,817 m
	Rotor Mean Diameter= 0,751 m
	Rotor Hub Diameter= 0,685 m
	Rotor Hub/Tip= 0,838
----------	----------
Stage 2	Stage 2
Gamma= 1,32	dVw: 353 m/s
R= 287	Q3 MEAN: 0,0224
Va= 200 m/s	PR= 0,65
Mach Absolute inlet= 0,34	Pin= 344,8 kPa
Vwin= 71 m/s	P3= 224,4 kPa
Alpha inlet= 20°	T3= 872
Vin= 213 m/s	P3= 224
Vin/Sqrt(T)= 6,865	A3= 0,216 m
Mach Relative inlet= 0,36	A3 annulus= 0,218 m
T/t inlet= 1,020	Theta= 40°
Q inlet= 0,0225	Stator Aspect Ratio= 1,80
TET= 959	Rotor Aspect Ratio= 4,00
Pin= 345	Vw0 MEAN: 327 m/s
A= 0,147	Vw3 MEAN: 26 m/s
A annlus= 0,156	Alpha 0 MEAN: 59°
NGV Height= 0,066 m	Alpha 3 MEAN: 7°
NGV Tip Diameter= 0,817 m	V3 MEAN: 202 m/s
NGV Mean Diameter= 0,751 m	V3/Sqrt(T3) MEAN: 6,837
NGV Hub Diameter= 0,685 m	M3 Relative MEAN: 0,35

NGV Hub/Tip= 0,838

Stage 3
Gamma= 1,32
R= 287
Va= 205 m/s
Mach Absolute inlet= 0,36
Vwin= 26 m/s
Alpha inlet= 7°
Vin= 206 m/s
Vin/Sqrt(T)= 6,991
Mach Relative inlet= 0,36
T/t inlet= 1,021
Q inlet= 0,0228
TET= 872
Pin= 224
A= 0,212
A annlus= 0,214
NGV Height= 0,081 m
NGV Tip Diameter= 0,924 m
NGV Mean Diameter= 0,844 m
NGV Hub Diameter= 0,763 m
NGV Hub/Tip= 0,825

Stage 4
Gamma= 1,32
R= 287
Va= 205 m/s
Mach Absolute inlet= 0,38
Vwin= 7 m/s
Alpha inlet= 2°
Vin= 205 m/s
Vin/Sqrt(T)= 7,317
Mach Relative inlet= 0,38
T/t inlet= 1,023
Q inlet= 0,0237
TET= 785
Pin= 140
A= 0,310
A annlus= 0,311
NGV Height= 0,117 m
NGV Tip Diameter= 0,961 m
NGV Mean Diameter= 0,844 m
NGV Hub Diameter= 0,727 m
NGV Hub/Tip= 0,756

Stage 5
Gamma= 1,32
R= 287
Va= 208 m/s
Mach Absolute inlet= 0,41
Vwin= 23 m/s
Alpha inlet= 6°
Vin= 209 m/s
Vin/Sqrt(T)= 7,922
Mach Relative inlet= 0,41
T/t inlet= 1,027
Q inlet= 0,0254
TET= 698

T3/t3 inlet= 1,020
Rotor Height= 0,082 m
Rotor Tip Diameter= 0,926 m
Rotor Mean Diameter= 0,844 m
Rotor Hub Diameter= 0,761 m
Rotor Hub/Tip= 0,822

Stage 3
dVw: 333 m/s
Q3 MEAN: 0,0237
PR= 0,62
Pin= 224,4 kPa
P3= 140,0 kPa
T3= 785
P3= 140
A3= 0,311 m
A3 annulus= 0,311 m
Theta= 0°
Stator Aspect Ratio= 1,80
Rotor Aspect Ratio= 4,00
Vw0 MEAN: 326 m/s
Vw3 MEAN: 7 m/s
Alpha 0 MEAN: 58°
Alpha 3 MEAN: 2°
V3 MEAN: 205 m/s
V3/Sqrt(T3) MEAN: 7,315
M3 Relative MEAN: 0,38
T3/t3 inlet= 1,023
Rotor Height= 0,117 m
Rotor Tip Diameter= 0,961 m
Rotor Mean Diameter= 0,844 m
Rotor Hub Diameter= 0,727 m
Rotor Hub/Tip= 0,756

Stage 4
dVw: 349 m/s
Q3 MEAN: 0,0251
PR= 0,59
Pin= 140,0 kPa
P3= 82,3 kPa
T3= 698
P3= 82
A3= 0,471 m
A3 annulus= 0,474 m
Theta= 0°
Stator Aspect Ratio= 1,80
Rotor Aspect Ratio= 4,00
Vw0 MEAN: 327 m/s
Vw3 MEAN: 23 m/s
Alpha 0 MEAN: 58°
Alpha 3 MEAN: 6°
V3 MEAN: 206 m/s
V3/Sqrt(T3) MEAN: 7,803
M3 Relative MEAN: 0,41
T3/t3 inlet= 1,026
Rotor Height= 0,198 m
Rotor Tip Diameter= 0,961 m
Rotor Mean Diameter= 0,763 m
Rotor Hub Diameter= 0,565 m
Rotor Hub/Tip= 0,588

Stage 5
dVw: 368 m/s
Q3 MEAN: 0,0282
PR= 0,55
Pin= 82,3 kPa
P3= 44,9 kPa
T3= 611
P3= 45
A3= 0,719 m
A3 annulus= 0,771 m
Theta= 0°
Stator Aspect Ratio= 1,80
Rotor Aspect Ratio= 4,00

Pin= 82
A= 0,465
A annlus= 0,468
NGV Height= 0,195 m
NGV Tip Diameter= 0,958 m
NGV Mean Diameter= 0,763 m
NGV Hub Diameter= 0,568 m
NGV Hub/Tip= 0,592

Vw0 MEAN: 288 m/s
Vw3 MEAN: 80 m/s
Alpha 0 MEAN: 54°
Alpha 3 MEAN: 21°
V3 MEAN: 223 m/s
V3/Sqrt(T3) MEAN: 9,023
M3 Relative MEAN: 0,47
T3/t3 inlet= 1,036
Rotor Height= 0,321 m
Rotor Tip Diameter= 1,085 m
Rotor Mean Diameter= 0,763 m
Rotor Hub Diameter= 0,442 m
Rotor Hub/Tip= 0,407

LPT EFFICIENCY PREDICTION

Total Work= 19,020
dT= 436
Umean= 242 m/s
Total dH/U2= 8,83
Warning!: The dH/U^2 is too High !
It requires 4 stages of HP turbines!

Stage 1
Stage HPT Power: 3,794 MW
Temperature Drop= 87,00 K
Umean: 262
dH/U2: 1,498
Va/Umean: 0,760
Stage Efficiency: 0,90

Stage 2
Stage HPT Power: 3,794 MW
Temperature Drop= 87,00 K
Umean: 301
dH/U2: 1,136
Va/Umean: 0,664
Stage Efficiency: 0,92

Stage 3
Stage HPT Power: 3,794 MW
Temperature Drop= 87,00 K
Umean: 319
dH/U2: 1,013
Va/Umean: 0,642
Stage Efficiency: 0,92

Stage 4
Stage HPT Power: 3,794 MW
Temperature Drop= 87,00 K
Umean: 304
dH/U2: 1,115
Va/Umean: 0,675
Stage Efficiency: 0,92

Stage 5
Stage HPT Power: 3,794 MW
Temperature Drop= 87,00 K
Umean: 288
dH/U2: 1,238
Va/Umean: 0,721
Stage Efficiency: 0,91

ROOT GEOMETRY

Stage 1
Vw0= 366 m/s
Alpha 0: 61°
Vw3= 78 m/s
Alpha 3: 21°
V3= 215 m/s
U INTER hub= 240 m/s
U EXIT hub= 259 m/s
V0= 417 m/s
Alpha inlet: 0°
Vin= 200 m/s
V1= 236 m/s
Alpha 1: 32°
V2= 392 m/s
Alpha 2: 59°
t3= 939 K
NGV Exit Gas Angle: 61°
Nozzle Deflection: 61°
Rotor Deflection: 92°
Nozzle Accel: 1,832
Rotor Accel: 1,658
Stator axial Exit Mach 0,33
Stator abs Exit Mach 0,69
Stator rel Exit Mach 0,39
Rotor axial Exit Mach 0,33
Rotor abs Exit Mach 0,36
Rotor rel Exit Mach 0,66
Exit Swirl: 21°
Reaction: 0,407

Stage 2
Vw0= 360 m/s

MEAN GEOMETRY

Stage 1
dVw: 405 m/s
Vw0: 334 m/s
Vw3: 71 m/s
Alpha 0: 59°
Alpha 3: 20°
V3: 212 m/s
U: 284 m/s
V0: 389 m/s
V1= 212 m/s
Alpha 1: 20°
V2= 408 m/s
Alpha 2: 61°
t3= 939 K
NGV Exit Gas Angle: 59°
Nozzle Deflection: 59°
Rotor Deflection: 80°
Nozzle Accel: 1,946
Rotor Accel: 1,923
Stator axial Exit Mach 0,33
Stator abs Exit Mach 0,64
Stator rel Exit Mach 0,35
Rotor axial Exit Mach 0,33
Rotor abs Exit Mach 0,36
Rotor rel Exit Mach 0,68
Exit Swirl: 20°
Reaction: 0,501

Stage 2
dVw: 353 m/s

TIP GEOMETRY

Stage 1
Vw0= 307 m/s
Alpha 0: 57°
Vw3= 66 m/s
Alpha 3: 18°
V3= 210 m/s
U INTER tip= 286 m/s
U EXIT tip= 309 m/s
V0= 366 m/s
Alpha inlet: 0°
Vin= 200 m/s
V1= 201 m/s
Alpha 1: 6°
V2= 424 m/s
Alpha 2: 62°
t3= 940 K
NGV Exit Gas Angle: 57°
Nozzle Deflection: 57°
Rotor Deflection: 68°
Nozzle Accel: 1,832
Rotor Accel: 2,114
Stator axial Exit Mach 0,33
Stator abs Exit Mach 0,60
Stator rel Exit Mach 0,33
Rotor axial Exit Mach 0,33
Rotor abs Exit Mach 0,35
Rotor rel Exit Mach 0,71
Exit Swirl: 18°
Reaction: 0,573

Stage 2
Vw0= 299 m/s

Alpha 0: 61°
Vw3= 29 m/s
Alpha 3: 8°
V3= 202 m/s
U INTER hub= 273 m/s
U EXIT hub= 288 m/s
V0= 412 m/s
Alpha inlet: 21°
Vin= 215 m/s
V1= 218 m/s
Alpha 1: 24°
V2= 374 m/s
Alpha 2: 58°
t3= 854 K
NGV Exit Gas Angle: 61°
Nozzle Deflection: 82°
Rotor Deflection: 81°
Nozzle Accel: 1,674
Rotor Accel: 1,715
Stator axial Exit Mach 0,35
Stator abs Exit Mach 0,71
Stator rel Exit Mach 0,38
Rotor axial Exit Mach 0,35
Rotor abs Exit Mach 0,36
Rotor rel Exit Mach 0,66
Exit Swirl: 8°
Reaction: 0,398

Stage 3
Vw0= 369 m/s
Alpha 0: 61°
Vw3= 8 m/s
Alpha 3: 2°
V3= 205 m/s
U INTER hub= 281 m/s
U EXIT hub= 275 m/s
V0= 422 m/s
Alpha inlet: 8°
Vin= 207 m/s
V1= 223 m/s
Alpha 1: 23°
V2= 349 m/s
Alpha 2: 54°
t3= 767 K
NGV Exit Gas Angle: 61°
Nozzle Deflection: 69°
Rotor Deflection: 77°
Nozzle Accel: 1,724
Rotor Accel: 1,567
Stator axial Exit Mach 0,37
Stator abs Exit Mach 0,77
Stator rel Exit Mach 0,41
Rotor axial Exit Mach 0,38
Rotor abs Exit Mach 0,38
Rotor rel Exit Mach 0,65
Exit Swirl: 2°
Reaction: 0,355

Stage 4
Vw0= 406 m/s
Alpha 0: 63°
Vw3= 31 m/s
Alpha 3: 9°
V3= 207 m/s
U INTER hub= 244 m/s
U EXIT hub= 214 m/s
V0= 455 m/s
Alpha inlet: 2°
Vin= 205 m/s
V1= 261 m/s
Alpha 1: 38°
V2= 319 m/s
Alpha 2: 50°
t3= 679 K

Vw0: 327 m/s
Vw3: 26 m/s
Alpha 0: 59°
Alpha 3: 7°
V3: 202 m/s
U: 319 m/s
V0: 383 m/s
V1= 202 m/s
Alpha 1: 7°
V2= 399 m/s
Alpha 2: 60°
t3= 854 K
NGV Exit Gas Angle: 59°
Nozzle Deflection: 78°
Rotor Deflection: 67°
Nozzle Accel: 1,804
Rotor Accel: 1,975
Stator axial Exit Mach 0,34
Stator abs Exit Mach 0,66
Stator rel Exit Mach 0,35
Rotor axial Exit Mach 0,35
Rotor abs Exit Mach 0,35
Rotor rel Exit Mach 0,70
Exit Swirl: 7°
Reaction: 0,500

Stage 3
dVw: 333 m/s
Vw0: 326 m/s
Vw3: 7 m/s
Alpha 0: 58°
Alpha 3: 2°
V3: 205 m/s
U: 319 m/s
V0: 385 m/s
V1= 205 m/s
Alpha 1: 2°
V2= 385 m/s
Alpha 2: 58°
t3= 767 K
NGV Exit Gas Angle: 58°
Nozzle Deflection: 65°
Rotor Deflection: 60°
Nozzle Accel: 1,865
Rotor Accel: 1,879
Stator axial Exit Mach 0,37
Stator abs Exit Mach 0,70
Stator rel Exit Mach 0,37
Rotor axial Exit Mach 0,38
Rotor abs Exit Mach 0,38
Rotor rel Exit Mach 0,71
Exit Swirl: 2°
Reaction: 0,500

Stage 4
dVw: 349 m/s
Vw0: 327 m/s
Vw3: 23 m/s
Alpha 0: 58°
Alpha 3: 6°
V3: 206 m/s
U: 288 m/s
V0: 386 m/s
V1= 206 m/s
Alpha 1: 6°
V2= 373 m/s
Alpha 2: 57°
t3= 680 K
NGV Exit Gas Angle: 58°
Nozzle Deflection: 60°

Alpha 0: 56°
Vw3= 24 m/s
Alpha 3: 7°
V3= 202 m/s
U INTER tip= 329 m/s
U EXIT tip= 350 m/s
V0= 360 m/s
Alpha inlet: 18°
Vin= 211 m/s
V1= 202 m/s
Alpha 1: 9°
V2= 424 m/s
Alpha 2: 62°
t3= 854 K
NGV Exit Gas Angle: 56°
Nozzle Deflection: 74°
Rotor Deflection: 70°
Nozzle Accel: 1,708
Rotor Accel: 2,093
Stator axial Exit Mach 0,34
Stator abs Exit Mach 0,61
Stator rel Exit Mach 0,35
Rotor axial Exit Mach 0,35
Rotor abs Exit Mach 0,35
Rotor rel Exit Mach 0,74
Exit Swirl: 7°
Reaction: 0,490

Stage 3
Vw0= 292 m/s
Alpha 0: 55°
Vw3= 6 m/s
Alpha 3: 2°
V3= 205 m/s
U INTER tip= 356 m/s
U EXIT tip= 363 m/s
V0= 356 m/s
Alpha inlet: 7°
Vin= 206 m/s
V1= 215 m/s
Alpha 1: 18°
V2= 422 m/s
Alpha 2: 61°
t3= 767 K
NGV Exit Gas Angle: 55°
Nozzle Deflection: 62°
Rotor Deflection: 79°
Nozzle Accel: 1,729
Rotor Accel: 1,967
Stator axial Exit Mach 0,37
Stator abs Exit Mach 0,64
Stator rel Exit Mach 0,39
Rotor axial Exit Mach 0,38
Rotor abs Exit Mach 0,38
Rotor rel Exit Mach 0,78
Exit Swirl: 2°
Reaction: 0,420

Stage 4
Vw0= 273 m/s
Alpha 0: 53°
Vw3= 18 m/s
Alpha 3: 5°
V3= 206 m/s
U INTER tip= 363 m/s
U EXIT tip= 363 m/s
V0= 341 m/s
Alpha inlet: 2°
Vin= 205 m/s
V1= 224 m/s
Alpha 1: 24°
V2= 433 m/s
Alpha 2: 62°
t3= 680 K

NGV Exit Gas Angle: 63°
Nozzle Deflection: 66°
Rotor Deflection: 88°
Nozzle Accel: 1,665
Rotor Accel: 1,220
Stator axial Exit Mach 0,40
Stator abs Exit Mach 0,89
Stator rel Exit Mach 0,51
Rotor axial Exit Mach 0,40
Rotor abs Exit Mach 0,41
Rotor rel Exit Mach 0,63
Exit Swirl: 9°
Reaction: 0,192

Stage 5
Vw0= 435 m/s
Alpha 0: 64°
Vw3= 139 m/s
Alpha 3: 34°
V3= 250 m/s
U INTER hub= 191 m/s
U EXIT hub= 167 m/s
V0= 482 m/s
Alpha inlet: 8°
Vin= 210 m/s
V1= 321 m/s
Alpha 1: 50°
V2= 370 m/s
Alpha 2: 56°
t3= 584 K
NGV Exit Gas Angle: 64°
Nozzle Deflection: 73°
Rotor Deflection: 105°
Nozzle Accel: 1,423
Rotor Accel: 1,152
Stator axial Exit Mach 0,44
Stator abs Exit Mach 1,01
Stator rel Exit Mach 0,67
Rotor axial Exit Mach 0,44
Rotor abs Exit Mach 0,53
Rotor rel Exit Mach 0,79
Exit Swirl: 34°
Reaction: 0,183

Rotor Deflection: 63°
Nozzle Accel: 1,881
Rotor Accel: 1,807
Stator axial Exit Mach 0,39
Stator abs Exit Mach 0,74
Stator rel Exit Mach 0,39
Rotor axial Exit Mach 0,40
Rotor abs Exit Mach 0,41
Rotor rel Exit Mach 0,73
Exit Swirl: 6°
Reaction: 0,500

Stage 5
dVw: 368 m/s
Vw0: 288 m/s
Vw3: 80 m/s
Alpha 0: 54°
Alpha 3: 21°
V3: 223 m/s
U: 288 m/s
V0: 355 m/s
V1= 208 m/s
Alpha 1: 0°
V2= 423 m/s
Alpha 2: 61°
t3= 590 K
NGV Exit Gas Angle: 54°
Nozzle Deflection: 60°
Rotor Deflection: 61°
Nozzle Accel: 1,698
Rotor Accel: 2,035
Stator axial Exit Mach 0,42
Stator abs Exit Mach 0,72
Stator rel Exit Mach 0,42
Rotor axial Exit Mach 0,44
Rotor abs Exit Mach 0,47
Rotor rel Exit Mach 0,90
Exit Swirl: 21°
Reaction: 0,638

NGV Exit Gas Angle: 53°
Nozzle Deflection: 55°
Rotor Deflection: 85°
Nozzle Accel: 1,666
Rotor Accel: 1,934
Stator axial Exit Mach 0,39
Stator abs Exit Mach 0,65
Stator rel Exit Mach 0,42
Rotor axial Exit Mach 0,40
Rotor abs Exit Mach 0,41
Rotor rel Exit Mach 0,85
Exit Swirl: 5°
Reaction: 0,401

Stage 5
Vw0= 215 m/s
Alpha 0: 46°
Vw3= 56 m/s
Alpha 3: 15°
V3= 216 m/s
U INTER tip= 386 m/s
U EXIT tip= 410 m/s
V0= 299 m/s
Alpha inlet: 5°
Vin= 209 m/s
V1= 269 m/s
Alpha 1: 39°
V2= 511 m/s
Alpha 2: 66°
t3= 591 K
NGV Exit Gas Angle: 46°
Nozzle Deflection: 51°
Rotor Deflection: 105°
Nozzle Accel: 1,433
Rotor Accel: 1,897
Stator axial Exit Mach 0,42
Stator abs Exit Mach 0,60
Stator rel Exit Mach 0,54
Rotor axial Exit Mach 0,44
Rotor abs Exit Mach 0,46
Rotor rel Exit Mach 1,08
Exit Swirl: 15°
Reaction: 0,360

C.2 3-Spool IPT

This section reports the results obtained for the three-spool engine IP turbine with the preliminary design tool.

Table 8.2 - 3-spool IPT preliminary design tool results

IPT inlet annulus geometry	IPT outlet annulus geometry
----------	----------
Stage 1	Stage 1
Gamma= 1.32	dVw: 463 m/s
R= 287	Q3 MEAN: 0.0188
Va= 156 m/s	PR= 0.63
Mach Absolute inlet= 0.24	Pin= 676.1 kPa
Vwin= 0 m/s	P3= 422.8 kPa
Alpha inlet= 0°	T3= 1020
Vin= 156 m/s	P3= 423
Vin/Sqrt(T)= 4.650	A3= 0.135 m
Mach Relative inlet= 0.24	A3 annulus= 0.155 m
T/t inlet= 1.009	Theta= 30°
Q inlet= 0.0157	Stator Aspect Ratio= 1.80
TET= 1129	Rotor Aspect Ratio= 4.00
Pin= 676	Vw0 MEAN: 375 m/s
A= 0.106	Vw3 MEAN: 88 m/s
A annlus= 0.106	Alpha 0 MEAN: 67°
NGV Height= 0.058 m	Alpha 3 MEAN: 29°
NGV Tip Diameter= 0.638 m	V3 MEAN: 179 m/s
NGV Mean Diameter= 0.580 m	V3/Sqrt(T3) MEAN: 5.616
NGV Hub Diameter= 0.522 m	M3 Relative MEAN: 0.29
NGV Hub/Tip= 0.818	T3/t3 inlet= 1.013
	Rotor Height= 0.078 m
	Rotor Tip Diameter= 0.714 m
	Rotor Mean Diameter= 0.637 m
	Rotor Hub Diameter= 0.559 m
	Rotor Hub/Tip= 0.783
----------	----------
Stage 2	Stage 2
Gamma= 1.32	dVw: 459 m/s
R= 287	Q3 MEAN: 0.0197
Va= 161 m/s	PR= 0.58
Mach Absolute inlet= 0.26	Pin= 422.8 kPa
Vwin= 88 m/s	P3= 243.8 kPa
Alpha inlet= 29°	T3= 905
Vin= 183 m/s	P3= 244
Vin/Sqrt(T)= 5.740	A3= 0.211 m
Mach Relative inlet= 0.30	A3 annulus= 0.233 m
T/t inlet= 1.014	Theta= 10°
Q inlet= 0.0191	Stator Aspect Ratio= 1.80
TET= 1020	Rotor Aspect Ratio= 4.00
Pin= 423	Vw0 MEAN: 382 m/s
A= 0.133	Vw3 MEAN: 76 m/s
A annlus= 0.151	Alpha 0 MEAN: 67°
NGV Height= 0.076 m	Alpha 3 MEAN: 25°
NGV Tip Diameter= 0.712 m	V3 MEAN: 178 m/s
NGV Mean Diameter= 0.637 m	V3/Sqrt(T3) MEAN: 5.915
NGV Hub Diameter= 0.561 m	M3 Relative MEAN: 0.31
NGV Hub/Tip= 0.788	T3/t3 inlet= 1.015
	Rotor Height= 0.112 m
	Rotor Tip Diameter= 0.772 m
	Rotor Mean Diameter= 0.660 m
	Rotor Hub Diameter= 0.547 m
	Rotor Hub/Tip= 0.709
----------	----------
Stage 3	Stage 3
Gamma= 1.32	dVw: 463 m/s
R= 287	Q3 MEAN: 0.0205
Va= 163 m/s	PR= 0.52

Mach Absolute inlet= 0.28
Vwin= 76 m/s
Alpha inlet= 25°
Vin= 180 m/s
Vin/Sqrt(T)= 5.981
Mach Relative inlet= 0.31
T/t inlet= 1.015
Q inlet= 0.0199
TET= 905
Pin= 244
A= 0.209
A annlus= 0.230
NGV Height= 0.113 m
NGV Tip Diameter= 0.759 m
NGV Mean Diameter= 0.646 m
NGV Hub Diameter= 0.533 m
NGV Hub/Tip= 0.701

Pin= 243.8 kPa
P3= 126.1 kPa
T3= 784
P3= 126
A3= 0.364 m
A3 annulus= 0.387 m
Theta= 10°
Stator Aspect Ratio= 1.80
Rotor Aspect Ratio= 4.00
Vw0 MEAN: 404 m/s
Vw3 MEAN: 59 m/s
Alpha 0 MEAN: 68°
Alpha 3 MEAN: 20°
V3 MEAN: 173 m/s
V3/Sqrt(T3) MEAN: 6.190
M3 Relative MEAN: 0.32
T3/t3 inlet= 1.016
Rotor Height= 0.174 m
Rotor Tip Diameter= 0.881 m
Rotor Mean Diameter= 0.707 m
Rotor Hub Diameter= 0.533 m
Rotor Hub/Tip= 0.604

IPT efficiency prediction

Total Work= 13.703
dT= 345
Umean= 274 m/s
Total dH/U2= 5.44
Warning!: The dH/U^2 is too High !
It requires 2 stages of HP turbines!

Stage 1
Stage HPT Power: 4.334 MW
Temperature Drop= 109.00 K
Umean: 287
dH/U2: 1.565
Va/Umean: 0.544
Stage Efficiency: 0.90

Stage 2
Stage HPT Power: 4.572 MW
Temperature Drop= 115.00 K
Umean: 306
dH/U2: 1.454
Va/Umean: 0.525
Stage Efficiency: 0.90

Stage 3
Stage HPT Power: 4.811 MW
Temperature Drop= 121.00 K
Umean: 319
dH/U2: 1.407
Va/Umean: 0.510
Stage Efficiency: 0.90

ROOT GEOMETRY

Stage 1
Vw0= 422 m/s
Alpha 0: 70°
Vw3= 100 m/s
Alpha 3: 33°
V3= 186 m/s
U INTER hub= 255 m/s
U EXIT hub= 264 m/s
V0= 450 m/s
Alpha inlet: 0°
Vin= 156 m/s
V1= 229 m/s
Alpha 1: 47°
V2= 397 m/s
Alpha 2: 67°
t3= 1005 K
NGV Exit Gas Angle: 70°
Nozzle Deflection: 70°
Rotor Deflection: 114°
Nozzle Accel: 2.381
Rotor Accel: 1.734
Stator axial Exit Mach 0.25
Stator abs Exit Mach 0.72
Stator rel Exit Mach 0.36
Rotor axial Exit Mach 0.25
Rotor abs Exit Mach 0.30
Rotor rel Exit Mach 0.64
Exit Swirl: 33°
Reaction: 0.374

Stage 2

MEAN GEOMETRY

Stage 1
dVw: 463 m/s
Vw0: 375 m/s
Vw3: 88 m/s
Alpha 0: 67°
Alpha 3: 29°
V3: 179 m/s
U: 301 m/s
V0: 406 m/s
V1= 179 m/s
Alpha 1: 29°
V2= 419 m/s
Alpha 2: 68°
t3= 1006 K
NGV Exit Gas Angle: 67°
Nozzle Deflection: 67°
Rotor Deflection: 97°
Nozzle Accel: 2.601
Rotor Accel: 2.338
Stator axial Exit Mach 0.25
Stator abs Exit Mach 0.64
Stator rel Exit Mach 0.28
Rotor axial Exit Mach 0.25
Rotor abs Exit Mach 0.29
Rotor rel Exit Mach 0.68
Exit Swirl: 29°
Reaction: 0.500

Stage 2

TIP GEOMETRY

Stage 1
Vw0= 338 m/s
Alpha 0: 65°
Vw3= 79 m/s
Alpha 3: 27°
V3= 175 m/s
U INTER tip= 319 m/s
U EXIT tip= 337 m/s
V0= 372 m/s
Alpha inlet: 0°
Vin= 156 m/s
V1= 157 m/s
Alpha 1: 7°
V2= 444 m/s
Alpha 2: 69°
t3= 1007 K
NGV Exit Gas Angle: 65°
Nozzle Deflection: 65°
Rotor Deflection: 76°
Nozzle Accel: 2.381
Rotor Accel: 2.825
Stator axial Exit Mach 0.25
Stator abs Exit Mach 0.58
Stator rel Exit Mach 0.25
Rotor axial Exit Mach 0.25
Rotor abs Exit Mach 0.28
Rotor rel Exit Mach 0.72
Exit Swirl: 27°
Reaction: 0.589

Stage 2

Vw0= 447 m/s
Alpha 0: 70°
Vw3= 92 m/s
Alpha 3: 30°
V3= 185 m/s
U INTER hub= 262 m/s
U EXIT hub= 259 m/s
V0= 475 m/s
Alpha inlet: 32°
Vin= 189 m/s
V1= 245 m/s
Alpha 1: 49°
V2= 386 m/s
Alpha 2: 65°
t3= 890 K
NGV Exit Gas Angle: 70°
Nozzle Deflection: 102°
Rotor Deflection: 114°
Nozzle Accel: 1.958
Rotor Accel: 1.572
Stator axial Exit Mach 0.27
Stator abs Exit Mach 0.80
Stator rel Exit Mach 0.41
Rotor axial Exit Mach 0.28
Rotor abs Exit Mach 0.32
Rotor rel Exit Mach 0.66
Exit Swirl: 30°
Reaction: 0.319

Stage 3
Vw0= 513 m/s
Alpha 0: 72°
Vw3= 78 m/s
Alpha 3: 26°
V3= 181 m/s
U INTER hub= 252 m/s
U EXIT hub= 252 m/s
V0= 538 m/s
Alpha inlet: 30°
Vin= 187 m/s
V1= 308 m/s
Alpha 1: 58°
V2= 368 m/s
Alpha 2: 64°
t3= 770 K
NGV Exit Gas Angle: 72°
Nozzle Deflection: 102°
Rotor Deflection: 122°
Nozzle Accel: 1.978
Rotor Accel: 1.195
Stator axial Exit Mach 0.30
Stator abs Exit Mach 0.99
Stator rel Exit Mach 0.57
Rotor axial Exit Mach 0.30
Rotor abs Exit Mach 0.33
Rotor rel Exit Mach 0.68
Exit Swirl: 26°
Reaction: 0.137

dVw: 459 m/s
Vw0: 382 m/s
Vw3: 76 m/s
Alpha 0: 67°
Alpha 3: 25°
V3: 178 m/s
U: 312 m/s
V0: 415 m/s
V1= 178 m/s
Alpha 1: 25°
V2= 420 m/s
Alpha 2: 67°
t3= 892 K
NGV Exit Gas Angle: 67°
Nozzle Deflection: 96°
Rotor Deflection: 93°
Nozzle Accel: 2.263
Rotor Accel: 2.361
Stator axial Exit Mach 0.27
Stator abs Exit Mach 0.69
Stator rel Exit Mach 0.30
Rotor axial Exit Mach 0.28
Rotor abs Exit Mach 0.31
Rotor rel Exit Mach 0.72
Exit Swirl: 25°
Reaction: 0.500

Stage 3
dVw: 463 m/s
Vw0: 404 m/s
Vw3: 59 m/s
Alpha 0: 68°
Alpha 3: 20°
V3: 173 m/s
U: 334 m/s
V0: 435 m/s
V1= 183 m/s
Alpha 1: 27°
V2= 425 m/s
Alpha 2: 67°
t3= 771 K
NGV Exit Gas Angle: 68°
Nozzle Deflection: 93°
Rotor Deflection: 95°
Nozzle Accel: 2.420
Rotor Accel: 2.320
Stator axial Exit Mach 0.29
Stator abs Exit Mach 0.78
Stator rel Exit Mach 0.33
Rotor axial Exit Mach 0.30
Rotor abs Exit Mach 0.32
Rotor rel Exit Mach 0.79
Exit Swirl: 20°
Reaction: 0.462

Vw0= 334 m/s
Alpha 0: 64°
Vw3= 65 m/s
Alpha 3: 22°
V3= 173 m/s
U INTER tip= 351 m/s
U EXIT tip= 365 m/s
V0= 371 m/s
Alpha inlet: 26°
Vin= 179 m/s
V1= 162 m/s
Alpha 1: 6°
V2= 459 m/s
Alpha 2: 69°
t3= 892 K
NGV Exit Gas Angle: 64°
Nozzle Deflection: 90°
Rotor Deflection: 75°
Nozzle Accel: 2.070
Rotor Accel: 2.840
Stator axial Exit Mach 0.27
Stator abs Exit Mach 0.61
Stator rel Exit Mach 0.27
Rotor axial Exit Mach 0.28
Rotor abs Exit Mach 0.30
Rotor rel Exit Mach 0.79
Exit Swirl: 22°
Reaction: 0.566

Stage 3
Vw0= 333 m/s
Alpha 0: 64°
Vw3= 47 m/s
Alpha 3: 16°
V3= 170 m/s
U INTER tip= 387 m/s
U EXIT tip= 416 m/s
V0= 371 m/s
Alpha inlet: 22°
Vin= 175 m/s
V1= 172 m/s
Alpha 1: 19°
V2= 491 m/s
Alpha 2: 71°
t3= 772 K
NGV Exit Gas Angle: 64°
Nozzle Deflection: 86°
Rotor Deflection: 89°
Nozzle Accel: 2.113
Rotor Accel: 2.860
Stator axial Exit Mach 0.29
Stator abs Exit Mach 0.65
Stator rel Exit Mach 0.30
Rotor axial Exit Mach 0.30
Rotor abs Exit Mach 0.31
Rotor rel Exit Mach 0.91
Exit Swirl: 16°
Reaction: 0.491

C.3 3-Spool LPT

This section reports the results obtained for the three-spool engine LP turbine with the preliminary design tool.

Table 8.3 - 3-spool LPT preliminary design tool results

LPT inlet annulus geometry	LPT outlet annulus geometry
----------	----------
Stage 1	Stage 1
Gamma= 1,32	dVw: 338 m/s
R= 287	Q3 MEAN: 0,0211
Va= 161 m/s	PR= 0,63
Mach Absolute inlet= 0,30	Pin= 131,8 kPa
Vwin= 0 m/s	P3= 83,3 kPa
Alpha inlet= 0°	T3= 698
Vin= 161 m/s	P3= 83
Vin/Sqrt(T)= 5,798	A3= 0,523 m
Mach Relative inlet= 0,30	A3 annulus= 0,548 m
T/t inlet= 1,014	Theta= 0°
Q inlet= 0,0193	Stator Aspect Ratio= 18,00
TET= 772	Rotor Aspect Ratio= 40,00
Pin= 132	Vw0 MEAN: 287 m/s
A= 0,380	Vw3 MEAN: 51 m/s
A annlus= 0,380	Alpha 0 MEAN: 61°
NGV Height= 0,173 m	Alpha 3 MEAN: 17°
NGV Tip Diameter= 0,873 m	V3 MEAN: 169 m/s
NGV Mean Diameter= 0,700 m	V3/Sqrt(T3) MEAN: 6,394
NGV Hub Diameter= 0,527 m	M3 Relative MEAN: 0,33
NGV Hub/Tip= 0,604	T3/t3 inlet= 1,018
	Rotor Height= 0,230 m
	Rotor Tip Diameter= 0,988 m
	Rotor Mean Diameter= 0,758 m
	Rotor Hub Diameter= 0,527 m
	Rotor Hub/Tip= 0,534
----------	----------
Stage 2	Stage 2
Gamma= 1,32	dVw: 324 m/s
R= 287	Q3 MEAN: 0,0230
Va= 161 m/s	PR= 0,60
Mach Absolute inlet= 0,32	Pin= 83,3 kPa
Vwin= 51 m/s	P3= 50,1 kPa
Alpha inlet= 18°	T3= 624
Vin= 169 m/s	P3= 50
Vin/Sqrt(T)= 6,379	A3= 0,753 m
Mach Relative inlet= 0,33	A3 annulus= 0,826 m
T/t inlet= 1,017	Theta= 0°
Q inlet= 0,0211	Stator Aspect Ratio= 18,00
TET= 698	Rotor Aspect Ratio= 40,00
Pin= 83	Vw0 MEAN: 251 m/s
A= 0,524	Vw3 MEAN: 72 m/s
A annlus= 0,549	Alpha 0 MEAN: 57°
NGV Height= 0,231 m	Alpha 3 MEAN: 24°
NGV Tip Diameter= 0,988 m	V3 MEAN: 176 m/s
NGV Mean Diameter= 0,758 m	V3/Sqrt(T3) MEAN: 7,057
NGV Hub Diameter= 0,527 m	M3 Relative MEAN: 0,37
NGV Hub/Tip= 0,533	T3/t3 inlet= 1,021
	Rotor Height= 0,347 m
	Rotor Tip Diameter= 1,104 m
	Rotor Mean Diameter= 0,758 m
	Rotor Hub Diameter= 0,411 m
	Rotor Hub/Tip= 0,372
LPT efficiency prediction	
	Stage 2
Total Work= 6,112	Stage HPT Power: 3,056 MW
dT= 148	Temperature Drop= 74,23 K

Umean= 258 m/s
Total dH/U2= 2,63
Warning!: The dH/U^2 is too High !
It requires 1 stages of HP turbines!

Stage 1
Stage HPT Power: 3,056 MW
Temperature Drop= 74,23 K
Umean: 268
dH/U2: 1,220
Va/Umean: 0,599
Stage Efficiency: 0,91

Umean: 280
dH/U2: 1,122
Va/Umean: 0,575
Stage Efficiency: 0,92

ROOT GEOMETRY

Stage 1
Vw0= 396 m/s
Alpha 0: 68°
Vw3= 73 m/s
Alpha 3: 24°
V3= 177 m/s
U INTER hub= 195 m/s
U EXIT hub= 195 m/s
V0= 428 m/s
Alpha inlet: 0°
Vin= 161 m/s
V1= 258 m/s
Alpha 1: 51°
V2= 312 m/s
Alpha 2: 59°
t3= 685 K
NGV Exit Gas Angle: 68°
Nozzle Deflection: 68°
Rotor Deflection: 110°
Nozzle Accel: 1,717
Rotor Accel: 1,210
Stator axial Exit Mach 0,31
Stator abs Exit Mach 0,83
Stator rel Exit Mach 0,50
Rotor axial Exit Mach 0,32
Rotor abs Exit Mach 0,35
Rotor rel Exit Mach 0,61
Exit Swirl: 24°
Reaction: 0,169

Stage 2
Vw0= 406 m/s
Alpha 0: 68°
Vw3= 133 m/s
Alpha 3: 40°
V3= 209 m/s
U INTER hub= 173 m/s
U EXIT hub= 152 m/s
V0= 437 m/s
Alpha inlet: 24°
Vin= 176 m/s
V1= 283 m/s
Alpha 1: 55°
V2= 327 m/s
Alpha 2: 61°
t3= 605 K
NGV Exit Gas Angle: 68°
Nozzle Deflection: 93°
Rotor Deflection: 116°
Nozzle Accel: 1,376
Rotor Accel: 1,155
Stator axial Exit Mach 0,33
Stator abs Exit Mach 0,90
Stator rel Exit Mach 0,59
Rotor axial Exit Mach 0,34
Rotor abs Exit Mach 0,44
Rotor rel Exit Mach 0,68
Exit Swirl: 40°

MEAN GEOMETRY

Stage 1
dVw: 338 m/s
Vw0: 287 m/s
Vw3: 51 m/s
Alpha 0: 61°
Alpha 3: 17°
V3: 169 m/s
U: 280 m/s
V0: 329 m/s
V1= 162 m/s
Alpha 1: 6°
V2= 368 m/s
Alpha 2: 64°
t3= 686 K
NGV Exit Gas Angle: 61°
Nozzle Deflection: 61°
Rotor Deflection: 70°
Nozzle Accel: 2,042
Rotor Accel: 2,268
Stator axial Exit Mach 0,31
Stator abs Exit Mach 0,63
Stator rel Exit Mach 0,31
Rotor axial Exit Mach 0,32
Rotor abs Exit Mach 0,33
Rotor rel Exit Mach 0,72
Exit Swirl: 17°
Reaction: 0,559

Stage 2
dVw: 324 m/s
Vw0: 251 m/s
Vw3: 72 m/s
Alpha 0: 57°
Alpha 3: 24°
V3: 176 m/s
U: 280 m/s
V0: 298 m/s
V1= 163 m/s
Alpha 1: 10°
V2= 387 m/s
Alpha 2: 65°
t3= 610 K
NGV Exit Gas Angle: 57°
Nozzle Deflection: 75°
Rotor Deflection: 75°
Nozzle Accel: 1,771
Rotor Accel: 2,371
Stator axial Exit Mach 0,32
Stator abs Exit Mach 0,60
Stator rel Exit Mach 0,33
Rotor axial Exit Mach 0,33
Rotor abs Exit Mach 0,37
Rotor rel Exit Mach 0,80
Exit Swirl: 24°
Reaction: 0,579

TIP GEOMETRY

Stage 1
Vw0= 225 m/s
Alpha 0: 54°
Vw3= 39 m/s
Alpha 3: 14°
V3= 166 m/s
U INTER tip= 343 m/s
U EXIT tip= 365 m/s
V0= 277 m/s
Alpha inlet: 0°
Vin= 161 m/s
V1= 200 m/s
Alpha 1: 36°
V2= 434 m/s
Alpha 2: 68°
t3= 686 K
NGV Exit Gas Angle: 54°
Nozzle Deflection: 54°
Rotor Deflection: 105°
Nozzle Accel: 1,717
Rotor Accel: 2,172
Stator axial Exit Mach 0,30
Stator abs Exit Mach 0,52
Stator rel Exit Mach 0,38
Rotor axial Exit Mach 0,32
Rotor abs Exit Mach 0,33
Rotor rel Exit Mach 0,85
Exit Swirl: 14°
Reaction: 0,391

Stage 2
Vw0= 182 m/s
Alpha 0: 49°
Vw3= 50 m/s
Alpha 3: 17°
V3= 168 m/s
U INTER tip= 386 m/s
U EXIT tip= 408 m/s
V0= 243 m/s
Alpha inlet: 14°
Vin= 165 m/s
V1= 260 m/s
Alpha 1: 52°
V2= 485 m/s
Alpha 2: 71°
t3= 612 K
NGV Exit Gas Angle: 49°
Nozzle Deflection: 62°
Rotor Deflection: 122°
Nozzle Accel: 1,469
Rotor Accel: 1,865
Stator axial Exit Mach 0,32
Stator abs Exit Mach 0,48
Stator rel Exit Mach 0,51
Rotor axial Exit Mach 0,33
Rotor abs Exit Mach 0,35
Rotor rel Exit Mach 1,01
Exit Swirl: 17°

Reaction: 0,171		Reaction: 0,310

Appendix D – T-AXI Input Files

The following sections provide the input files developed in T-AXI for the design of the considered turbines. The essential results obtained are reported in the Chapter 6, while the list of the complete blading would result excessively long to be published in the work. The input files are therefore provided in the following sections, thus allowing in every moment the reproduction of the results obtained.

D.1 2-Spool LPT

Init File

```
1               ! Units                       [1-SI:2-English]
2 1 1 1         ! Design Options
5               ! N Stages
36.834          ! Mass Flow Rate              [kg/s]
7218.36         ! RPM                         [rpm]
514373.36       ! Inlet Total Pressure        [Pa]
1045.38         ! Inlet Total Temperature     [K]
0.              ! Alpha 1 - First Stage       [deg]
0.320           ! Mach 1 - First Stage        [-]
1.441           ! Inlet Duct Length/N1 Axial Width Ratio [-]
0 0           ! Hub and Casing slope upstream of N1 [deg]
1.32            ! Ratio of Specific Heats     [-]
0.287           ! Gas Constant                [kJ/kg*K]
0.0009          ! Ratio of clearance/(tip radius)
```

Stage File

```
LEMC  Stage Data for LPT 5 stage meanline design
  1          2          3          4          5     ! Comment Stage
59.0       59.0       61.0       62.0       62.5    ! Alpha 0 [deg]
0.64       0.66       0.68       0.70       0.66    ! Mach 0  [-]
959        872        785        698        611     ! T3      [K]
0.8        0.8        0.8        0.8        0.8     ! Stator Zweifel no.
0.8        0.8        0.8        0.8        0.8     ! Rotor Zweifel no.
0.08       0.05       0.05       0.05       0.05    ! Stator Phi Coef.
0.12       0.1        0.1        0.1        0.05    ! Rotor Phi Coef.
1.8540     1.8611     1.9992     2.7541     4.5374  ! Stator AR
3.5065     3.7026     4.4733     6.1180     6.1180  ! Rotor AR
1.0        1.000      1.000      1.100      1.100   ! Rotor Axial V Ratio
0.231      0.38       0.3        0.51       0.34    ! NGV Row Space Coef.
0.575      0.47       0.472      0.63       0.567   ! Rot Row Space Coef.
0.3213     0.3776     0.4263     0.4321     0.3973  ! Stator Mean R [m]
0.3400     0.3817     0.4100     0.4200     0.4000  ! Rotor Mean R [m]
```

D.2 3-Spool IPT

Init File

```
1               ! Units                       [1-SI:2-English]
2 1 1 1         ! Design Options
3               ! N Stages
33.582          ! Mass Flow Rate              [kg/s]
9021.55         ! RPM                         [rpm]
676101.27       ! Inlet Total Pressure        [Pa]
1128.94         ! Inlet Total Temperature     [K]
0.              ! Alpha 1 - First Stage       [deg]
0.240           ! Mach 1 - First Stage        [-]
1.441           ! Inlet Duct Length/N1 Axial Width Ratio [-]
0 0           ! Hub and Casing slope upstream of N1 [deg]
1.32            ! Ratio of Specific Heats     [-]
0.287           ! Gas Constant                [kJ/kg*K]
0.0009          ! Ratio of clearance/(tip radius)
```

Stage File

```
LEMC  Stage Data for IPT 3 stage meanline design
  1          2          3      ! Comment Stage
67.0       69.0       70.0     ! Alpha 0           [deg]
0.64       0.69       0.78     ! Mach 0            [-]
1020       905        784      ! T3                [K]
0.8        0.8        0.8      ! Stator Zweifel No. [-]
0.8        0.8        0.8      ! Rotor Zweifel No.  [-]
0.30       0.28       0.28     ! Stator Phi Coef.  [-]
0.34       0.30       0.30     ! Rotor Phi Coef.   [-]
2.1363     2.5913     3.5913   ! Stator Aspect Ratio
4.0419     4.7934     5.9776   ! Rotor Aspect Ratio
1.0        1.000      1.000    ! Rotor Axial V Ratio
0.231      0.38       0.3      ! Stat Row Space Coef.
0.575      0.47       0.472    ! Rot Row Space Coef.
0.2971     0.3380     0.3306   ! Stat Mean R       [m]
0.3112     0.3360     0.3500   ! Rot Mean R        [m]
```

D.3 3-Spool LPT

Init File

```
1               ! Units                       [1-SI:2-English]
2 1 1 1         ! Design Options
2               ! N Stages
34.767          ! Mass Flow Rate              [kg/s]
7048.94         ! RPM                         [rpm]
131785.03       ! Inlet Total Pressure        [Pa]
772.03          ! Inlet Total Temperature     [K]
0.              ! Alpha 1 - First Stage       [deg]
0.36            ! Mach 1 - First Stage        [-]
0.8             ! Inlet Duct Length/N1 Axial Width Ratio [-]
0 0           ! Hub and Casing slope upstream of N1 [deg]
1.32            ! Ratio of Specific Heats     [-]
0.287           ! Gas Constant                [kJ/kg*K]
0.0009          ! Ratio of clearance/(tip radius)
```

Stage File

```
LEMC  Stage Data for LPT 2 stage meanline design
  1          2       ! Comment Stage
61.0       61.0      ! Alpha 0  [deg]
0.70       0.74      ! Mach 0   [-]
698        624       ! T3       [K]
0.8        0.8       ! Stator Zweifel No.  [-]
0.8        0.8       ! Rotor Zweifel No.   [-]
0.08       0.05      ! Stator Phi Coef.   [-]
0.1        0.1       ! Rotor Phi Coef.    [-]
4.5781     5.6073    ! Stator Aspect Ratio
6.1180     6.1180    ! Rotor Aspect Ratio
1.1        1.1       ! Rotor Axial V Ratio
0.51       0.34      ! Stator Row Space Coef.
0.63       0.567     ! Rotor Row Space Coef.
0.3500     0.3800    ! Stator Mean Radius [m]
0.3600     0.3700    ! Rotor Mean Radius  [m]
```